People's Democratic Republic of Algeria.

Ministry of Higher Education and Scientific Research.

University of Médéa



Faculty of Technology

Department of: Process Engineering And Environment
Option: Process Engineering Of Materials.

In view of obtaining a Master's degree in process engineering of materials

Theme:

Modeling the prediction of the permeability of organic-inorganic hybrid polymers

Realized by:

ANISSA HABIRECHE

Proposed and directed by:

-Pr. KREA MOHAMED.

-Dr. HASNAOUI HANAA.

COLLEGE YEAR
2017/2018

THANKS

We thank ALLAH Almighty for having given us the health and the will to begin and end this memory, to be our best confidant and to allow us to realize our dreams. Thank you for guiding us and always be with us.

The realization of this memoir has been possible thanks to the help of several people to whom we would like to express my gratitude.

First of all, this work would not be so rich and could not have been done without the help and the framer: ***Pr. KREA Mohamed****. I thank him for the quality of his exceptional supervision, for his patience, his rigor and above all for his confidence, his remarks and his advice, his availability and his kindness during my preparation of this memoir.*

My deepest gratitude, my thanks are addressed to ***Dr. HASNAOUI HANAA*** *for her practical help and moral support and encouragement, and for her patience, her rigor and especially for her trust, her remarks and her advice, her availability and her kindness during our preparation for this memory.*

To all the members of the ***jury*** *for having accepted to evaluate this work and for all their remarks and criticisms, as well as my teachers for their generosity and the great patience which they knew how to show despite their academic and professional duties*

To all my teachers who introduced us to authentic values, sign of deep respect and deep love one by one.

My deepest thanks also go to all the people who helped me and supported me from law or order.



DEDICATION

A MES PARENTS, POUR LE SOUTIEN QU'ILS M'ONT APPORTÉ DURANT TOUTES SES ANNÉES D'ÉTUDES. QU'ILS SOIENT ASSURÉS DE TOUT MON AMOUR.

A IBRAHIM DEUXIÈME PÈRE POUR LEUR SOUTIEN MORAL. ET POUR LEUR GENTILLESSE ET LEUR DISPONIBILITÉ.

A ABD ERRAHIM, L'ÉPOUX QUI M'A ACCOMPAGNÉ TOUT AU LONG DE CE TRAVAIL.

A MA FAMILLE SPÉCIALEMENT MES SŒURS. ET LES PETITES ENFANTS NADHIR, CHOROUK, RANIA, RAYEN, RAHIM, AMIR, ANESS ET HAITHEM.

A MES CAMARADES INTIMES, DE CLASS ET DE LA PROMO POUR NOS SOUVENIRS, NOTRE ANNÉE SCOLARITÉ

ملخص:

في هذا العمل ، تم إنشاء نموذج للعلاقة الهيكلية - الكمية للتنبؤ بنفاذية 45 بوليمر هجين في درجات حرارة مختلفة لغاز ثاني أكسيد الكربون. مع تحديد 3222 واصف من ثلاث وحدات مكررة وتم اختيار الأهم من خلال الاحتفاظ المتكرر بطريقة متكررة بالمعلومات. واستخدمت مواصفات مختارة بالإضافة إلى درجة الحرارة كمدخلات لتطوير نموذج الشبكة العصبية الاصطناعية. تم تقييم هذه النماذج غير الخطية من خلال بعض طرق التحقق الداخلية والخارجية. أشارت النتائج التي تم الحصول عليها إلى قدرة الممتازة على التنبؤ بنفاذية هذه البوليمرات المحددة لغاز ثاني أكسيد الكربون مع مقاييس إحصائية مرضية :

$Z \approx 1$, RMSE=0.23, $Q^2_{test} = 0.8$, $Q^2_{train} = 0.604$

الكلمات المفتاحية:

البوليمرات المهجنة ، النفاذية ، البنية ، الشبكة العصبية الاصطناعية ، الواصفات ، IRIV

Résumé:

Dans ce travail, un modèle de relation structure-propriété quantitative (QSPR) a été établi pour prédire la perméabilité de 45 polymères hybrides à différentes températures pour le dioxyde de carbone gazeux. Avec 3222 descripteurs ont été déterminés à partir de trois unités récurrentes (trimère) et les plus importants ont été sélectionnés au moyen d'une méthode de variables informatives retenant itérativement (IRIV). Les descripteurs sélectionnés en plus de la température ont été utilisés comme intrants pour développer un modèle de Réseau Neuronal Artificiel (RNA). Ces modèles non linéaires ont été évalués par des méthodes de validation internes et externes. Les résultats obtenus indiquent l'excellente capacité de l'RNA à prédire la perméabilité de ces polymères fixés pour le gaz CO_2 avec des paramètres statistiques satisfaisants :

$Z \approx 1$, RMSE=0.23, $Q^2_{test} = 0.8$, $Q^2_{train} = 0.604$

Mots clés:

Polymères hybrides, perméabilité, structure, réseau neuronal artificiel (RNA), descripteurs, IRIV.

Abstract:

In this work, a quantitative structure–property relationship (QSPR) model was established to predict permeability of 45 hybrid polymers at different temperatures for carbon dioxide gas. With 3222 descriptors was determined from three repeating units (trimer) and the most important were selected by means of an iteratively retaining informative variables (IRIV) method. The selected descriptors in addition to the temperature were used as the inputs to develop an artificial neural network (ANN) model. These nonlinear models were assessed by some internal and external validation methods. The obtained results indicated the excellent ability of ANN to predicting the permeability of this set polymers for CO_2 gas with satisfying statistical parameters: Z≈1, RMSE=0.23, $Q^2_{test} = 0.8$, $Q^2_{train} = 0.604$

Key words:

Hybrid polymers, permeability, Structure, Artificial Neural Network (ANN), descriptors, IRIV.

Contents

Thanks

DEDICATION

Abstract

Contents

LIST OF FIGURES

LIST OF TABLES

LIST OF ACRONYMS

GENERAL INTRODUCTION ……..…….…….1

Chapter I: Bibliographic summary

Part-1-Introduction to hybrid materials

1. Introduction …… 2
2. Definitions: Hybrid Polymers, Blends and Nanocomposites …….…..2
   - 2.1.Hybrid Polymers ……..…….....2
   - 2.2.Blends …….…..4
   - 2.3.Nanocomposites ……...5
3. Classification and hybrid materials ……..6
   - 3.1.Preparing class I hybrid material …….…….….6
   - 3.2.Preparing class II hybrid material …...……..7
4. Process of elaboration of hybrid materials …….….7
   - 4.1.Physical development …….…..8
     - 4.1.1. Ion deposition ……...…8
     - 4.1.2. Cathode sputtering ……..….8
     - 4.1.3. Laser ablation deposition ……8
   - 4.2.Chemical deposition …… 9
     - 4.2.1. Non-assisted procedure ……....9
     - 4.2.2. Plasma assisted process ……9
5. Conclusion ……10

Part -2- Characteristics and applications of hybrid materials

1. Introduction …….……11
2. Characteristics of hybrid materials ……..11
2.1. Low deformations ……...……11
2.2. Large deformations, fracture behavior ……...….12
2.2.1. Hybrid materials with high organic polymer content ……..13
2.2.2. Hybrid materials with high inorganic content …...……...…..13
2.3. Hardness ……..14
2.4. Mechanical properties of organic–inorganic hybrid films ……..14
2.4.1. Sol–gel silicas modified by hydrophobic –CH3 group ….…...14
2.4.2. Epoxy-modified silica hybrid materials …….……..15
2.4.3. (Meth)acrylate modified silica hybrid materials ….…….……15
3. Applications of hybrid organic-inorganic membranes …….…….……15
3.1. Reduction of membrane fouling ……..16
3.2. Pressure-driven water filtration ……..…….16
3.3. Membrane contactor applications ……...…17
3.4. Organic solvent nanofiltration …….17
3.5. Hydrophilic pervaporation ……..17
3.6. Organophilic pervaporation …….……18
3.7. Gas separation …….18
4. Conclusion …….21

Part -3- Synthesis of Organic-inorganic hybrid membranes

1. Introduction …. ……..…22
2. Synthesis methodologies of hybrid organic-inorganic membranes ……22
2.1.Sol-Gel Process …….. …….. …….. ……22
2.2.Self-Assembly Process …….. …… ……..27
2.3.Assembling or Dispersion of Nanobuilding Blocks (NBBs) …….. 30
2.3.1 Clusters ……..……..…….30
2.3.2 Organically in Situ- or Post-Functionalized Nanoparticles....31
2.3.3 Layered Compounds …..……. ..…..31

2.3.4 Core-Shell Nanocomposites ……..……...…32

2.3.5 Hierarchical Structures …….. ….…..…...33

2.4.Interpenetrating Networks (IPNs) ……..……..…….34

3. Class II hybrid organic-inorganic membranes synthesis method ……...…35

3.1.Dip-coated organic-inorganic hybrid membranes …….....36

3.1.1. Polymer (PDMS) coated ceramic membranes ……37

3.1.2. (Co)-condensed membranes based on sol-gel chemistry ..…38

3.2.Post-synthetic organic-inorganic hybrid membranes …….....38

3.2.1. Grafted organic-inorganic membranes with a direct oxygen bond……...…39

3.2.2. Condensation via a heteroatom …….…..39

3.2.2.1.Organosilane-modified membranes ……... …39

3.2.2.2.Organophosphonic acid-modified membranes …….. 40

3.2.3. Organometallic-modified hybrid membranes ……..41

4. Conclusions …….. …… ……..……. …….. ..41

Chapter II: NEURONAL MODELING FOR THE PREDICTION OF PERMEABILITY

1. Introduction ……...…….42
2. Part-1- : Development of the database ……..…..……43

2.1.Software and materials used ……. ……..……..43

2.2.Collection of data …… …….……. ……..……43

2.3.Polymers collected used in this work …….…...44

2.4.Drawing of molecules by ChemDraw ……. ……....54

2.5.Molecular modeling of trimers by HyperChem ……..……..… 55

2.6.Descriptor calculation by DRAGON ……..……57

2.7.Collection of data in an EXCEL file …….…..… ….62

3. Part 2- Reduction of the number of descriptors ……...…...…..63

3.1.Pretreatment of the database:…….……63

4. Part-3. Neural modeling for the prediction of permeability …….…...…66

4.1.Distribution of data ……..……..66

4.2.Optimization and design of the neural network ……67

4.3.Optimization of the CO_2 prediction network architecture ……....70
4.3.1. Step 1: Effect of the learning algorithm ……..71
4.3.2. Step 2: Effect of standardization ……..…..……73
4.3.3. Step 3: Activation function effect …….……..….74
4.3.4. Step 4 ……..74
A. Effect of the number of neurons …….. ……74
B. Effect of the number of hidden layers ……..……..75
5. Result of the optimization ……..……...…….79
6. Statistical parameters ……..…….……..79
6.1.Coefficient of correlation R …….…..79
6.2.Prediction coefficient(Q^2_{train})……...……80
6.3.Prediction coefficient (Q^2_{test})…….…..……..80
6.4.Performance factor (C)…… ….……..……...…80
6.5.Average absolute relative error (AARE) ……..…..…80
7. Results analysis …..... 81
8. Conclusion …… …...…….82
General conclusion ……..… …….……83
References

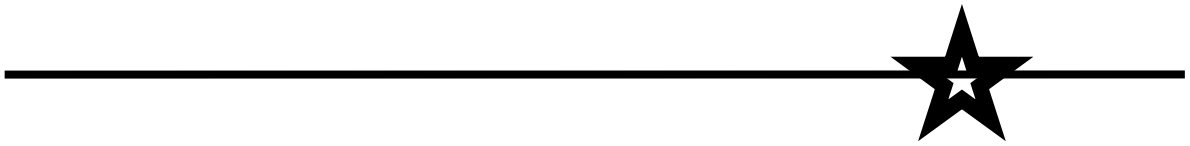
List of Figures

Fig. 1.1	Selected interactions typically applied in hybrid materials and their relative strength	3
Fig.1.2	The different types of hybrid materials.	5
Fig 1.3	Interpenetrating network	6
Fig 1.4	Particulate Nanocomposite	6
Fig 1.5	Hybrid precursor	7
Fig 3.1	hydrolisation of TEOS	23
Fig 3.2	Schematic super hydrophobic surfaces prepared through the sol-gel derived organic-inorganic hybrid emulsion	23
Fig 3.3	Description of technologies and products of the sol-gel process	24
Fig 3.4	Organically functionalized trialkoxysilanes	26
Fig 3.5	Schematic illustration of covalent bonds and hydrogen bonds between NH2-ZIF-8 and PA	27
Fig 3.6	Fundamental reaction steps in the sol–gel process based on tetrialkoxysilanes	27
Fig 3.7	Representation of mesoporous M41S compounds	28
Fig 3.8	Synthesis of mesoporous compounds in the presence of template	29
Fig 3.9	Different methods for the synthesis of organic-inorganic hybrid mesoporous silica	30
Fig 3.10	Schematic representation of different kinds of composites produced from interaction of layer compound with polymers	32
Fig 3.11	TEM of polystyrene-coated Fe_2O_3 particles	32
fig 3.12	Hierarchical structure of lobster cuticle	33
Fig 3.13	Schematic representation of IPNs	35
Fig 3.14	Schematic overview of the different synthesis approaches resulting in class II hybrid organic-inorganic membranes	36
Fig 3.15	Schematic representation of the different precursors	37
Fig 3.16	Schematic representation of the influence of water on the grafting of organosilane with multiple reactive groups	40
Fig II.1	Flowchart of the different stages of realization of the database	43
Fig II.2	Stage of representation of the structures by ChemDraw	55
Fig II.3	HyperChem version 8.0.7 for molecular modeling of trimers	56
Fig II.4	Step of the pre-optimizations of the molecules respectively	57
Fig II.5	The interface of the DRAGON software version 5.5	58
Fig II.6	First steps for calculating descriptors by DRAGON	58
Fig II.7	Second steps for calculating descriptors by DRAGON	59
Fig II.8	Third step for calculating descriptors by DRAGON	59
Fig II.9	Fourth step for calculating descriptors by DRAGON	60
Fig II.10	Fifth step for calculating descriptors by DRAGON	60
Fig II.11	The database of final descriptors	62
Fig II.12	The flow chart of IRIV algorithm. The number of the variables, P, changes after removing the uninformative and interfering variables	64
Fig II.13	General schematization and distribution of the contents of the database	66
Fig II.14	Flowchart of Optimal Static Neural Network (OSNN) Methodology	69
Fig II.15	Effect of the learning algorithm on the performance of the neural	70

	network	
Fig II.16	Effect of normalization on the learning performance of the neural network, train LM	72
Fig II.17	Effect of normalization on the learning performance of the neural network, BR train	72
Fig II.18	Effect of the activation function on the performance of the neural network	73
Fig II.19	Effect of number of neurons of the hidden layer on the learning performance of the neural network	74
Fig II.20	Effect of the number of hidden layers on the learning performance	75
Fig II.21	Optimized CO_2 neuron network architecture	77
Fig II.22	the permeability estimated as a function of the experimental permeability for CO_2 and their linear equation by the postreg function of MATLAB	78
Fig II.23	Comparison between the experimental permeability and the estimated permeability for CO_2	80

List of tables

Number	Title	Page
Table 1.1	Different possibilities of compositions and structures of hybrid materials	2
Table 1.2	Different chemical interactions and their respective strength	4
Table 1.3	Comparison of Techniques Used to Develop Hybrid Layers	10
Table 2.1	Influence of the gas / polymer system and temperature on D, S, and P_e	21
Table 3.1	Ion Exchange Capacity (IEC), water uptake (WU), proton diffusion coefficient (U_H^+), and separation factor of some reported membranes	34
Table II.1	Selected hybrid membranes and their permeability	54
Table II.2	Number of descriptors calculating by DRAGON.	61
Table II.3	Calculation results of molecular descriptors for CO2	65
Table II.4	The meanings of some Matlab instruction.	67
Table II.5	Codes of different learning functions using in the test	68
Table II.6	Standardization algorithms.	71
Table II.7	Different activation functions using in the design phase of the neural model	73
Table II.8	Structure of optimized neural networks	76
Table II.9	The values of the statistical parameters	80



General Introduction



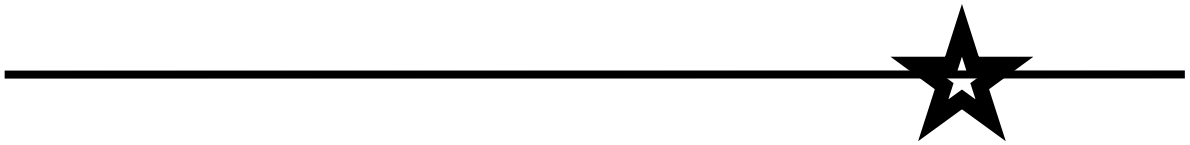
General Introduction

Polymers are now well-accepted for a wide variety of applications. The growth in their use has continued in the last two decades or more when demand for traditional materials like metals, ceramics and glasses has remained static or even fallen [1]. Currently, and in the field of high technology, which prompt the direction of research towards a new kind of material: hybrid organic-inorganic polymers, with their interfaces consequently playing an important role in their properties and generating unusual features and improved performances. One important brand of development of these hybrid materials deals with those destined to membrane separation process [2].

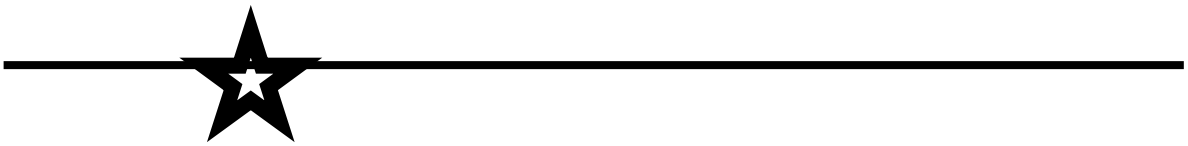
This work fits into this context and is a logical continuation of the previous work carried out in the Materials and Environmental Laboratory (MEL) on the exploitation of experimental data for the collection and validation of published permeability and solubility prediction models for a wide range of film-forming materials used either in separation processes or as packaging of pharmaceuticals or agri-food products. It consists in enriching the existing polymer database with new hybrid materials and in predicting their permeability to gases by means of determining the relationship between the microstructure of these materials and the property of permeability to the different gases.

This work is organized into two chapters:

- The first deals with the potential of hybrid materials for membranes, where we highlight and categorize the wide diversity of hybrid organic-inorganic membranes. We focus in this review on the preparation, proprieties, application and synthesis of class II hybrid O-I membranes for the presence of covalent bonds between organic and inorganic moieties that show promise for enhanced molecular separations in gas separation especially for CO_2 case.
- The second part is devoted to the modeling method for the prediction of permeability consisting of digitalizing hybrid polymers, optimizing their 3D structures and determining their descriptor. It also contains a method for reducing the size of descriptors number by IRIV, the neuronal modeling, optimization of the parameters of neural networks and the results of the application of the prediction model followed by interpretations of these results.
- In the end a conclusion pinched from this work.



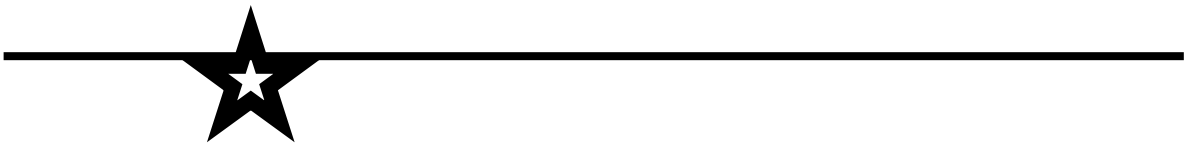
Chapter I: Summary bibliographic





Part-1-

Introduction to hybrid materials



1. Introduction:

Recent technological breakthroughs and the desire for new functions generate an enormous demand for novel materials. Many of the well-established materials, such as metals, ceramics or plastics cannot fulfill all technological desires for the various new applications. Scientists and engineers realized early on that mixtures of materials can show superior properties compared with their pure counterparts. One of the most successful examples is the group of composites which are formed by the incorporation of a basic structural material into a second substance, the matrix. Usually the systems incorporated are in the form of particles, whiskers, fibers, lamellae, or a mesh. Most of the resulting materials show improved mechanical properties and a well-known example is inorganic fiber-reinforced polymer [3].

Hybrid materials refer to any of a class of materials in which organic and inorganic components intimately mixed. This however does not mean that simple physical mixtures of organic and inorganic compounds are hybrid materials. The rider is that the mixing be at the nanometric scale [3].

1. Definitions: Hybrid Polymers, Blends and Nanocomposites:

1.1.Hybrid Polymer:

Hybrid polymer is a system in which both organic and inorganic species coexist. The term hybrid polymer is used for many different systems spanning a wide area of different materials, such as crystalline highly ordered coordination polymers, amorphous sol–gel compounds, and polymer with and without interactions between the inorganic and organic units.

Before the discussion of synthesis and properties of such materials, we try to delimit this broadly-used term by taking into account various concepts of composition and structure (Table 1.1) [4].

Table1. 1: Different possibilities of compositions and structures of hybrid materials.

Matrix:	*crystalline* ↔ *amorphous* *organic* ↔ *inorganic*
Building blocks:	*molecules* ↔ *macromolecules* ↔ *particles* ↔ *fibers*
Interactions between components:	*strong* ↔ *weak*

The most wide-ranging definition is the following: a hybrid polymer is a material that includes two moieties blended on the molecular scale. Commonly one of these compounds is inorganic and the other one organic in nature.

A more detailed definition distinguishes between the possible interactions connecting the inorganic and organic species.

Because of the gradual change in the strength of chemical interactions it becomes clear that there is a steady transition between weak and strong interactions (Fig. 1.1) [4].

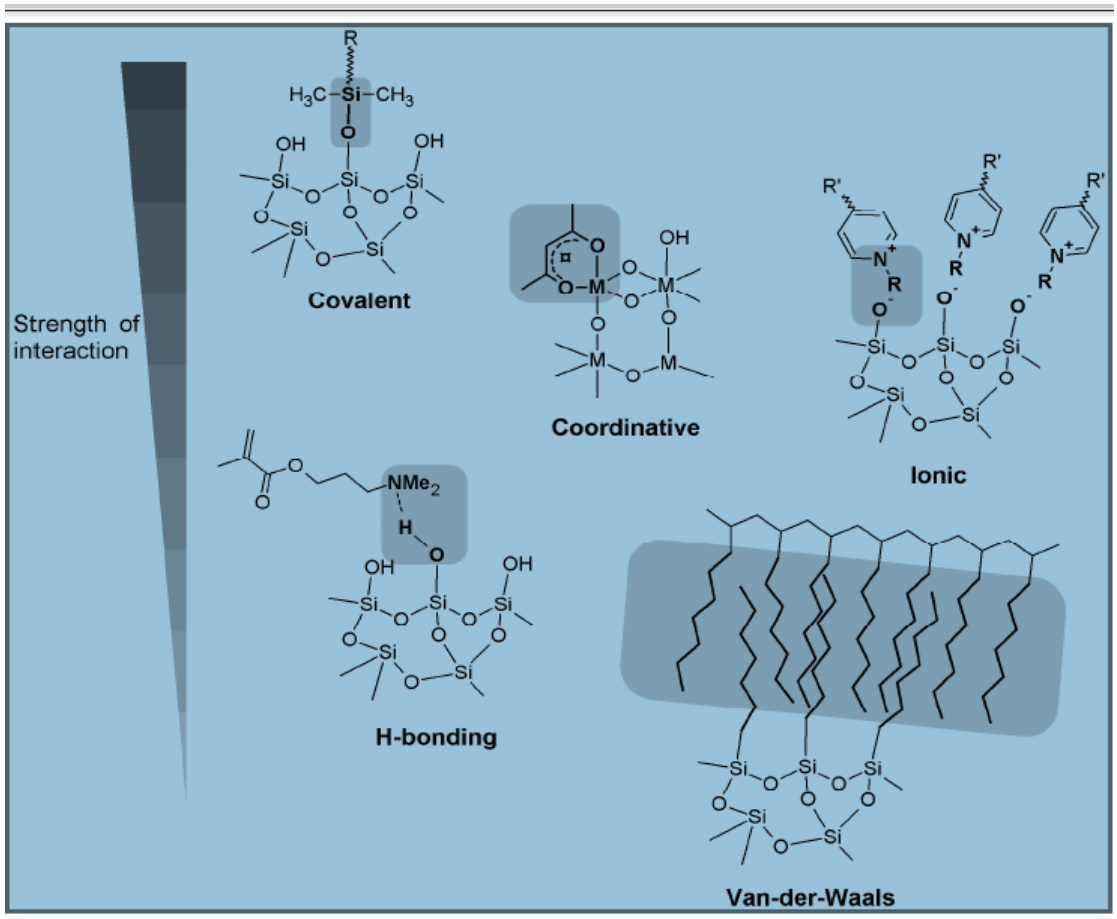


Fig1. 1. Selected interactions typically applied in hybrid materials and their relative strength.

For example, there are hydrogen bonds that are definitely stronger than for example weak coordinative bonds. Table 1.2 presents the energetic categorization of different chemical interactions depending on their binding energies [5].

Table1. 2: Different chemical interactions and their respective strength.

Type of interaction	*Strength [kJmol^{-1}]*	*Range*	*Character*
Van der Waals	50	Short	nonselective, nondirectional
H-bonding	5–65	Short	selective, directional
Coordination bonding	50–200	Short	directional
Ionic	50–250[a]	Long	nonselective
Covalent	350	Short	predominantly irreversible

a Depending on solvent and ion solution; data are for organic media.

Hybrids can either be homogeneous systems of miscible organic and inorganic components or they can be heterogeneous with dimension scales of the order of a few Angstrom to a few nanometres. At such scales, the properties of the resultant material are not just the result of the individual properties of the materials, but the scale of the interaction between the two components contributes significantly to the properties of the resultant material [3].

The precursors commonly used to develop hybrids, are called ORMOCERS (ORganicallyMOdifiedCERamics) if the mineral element is any metal (titanium, zirconium, aluminum ...) and more specifically ORMOSILS (ORganicallyMOdifiedSIloxanes) if the mineral element is the silicon atom. The general formula of ORMOSILS is RxSi (OR ') $_{4-x}$. R is an organic moiety that can be either inert or susceptible to thermal or UV irradiation polymerization. (OR ') is an alkoxide group for forming the mineral network by hydrolysis and condensation (sol-gel process) [5].

1.2.*Blends*:

Blends are formed if no strong chemical interactions exist between the inorganic and organic building blocks. One example of such a material is the combination of inorganic clusters or particles with organic polymers (fig 1.2a). In this case a formed material consists of a continuous phase, organic polymer with

entrapped discrete inorganic moieties. Other blend is formed if an inorganic and an organic network interpenetrate each other without strong chemical interactions, so called interpenetrating networks (IPNs) are formed (fig 1.2b). Both blend materials belong to class I hybrids [4].

1.3.*Nanocomposites*:

The term nanocomposite is used if one of the structural units, either the organic or the inorganic, is in a defined size range of 1–100 nm. Commonly, the term nanocomposites is used if discrete structural units in the respective size regime are used and the term hybrid materials is more often used if the inorganic units are formed *in situ* by molecular precursors, for example applying sol–gel reactions [4].

Examples of discrete inorganic units for nanocomposites are nanoparticles, nanorods, carbon nanotubes and galleries of clay minerals (Fig.1.2 c and d). Usually a nanocomposite is formed from these building blocks by their incorporation in organic polymers [4].

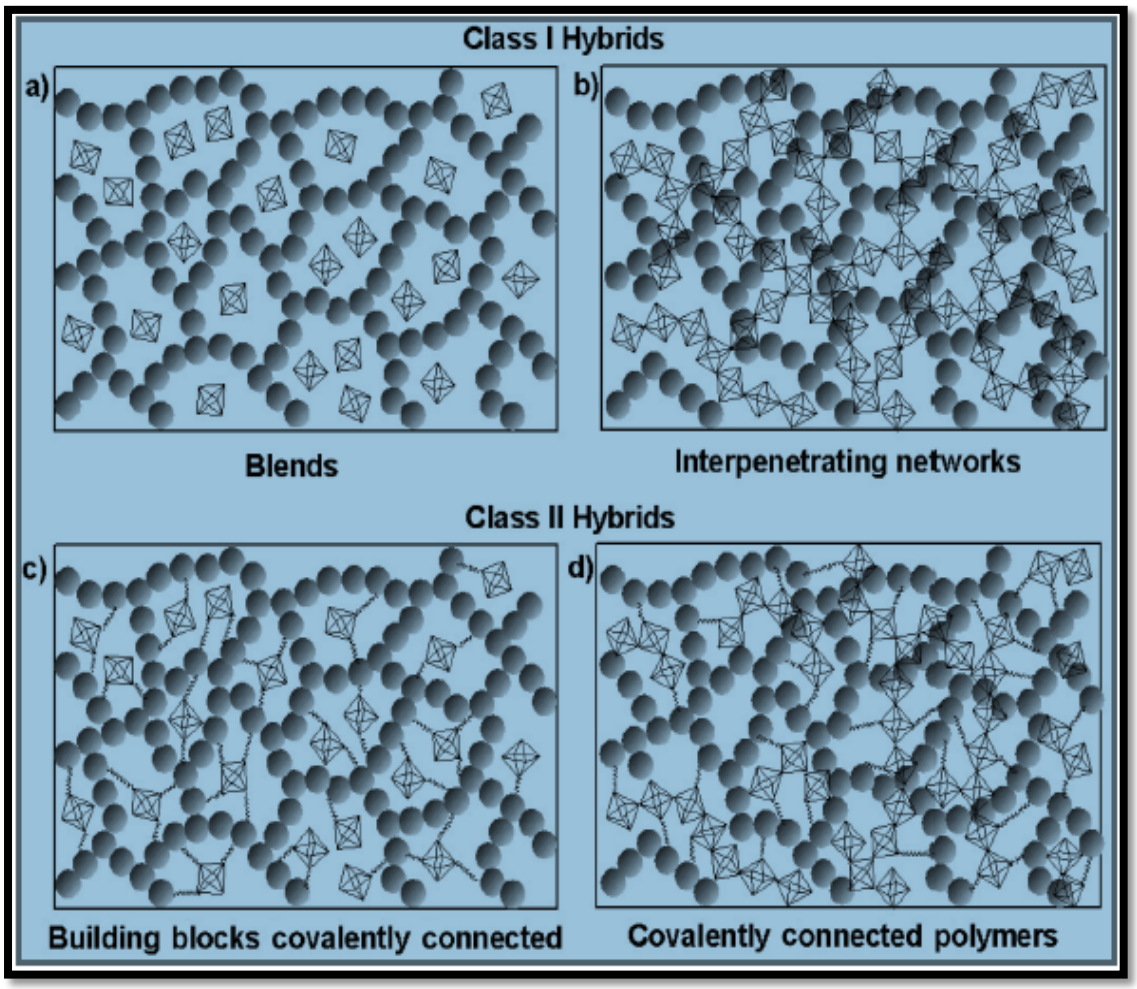


Fig. 1.2: The different types of hybrid materials.

2. Classification of Hybrid materials:

- *Class I* hybrid materials are those that show weak interactions between the two phases, such as Van Der Waals, hydrogen bonding or weak electrostatic interactions.
- *Class II* hybrid materials are those that show strong chemical interactions between the components, such as covalent and ion covalent bonds.

2.1.Preparing class I hybrid material:

To prepare a class I hybrid material, two methods are used:

The first method consists of a dispersion of a mineral network through an organic network. The training reactions of each network must be simultaneously without bringing about in homogeneity. The result is an interpenetrating network (Fig 1.3) without resorting to strong interactions (i.e. covalent bonds) [5].

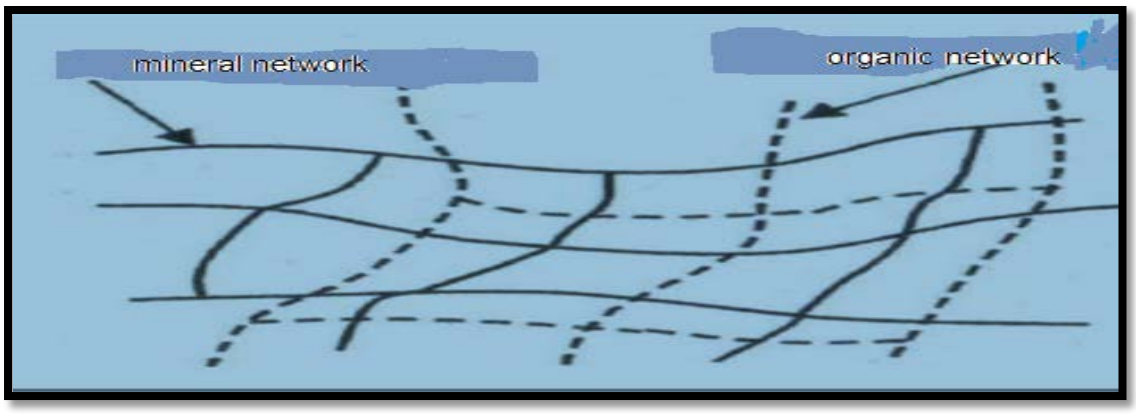


Fig. 1.3: Interpenetrating network.

The second possibility is to introduce the mineral or organic part under form of colloidal particles (sizes of a few tens of nanometers). There is forming a particulate nanocomposite with a weak matrix-particle bond. This case is illustrated in (Fig 1.4). The synthesis of this type of materials is carried out at the liquid state [5].

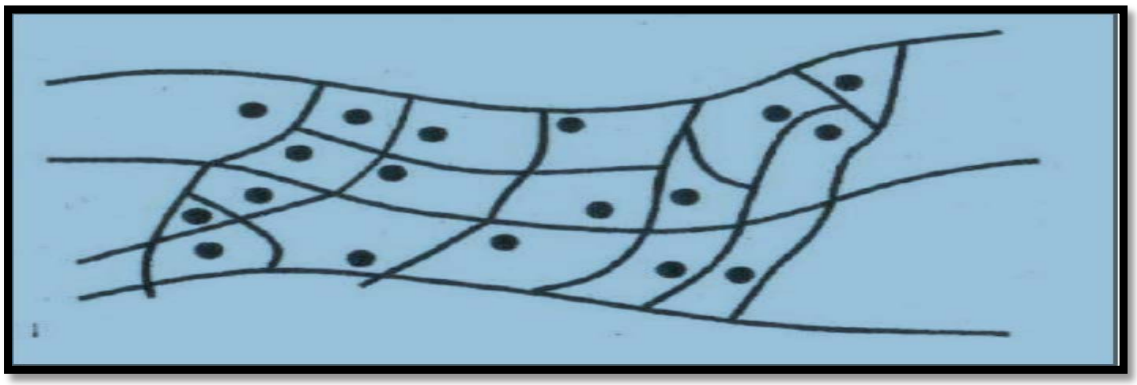


Fig 1.4: Particulate Nanocomposite

Regardless of the method used, class I corresponds to a hybrid system where the organic component is trapped in an inorganic network. Only hydrogen, Van der Waals or ionic bonds bring the cohesion of the entire structure. The links between the two phases are weak but this class of materials has a wide diversity of structures and final properties [5].

2.2.preparing class II hybrid material:

With regard to obtaining class II hybrid films, mixed (or hybrid) precursors that already carry an organic part and a mineral part such as organoalkoxysilanes are used, as shown in the example presented in (Fig 1.5) [5].

Class II corresponds to a system where the organic component is bound to the inorganic network by strong bonds such as covalent or ion covalent bonds.

Depending on its nature, the organic group can act as a modifier, conferring on the silicon oxide network new properties or as a trainer of new chemical bonds.

In the latter case, the group may be, for example, a vinyl group for generating an organic polymer simultaneously or later to the mineral network. This group can also carry a reactive function ensuring compatibility with the various components of the network [5].

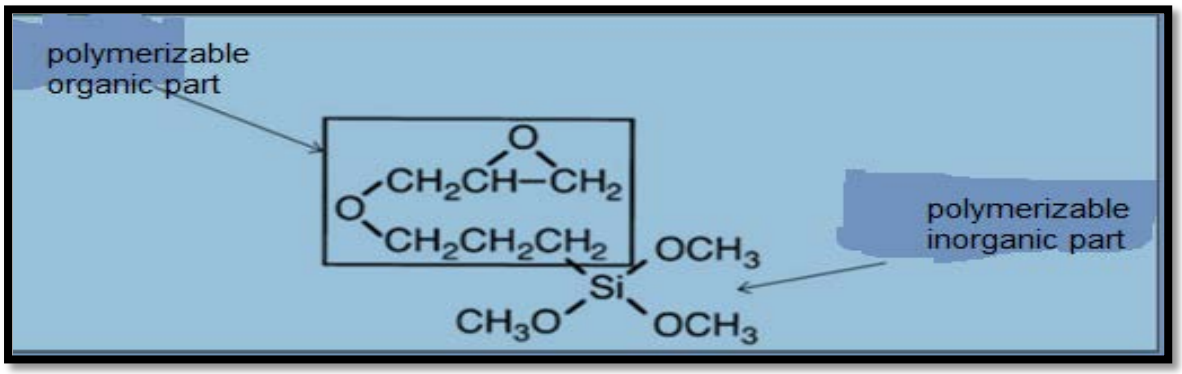


Fig 1.5: Hybrid precursor

3. Process of elaboration of hybrid materials:

The processes for producing hybrid materials are essentially of two types, physical and chemical processes. The former used the PVD (Physical Vapor Deposition), electron beam or laser ablation methods; the latter use methods such as CVD (Chemical Vapor Deposition) or sol-gel. In order to be able to define the advantages and the disadvantages of these processes, a synthetic description is necessary in the first place [5].

3.1.Physical development:

Three deposition methods can be distinguished according to the method used to generate the ionic or atomic beam. These beams can be generated using an ion gun, electric discharge, sputtering or laser ablation [5].

3.1.1. Ion deposition:

Ion Beam Sputtering (IBS) is a technique that involves eroding a target of material to be deposited with ions. Ions are often neutralized by an electron beam just before the target. The atoms are emitted in a privileged direction forming a cone, also called ejection pen. The substrate to be coated is placed in the trajectory of the atomized atom. The low working pressure allows an average free path of the pulverized material of several tens of centimeters

Ion bombardment controls the morphology, composition and physical properties of the coating during its growth, which is a considerable advantage of this method. However, the high cost, the congestion related to the experimental device and the low deposition rate make this method less attractive [5].

3.1.2. Cathode sputtering:

This sputtering method is a process based on sputtering a solid target from plasma generated in a low pressure gas. Depending on the nature of the target, two types of sputtering are possible: cathode sputtering (CS) and sputtering radio frequency (RF).

RF cathodes make it possible to produce plasmas even if the material is an electrical insulator. The magnetron effect consists of confining the free electrons on the surface of the target in a magnetic field in order to increase the ionization efficiency [5].

3.1.3. Laser ablation deposition:

Pulsed Laser Deposition (PLD) is a depot technique that uses pulsed laser beam. The beam is focused on a target placed in an ultra-vacuum enclosure. The laser pulses allow the vaporization of materials in the form of plasma. The plume of material thus ejected perpendicularly to the target is condensed on a substrate placed opposite to form a coating. The benefits of PLD are multiple. It is a laboratory process for depositing a multitude of materials ranging from semiconductors to polymer materials [5].

3.2. Chemical deposition:

Two categories of chemical deposits are considered according to whether or not they are supported by plasma.

3.2.1. Non-assisted procedure:

This process makes it possible to produce deposits on a heated substrate, from the decomposition of gaseous precursors, most often hydrocarbons, hydrides but also fluorides, chlorides, bromides, iodides and organometallics. The thickness of deposits can range from micrometers to tens of millimeters with deposition rates ranging from a few micrometers to several tens of micrometers per hour. The deposited materials are dense, close to the theoretical density of the diamond, they are very adherent on the substrates, and can cover parts of complex shapes with a good homogeneity in thickness. The granular structure and the crystallographic growth orientation can be controlled. This technique, however, has a major disadvantage, the temperature limit that can support the substrate. This temperature is generally included, depending on the materials to be deposited, between 500 ° C and 2000 ° C [5].

3.2.2. Plasma assisted process:

The plasma-assisted chemical process, Plasma Enhanced Chemical Vapor Deposition (PECVD) or Plasma Assisted Chemical Vapor Deposition (PACVD), is a technique that allows for the production of deposits from gaseous precursors and chemical reactions assisted by an electric discharge, by means of an electric arc (thermal plasma) or a radio-frequency alternating discharge (cold plasma).

The main advantage of the PECVD process over the unassisted process is the possibility of depositing layers on substrates which are maintained at temperatures below <300 ° C. The main limitation of the PECVD process is the difficulty of depositing pure materials and the interaction of the plasma with the substrates which can possibly lead to heterogeneities on parts of complex geometry.

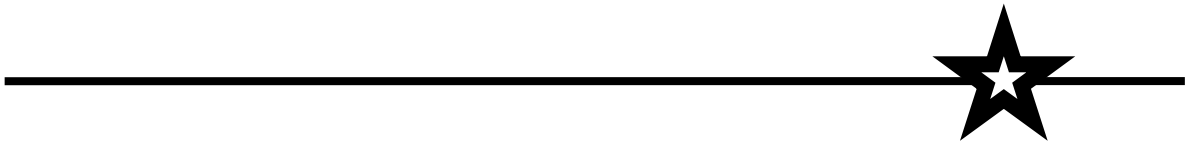
To finish this description a comparison of the different techniques of elaboration of hybrid materials is given in Table 1.3 [5].

Table 1.3: Comparison of Techniques Used to Develop Hybrid Layers.

Technical	Characteristics
Laser ablation	-Very expensive equipment, -Very low deposition rate, -possibility of depositing a large variety of even complex compounds while preserving stoichiometry.
Cathodic spraying	-Relatively low deposition rate complex structure of deposits, -production of thin and dense layers, limited surfaces.
Cathode sputtering in reactive condition	-Quite high deposition rate, -same characteristics as sputtering
CVD (Chemical Vapor Deposition) or sol-gel.	Expensive equipment, very low deposition rate, production of high quality thin films, vacuum control, simple structure deposition.
Ionic deposition	Deposit rate quite high, obtaining very adherent layers, having a good covering power and having a low porosity. The mechanisms involved are not clearly known and this technique is difficult to implement.

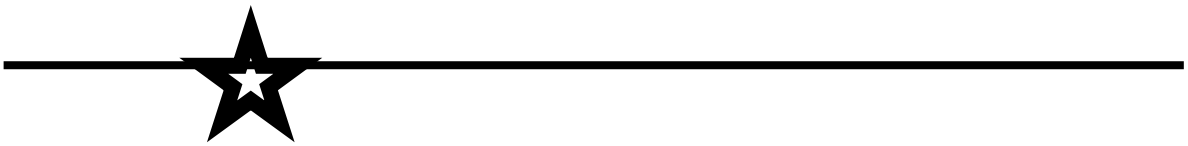
4. Conclusion:

- Depending on the nature of the bonding between the organic and inorganic phases, two classes of organic– inorganic hybrids have been defined.
- At this first part of the first chapter consisted in setting out generalities on the chemistry of the material, the methods of its elaboration.
- In order to choose the best method for developing the hybrid film, a comparison of the methods of preparation has been made.



Part-2-

Characteristics and applications of hybrid polymers



1. Introduction:

There is almost no limit to the combinations of inorganic and organic components in the formation of hybrid materials. Therefore, materials with novel composition–property relationships, that have not yet been possible, can be generated. Because of the plethora of possible combinations, this introductory chapter can only present some selected examples. Many of the resulting hybrid materials properties and applications depends of the precursors properties and the reader is therefore referred to the following chapter.

Organic–inorganic (O–I) hybrid materials are covering a large range of materials from oxides (ceramics) to polymers depending on the organic–inorganic ratio. Due to the easy tuning of the initial organic inorganic composition, the chemistry and the processing conditions, a continuous evolution of the mechanical properties is expected despite the different modes of fracture and deformation observed for glasses and polymers. Depending on the composition, the hybrid materials present various mechanical behaviors and require specific techniques adapted for each class of materials (polymers or ceramics) [6].

2. Characteristics of hybrid materials:

The main aim of this part is to review the necessity to realize a complete study of the mechanical properties of O–I hybrid materials. Nevertheless, it is important to remember that the properties are strongly linked to the material's nanostructure. This is a point of paramount importance that will be developed in this Part 2.

2.1.Low deformations:

The main technique used to characterize the elastic behavior of bulk hybrid materials is the dynamic thermo mechanical analysis (DMTA) in various modes: tension or shear. Based on the principle of the conservation of the mechanical energy, this technique allows the measurement of the storage modulus E9 (in tension mode) or G9 (in shear mode) and the loss factor tand (corresponding to the dissipation of energy during solicitation) as a function of the temperature. Usually, the study of hybrid materials having a component constituted by polymer is performed by comparison with the corresponding neat polymer [6].

For each hybrid composition, the polymer main relaxation Tg, corresponding to the glass transition, is always expected to be observed. Its position and intensity allow characterizing of the reduction in mobility of the macromolecules. The results obtained from DMTA are generally complementary and in good agreement with those obtained by DSC (differential scanning calorimetric). The glass transition temperature Tg observed by DSC in hybrid materials corresponds to the glass transition of the organic domains. The glass transition temperature increases with the inorganic content while the apparent variation of heat capacity at T_g decreases [6].

By introducing an inorganic component in the polymer network, reinforcement is expected when the miscibility between the two components is promoted. Phase separation at the nanometer scale can be analyzed by using SAXS experiments which are very useful to get a better understanding of the mechanical behavior of hybrids. Consequently, when weak interactions are developed between the organic and inorganic components, an increase in T_g is frequently observed, corresponding to a loss in mobility of the macromolecules [6].

For hybrid materials mostly constituted by metallic oxide component, the observed behavior is due to the relaxation of the polymer phase and in relation with the interactions with the inorganic phase. Because the relaxations due to the inorganic components occur at higher temperatures they cannot be observed without the degradation of the polymer. Usually, materials mostly constituted by metallic oxide present interesting mechanical properties due to the strong interactions developed between the continuous metal ox phase (contributing to the strength of the material) and the flexible polymer phase (providing more toughness to the oxide network) [6].

2.2. Fracture behavior:

The most classical tests used to characterize the elastic–plastic and fracture behavior of hybrid materials are those already used for polymers and ceramics: uniaxial tests (tension, compression) or flexural tests (three or four points) to determine the elastic modulus and the ultimate properties.

Nevertheless, these latter properties are strongly dependent on the O–I composition and the separation in polymer-rich and doxide-rich hybrid materials is necessary [6].

2.2.1. Hybrid materials with high organic polymer content:

Elastic properties of a polymer-rich hybrid material are governed by the properties of the polymer. It is often measured by tensile or compression tests. In the glassy state, reinforcement is only slightly dependent on the oxide content (below 20 wt% of inorganic component). But in the rubbery state, the presence of inorganic fillers has a great influence on the elastic modulus by increase or decrease.

For low inorganic content (15 wt %), the behavior of hybrids is generally the same as the neat organic polymer but with a higher elongation aptitude. By increasing the filler content, the material becomes more and more brittle and the yield stress of the polymer increases at the same time.

The fracture properties of hybrid materials and the modification of mechanical behaviors' are in relation with the nanostructure of the inorganic phase (composition and size).

The total work for fracture per ligament unit is a linear function of the ligament. At any given temperature, the enhancement of fracture toughness is relative to the silica content and accompanied by an increase in modulus and yield stress. The essential work increases linearly with temperature, more especially when silica particles are present. [6]

2.2.2. Hybrid materials with high inorganic content:

The mechanical properties of a nanocomposite mostly composed of polymers depend essentially on those of the polymeric phase whereas the properties of material with a high inorganic content present tunable behaviors between plastic and brittle behaviors.

These behaviors prevent direct comparison between the properties of the hybrid and those of the polymer. Indeed, these materials present different fracture modes. A change in behavior is expected to be observed when raising the inorganic content in the hybrid material. Under elevated load, two distinct behaviors are expected:

- *Brittle behavior:*

The mechanical properties of these hybrids can be compared to those of inorganic xerogels or aerogels.

The high porosity, a consequence of an incomplete condensationof the alkoxides, induces low elastic modulus and toughness.

The impregnation of the oxide network by a polymer solution or the simultaneous inorganic and organic polymerizations contribute to the improvement of the mechanical responses.

➢ *Plastic behavior:*

The polysiloxanes are inorganic polymers with elastomeric behavior. Whereas the usual plastics cannot stretch or deform easily, the main quality of an elastomeric is its high elastic elongation. Consequently, the uniaxial tests are used to determine the tensile modulus but also the toughness from the stress–strain (s–e) curves.

Toughness can be obtained from the measurement of the area underneath the s–e curve that represents the energy a sample can absorb before breaking. The ideal material should be strong and tough, bend instead of breaking. By designing composites with elastomers, toughness is partially lost in order to get a stronger material. The efficient reinforcement of elastomers is commonly obtained by generating in situ some metal oxide based particles (by sol–gel process), which would act as cross-linking agents bonded to the PDMS elastomers via M–O–Si bonds.

The molecular weight of the PDMS influences directly the morphology of the final material and particularly the size of the domains which undergo elastic deformation [6].

2.3.Hardness:

An important mechanical parameter has to be considered to complete the characterization of the materials: the hardness H, which can be related to wear resistance and consequently is fundamental for many applications. The hardness of a material is commonly determined by an indentation test: pencil test or by the measurement of the residual indent after the loading and unloading a pyramidal indenter [6].

2.4.Mechanical properties of organic–inorganic hybrid films:

We shall focus in the following section on class II hybrid materials:

2.4.1. Sol–gel silicas modified by hydrophobic –CH_3 groups:

The substrate influences on the elastic modulus and hardness measurements also the sensitivity of indentation techniques towards the concentration gradient.

The organic group for these materials is only a methyl –CH3 group. Without the polymer group, a brittle behaviour was reported. An extensive survey of the response as a function of coating thickness was made. A drastic increase of hardness

as a function of penetration depth was reported for the thinnest coatings (0.5 mm) while the hardness response was almost a plateau for the 4 mm thick film within the investigated range.

Interestingly, as expected, elastic response is affected by the substrate in the same range of indenter penetration. Under elevated load the thinnest films showed only delamination and chipping while the thickest films show first radial cracks that were followed by delaminating and chipping [6].

2.4.2. Epoxy-modified silica hybrid materials:

These hybrids were formed from silica nanoparticles or precursors obtained by hydrolysis–condensation of silicon or transition metal alkoxides and glycidoxypropyltrimethoxysilane (Glymo) as coupling agent. The epoxy function can be maintained to modify the hybrid network or polymerized when reactions with amines are carried out, then it will contribute to the formation of the network. Hardness testing showed variation of modulus and hardness as a function of the composition [6].

2.4.3. (Meth)acrylate modified silica hybrid materials:

All the resulting films were transparent. Moreover, nanoindentation tool was shown to yield elastic modulus and hardness data with good reliability. As expected thickness of the film, filler content and chemical composition are shown to influence the mechanical response [6].

3. Applications of hybrid organic-inorganic membranes:

Hybrid polymers represent a highly emerging class of multifunctional materials that are expected to be relevant for advanced applications such as:

- Coating against corrosion
- Medicinally important compounds that target diseases as cancer
- Micropollutant purifiers: to purify sea water.
- Selective systems of metals extraction
- Electrical and Optical Materials
- Domestic application concerns a novel inhibitor composition using to protect the metal, removing of scale deposits in boilers, in cooling water systems or in closed water loop fountains.
- Glasses self watching etc.

Since the 1990s, many groups have been working on the development of high-quality class II hybrid organic-inorganic membranes for a variety of applications. All synthesis routes described in the previous sections have been utilized with a multitude of organic functional groups on different inorganic membranes. The hybrid organic-inorganic membranes obtained showed a clear enhancement of the performance in the applications of interest, as described below. In each case, they combine the high thermal, chemical and mechanical stability of the inorganic membranes with the surface or structural functionality of the incorporated organic groups. They owe their ameliorated properties to the combination of the advantages of both of the organic and inorganic assets. Compared to the purely inorganic, non-hybrid versions of the membranes, they can profit from a changed surface affinity, an altered surface charge, and/or an adjusted microstructure, such as a decreased pore size [6].

The sections below give an overview of the literature on membrane applications in which the use of hybrid organic-inorganic membranes has proven advantageous:

3.1.Reduction of membrane fouling:

Organic modification has been applied to reduce the fouling of the intrinsically hydrophilic native inorganic membranes. It was concluded that the organic membrane modification efficiently mitigated flux decline during filtration. Similar positive anti-fouling effects were also found when grafting with perfluoroalkylsilanes.

Also in water filtration, grafting has recently been explored as a way to sustainable fouling mitigation.

In this study, fouling reduction of commercially available Titania nanofiltration membranes has been envisaged; compared to the intrinsically more hydrophobic polymeric nanofiltration membranes, the. The best performing membrane remained un fouled (no irreversible fouling) in a wide variety of studied fouling conditions, including pulp and paper effluent streams, and olive oil waste waters. Moreover, in olive oil waste water filtration it shows not only superior flux. In filtration of real surface water, the retention of humics was similarly high for both grafted and un grafted nanofiltration membranes [6].

3.2.Pressure-driven water filtration:

Back in 1995, the grafting of butyl phosphonic acid to decrease the charge of the membrane and thus the adsorption of proteins such as BSA (Bovine Serum Albumin). This leads to an extensive increase of the protein retention in ultrafiltration from 48 to > 99%. However, the grafted Titania UF membrane was strongly hydrophobic, and required pre-wetting with an ethanol-water mixture before use. The resulting process flux of the hybrid membrane was about of factor of 2 lower than that of the unmodified Titania membrane.

More recently, grafting of ceramic tight UF membranes (5 and 10 nm γ-alumina membranes) was applied to increase their heavy metal ion removal performance. In particular, the low-cost biopolymer alginate, which has high heavy metal adsorption capacity, was grafted.

Another example of pressure-driven water filtration is reverse osmosis (RO), which is a widely used technique to produce high-purity water, e.g. to make drinking water from seawater. Large-scale RO is currently carried out with polymeric membranes.

Recently, grafting of organic groups has also been applied to reduce fouling of membranes in pressure-driven filtrations involving water. As the application aim is essentially different from improving the intrinsic separation properties of the membrane, this will be described in a separate section below [6].

3.3.Membrane contactor applications :

Membrane contactor applications typically require macroporous membranes (for high flux) that are non-wetted by the mainly aqueous liquid feed. Moreover, for easy operation, wetting should be avoided also at a transmembrane pressure of a few bars [6].

3.4.Organic solvent nanofiltration:

Modification of tight mesoporous membranes in order to specifically enhance their flux performance in apolar solvent filtration was first studied in this century using post-synthesis organosilane grafting (silanation).

From this research it is clear that for a correct modification inside the small mesopores, it is important to carefully choose the size and amount of reactive groups of the organosilanes. The studies mentioned, hydrophobization of the inner membrane

surface by the organoschlorosilane grafting was shown, most clearly by the enhanced permeation of apolar solvents as hexane, or toluene.

The hydrophobic nature of a silanated membrane leads to solvent transport that fits viscous flow behavior: the fluxes of all solvents vary according to their viscosities so that viscosity times flux is a constant, independent of the solvent. The results to those of fully inorganic silica where compared to the Titania membranes. The hydrophilic inorganic membranes showed a drastic flux decline for hexane during the first minutes of filtration. This loss of permeability was attributed to the presence of trace amounts of water in hexane, adsorbing onto the hydrophilic pore surface [6].

3.5.Hydrophilic pervaporation:

Of notable relevance is the substantial hydrothermal stability of HybSi membranes. While silica membranes show high performance as dehydrating pervaporation membranes, long-term exposure to water leads to pore size changes even at temperatures as low as ~70°C. Consequent permeability and selectivity changes result insubstantial decrease of the pervaporation performance. While methylated silica, prepared by in-situ incorporation of pendant methyl groups, was shown to have improved stability up to 95°C for more than 1 year, higher temperatures similarly led to a fast decline in selectivity. Considering that many dewatering applications require substantially higher operation temperatures, the development of organically bridged silica, or HybSi®, membranes that showed stability up to at least 150°C for several years raised new interest in inorganic membranes for pervaporation [6].

3.6.Organophilic pervaporation:

As organic modification of inorganic membranes typically changes the polarity of the membranes from intrinsically hydrophilic to more hydrophobic, different groups have studied the possibility to change the pervaporation (or vapor permeation) behavior of microporous metal oxide membranes. The objective was to obtain membranes that preferentially permeate the more apolar component of a solvent mixture, altering the typical dehydration behavior of the native microporous metal oxide membranes.

Selective pervaporation of organic compounds can also be carried out with inorganic silica-based membranes by incorporation of pendant groups using sol-gel dip-coating methods [6].

3.7.Gas separation:

The first incentive for creating hybrid organic-inorganic membranes was an increase in the gas separation performance of existing mesoporous metal oxide or glass. Grafting introduced gas transport mechanisms other than the low-selective Knudsen diffusion of the mesoporous supports. Both silanation and phosphonic acid grafting using primarily apolar long alkyl or perfluoroalkyl groups were applied for this purpose. Depending on the groups grafted, surface diffusion or solubility of a particular gas could be enhanced. The research in the 1990s resulted in an only modest selectivity increase.

Permeability (P) is the ability of a molecule to pass through a solid medium (i.e. polymer). Permeability is the measurement over time of the quantity of a species that crosses through a polymer film subjected to a difference in concentration of the species considered [5].

The first law of Fick is the most commonly used equation to describe the transport of a gas through a polymer film in the ideal case (simple and non-plasticizing gases). The specific flow J of the permeating gas is equal to:

$$J = -D\left(\frac{\partial C}{\partial x}\right) \quad \text{..... (1)}$$

With D: the diffusion coefficient (or diffusivity) of the gas ($m^2.s^{-1}$); C: the concentration of gas in the membrane ($mol.m^{-3}$) and x: the thickness of the film (m)

If we consider a linear relationship between the gas pressure and its concentration at the interface (Henry's Law), the following equation applies:

$$P = S * C \quad \text{..... (2)}$$

With S: solubility of the gas in the polymer film ($mol.m^{-3}.Pa^{-1}$)

P: gas pressure in the polymer film (Pa)

Assuming that S and D are independent of gas concentration, the integration of the law of Fick over the entire thickness of the polymer film gives the expression of the specific flow of gas J through the film:

$$J = D * S\frac{\Delta P}{\mathrm{d}} \quad \text{..... (3)}$$

The capacity of a film to transport a gas is described by the permeability coefficient Pe defined by:

$$Pe = D * S = \frac{Qte\ permeant\ *Thickness\ film}{Area\ film * Time * \Delta P_{\text{permeant}}^{x/y}} \quad \text{..... (4)}$$

And x/y = upstream / downstream.

P_e is expressed in $mol.m^{-1}.s^{-1}.Pa^{-1}$. However according to the applications of many other units are used.

The coefficient of permeability P_e is an intrinsic property of the polymeric material. It is independent of film thickness and upstream / downstream pressure difference (driving force).

The diffusion coefficient D (in $m^2.s^{-1}$) is the kinetic parameter of global transport. As we have seen, it describes the mobility of the penetrant in the membrane and depends mainly the size of the penetrant molecule, movements of the segments of polymer chains and free volume thereof [5].

The solubility coefficient S is the thermodynamic magnitude of the overall transport. He represents the amount of dissolved gas molecules in the membrane under the conditions balance. It is related to the gas / polymer interactions and the free volume of the membrane [5].

The coefficient of permeability P_e generally follows the Arrhenius law:

$$P_e = P_0 exp^{(\frac{-Ep)}{RT}} \quad \text{..... (5)}$$

With P_0: pre-exponential permeability factor equal to $D_0.S$ ($mol.m^{-1}.s^{-1}.Pa^{-1}$)

E_p: activation energy of global transport.

A: The perfect gas constant ($J \cdot mol^{-1} \cdot K^{-1}$)

Several other quantities are also used to characterize the passage of gas through a movie:

- Permeation rate: This is the coefficient of permeability without take into account the difference in pressure:

$$\text{Permeation rate} = \frac{\text{Permeant } \textit{quantity} * \text{Thickness film}}{\text{Area .Time}} \quad \text{..... (6)}$$

- Permeation: This is the coefficient of permeability regardless of the thickness of the movie. When the thickness of the film is unknown, we prefer to use permeance rather that permeability:

$$permeance = \frac{Qte\ permeant * Thickness\ film}{Area\ film * Time * \Delta P^{x/y}_{permeant}} \quad \text{..... (7)}$$

- The gas flow varies with thickness and pressure. It is inversely proportional to thickness.
- The influence of the nature of the permeating gas, the structure of the polymer, and the temperature on the permeability of a film is a result of the coupled influence of these parameters on D and S. Table 2.1 summarizes the generally observed effect of both protagonists of transport, gas and polymer, and temperature on D, S, and P_e.

Table 2.1: Influence of the gas / polymer system and temperature on D, S, and P_e

Influencing parameter	Effect on D	Effect on S	Effect on Pe
Gas size	- -	+	-
Condensability of the gas	0	+	+
Curing	-	0	-
crystallinity	-	-	-
Flexibility of the chains	+	0	+
Temperature	++	-	+

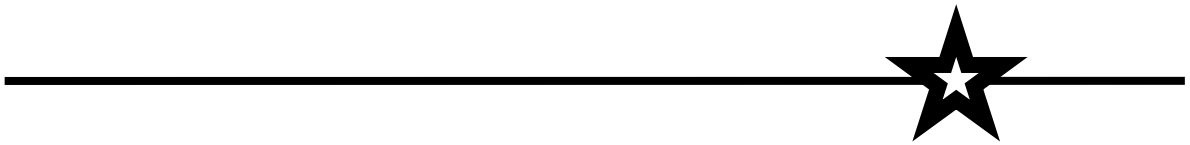
(-) no efficient influence of the parameter.

(+) efficient influence of the parameter.

The permeability of the polymers to different gases generally ranks, depending on the nature of the permeant, in an order that is only slightly influenced by the chemical nature of the material. In other words, there are two categories of gas: fast gases and slow gases. The first category gathers, on the one hand, the gases which have a high mobility (i.e He and H_2), and on the other hand, the gases whose polar character makes them soluble in polymers. The category of slow gases concerns gases that are both poorly soluble and not very mobile, it generally includes molecules that are devoid of dipole moment and have a diameter greater than 3 Å: O_2, N_2, CH_4 gases and most of the polyatomic molecules are part of this category [5].

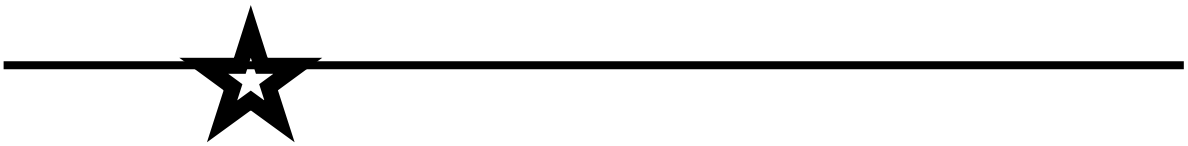
4. Conclusion:

- The development of hybrid membranes and their use in separation applications have evolved strongly in the last decade. This opens new opportunities to replace current energy-intensive separation processes or convert them into hybrid processes.
- The resulting hybrid materials are very interesting model compounds to establish an accurate relation between the microstructure of the hybrid material and their mechanical properties.
- The microstructure of O–I hybrid materials depends not only on the nature of the organic and inorganic components but also on the synthesis procedure.



Part-3-

Synthesis of hybrid polymers



1. Introduction:

The 'hybrid membranes' encompass a very wide range of materials that needs a more detailed description. Membranes can be mainly polymeric with embedded inorganic nanoparticles, ceramic with an organic phase grafted onto the surface, or even consisting of a network structure with both organic and inorganic moieties built-in. The difference between these classes of membranes is very large with respect to the membranes synthesis, properties and behavior. Also, the structure of the support system can be very different, ranging from intrinsically asymmetric in several polymeric systems, or asymmetrically built up of different layers in ceramic ones. It is therefore important to clearly stipulate the dominant phase of the membrane being inorganic-organic or organic-inorganic hybrid materials in which the last word stipulates the dominant phase [7].

Inorganic-organic hybrid membranes are widely applied and combine the benefits of both inorganic and organic phases. However, the dominant phase in these membranes is organic and their preparation is very different from those of the organic-inorganic materials. Therefore, in this review, we will describe only hybrid membranes made from organic and inorganic and belonging to class II hybrid [7].

2. Synthesis methodologies of hybrid organic-inorganic membranes:

Organic-inorganic hybrid membranes are obtained through (1) sol-gel process; (2) self-assembly process; (3) assembling or dispersion of nanobuilding blocks; (4) hierarchical structures and (5) interpenetrating networks.

2.1. *Sol-Gel Process:*

In 1846, Ebelmanl and Graham reported that the hydrolysis of tetraethylorthosilicate (TEOS) as shown in (fig 3.1) [8]. Under acidic conditions produced SiO_2 in the form of fibers.

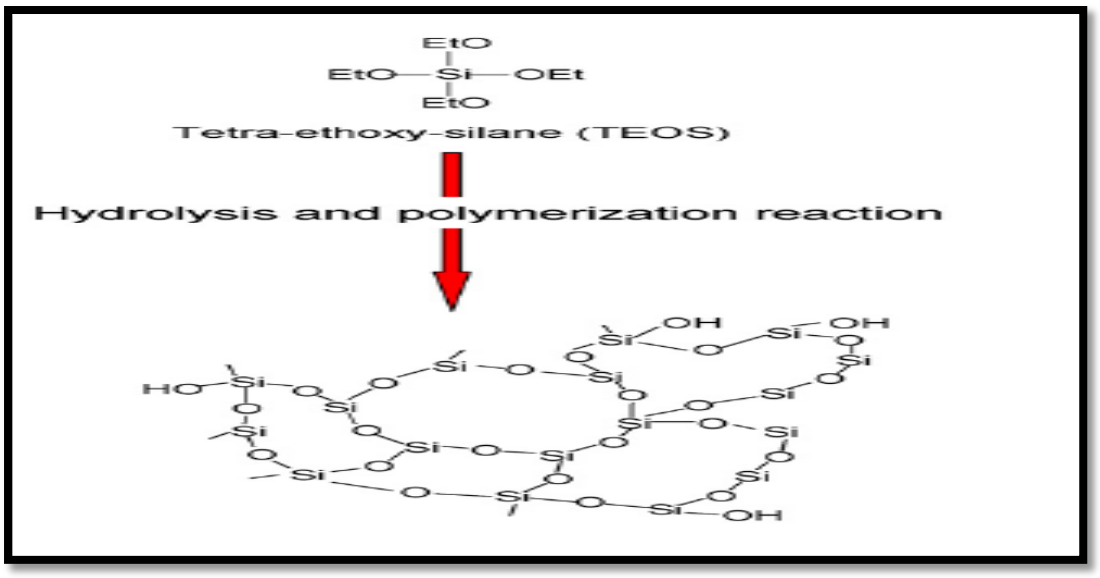


Fig 3.1: hydrolisation of TEOS.

In 1950s, a number of phenylsilsesquioxane-alkylsilsesquioxane copolymers that were the first successful commercial organic-inorganic hybrid polymers. The sol-gel process is a cheap and low-temperature method for producing transparent and homogenous solid materials with high purity from small molecules and for controlling the chemical composition of products. Compounds produced by the sol-gel process have many applications in super hydrophobic surfaces (shown in fig 3.2), electrolyte, biosensors, corrosion protection, etc [7].

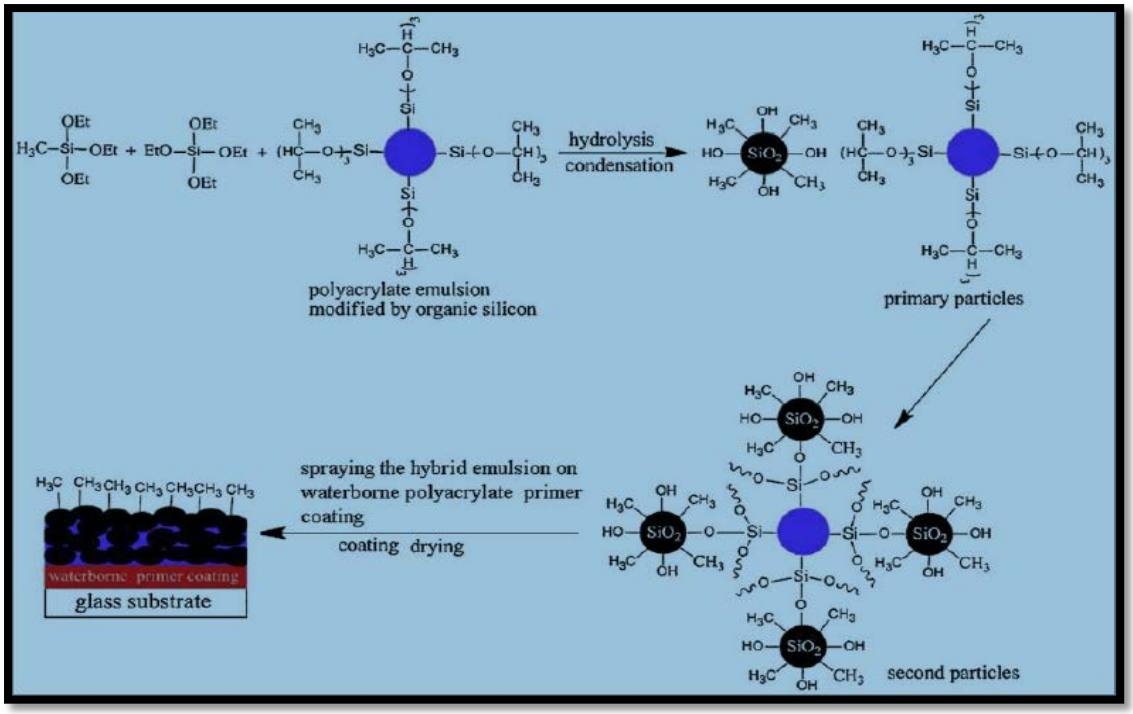


Fig 3.2: Schematic super hydrophobic surfaces prepared through the sol-gel derived organic-inorganic hybrid emulsion.

This process is carried out in water and organic solvents and its precursors are usually metal halides (in organic solvents) and metal alkoxides such as $Si(OR)_4$, $SiR'(OR)_3$, $Ti(OR)_4$, etc. As seen in (fig 3.3), these materials are subject to a series of hydrolysis (or non-hydrolytic process in organic solvents) and condensation reactions that through nucleophilic substitution mechanisms result in sol formation [7].

Sol is a colloidal solution in which individual particles interact weakly with each other and due to cross-linking reactions, converts into an integrated network (wet gel). This structure with further drying processes converts to gel.

In spite of silicon alkoxides, hydrolysis reactions of other metal alkoxides in water are too fast. The hydrolysis reaction of silicon alkoxides is typically acid-or base-catalyzed. Silica networks formed under acid-catalyzed conditions are dense and those of formed in the presence of base are porous and loose [7].

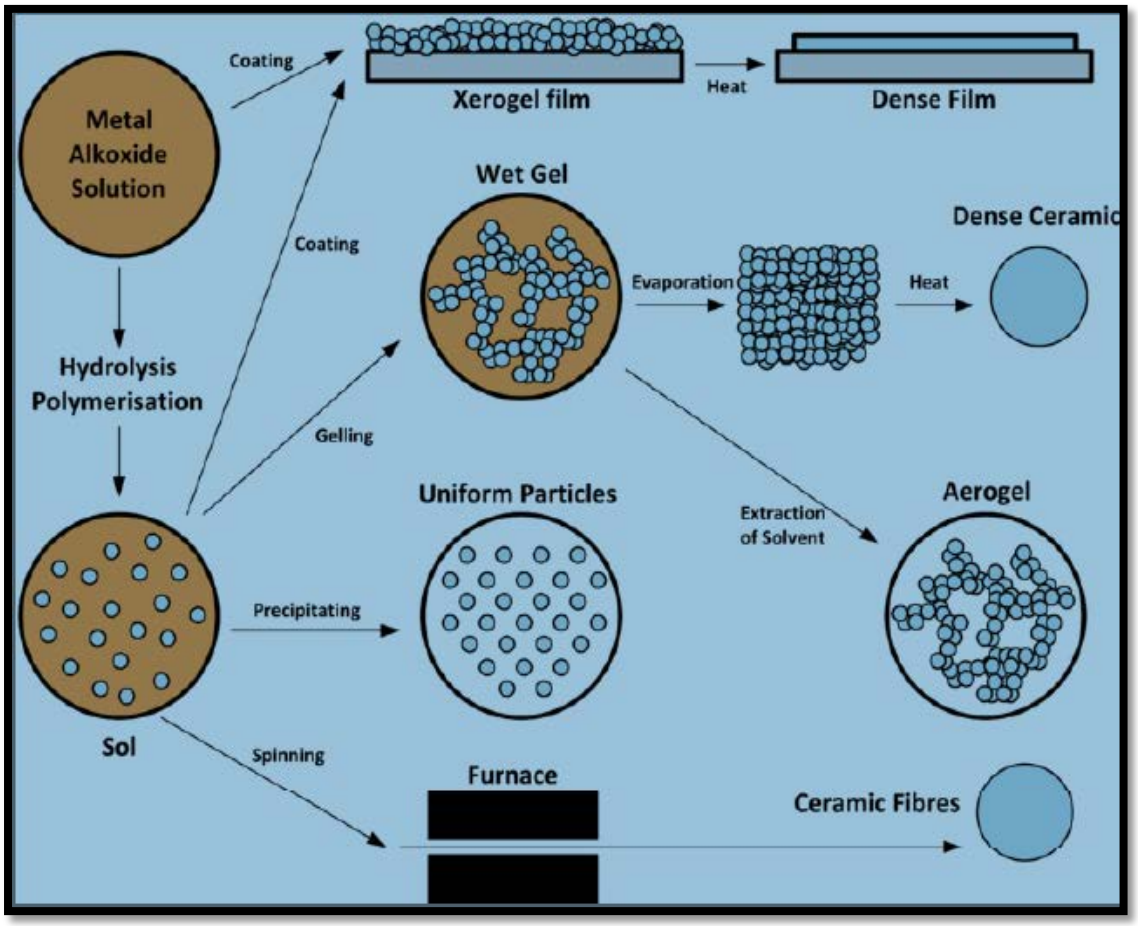


Fig 3.3: Description of technologies and products of the sol-gel process.

A suitable way for modifications of properties of materials obtained from this method is the introduction of organic groups (R) into their structure. For example, the Si–C bond does not hydrolyze in most sol-gel processes and organic groups can be incorporated covalently into the network of inorganic gel using silsesquioxanes [$(\boldsymbol{R-Si_{1.5}})_{\boldsymbol{n}}$(*n* = even number)], such as $\boldsymbol{R'(OR)_2Si-R-Si(OR)_3}$Compounds or derivatives of tetrafunctional silicon alkoxide [organically modified silicates (ORMOSILs)], such as TEOS,$\boldsymbol{R'Si(OR)_3}$, *etc* [7].

If an organic group remains stable and does not hydrolyze during sol-gel processes it is defined as a network modifier. On the other hand, if it can react with other monomers or with itself (e.g., –CH=CH2) it is named as a network builder.

Moreover, if it is a reactive functional group, such as $–NH_2$, it is specified as a network functionalizer (fig 3.4). These materials belong to class II interactions of organic-inorganic hybrid polymers [7].

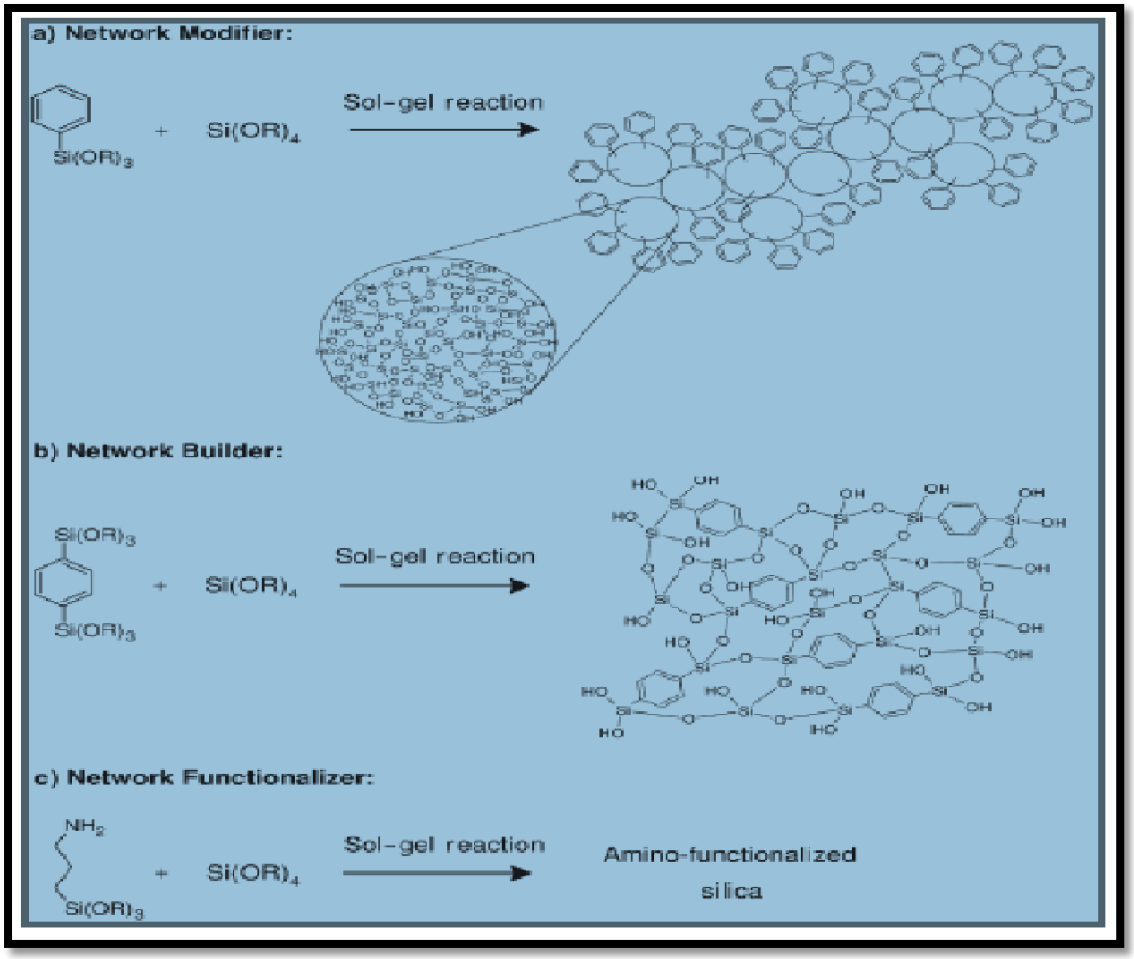


Fig 3.4: Organically functionalized trialkoxysilanes,$\boldsymbol{R'Si(OR)_3}$, used as (a) modifier; (b) builder and (c) functionalizer of silica-based network through the sol-gel process.

Another example of using sol-gel processes is the synthesis of microporous zeolites (or molecular sieves); for example see the (fig 3.5) [9]. These materials are framework aluminosilicate and have a three-dimensional structure with high internal surface area and an ordered crystalline structure. Zeolites with high silica contents are synthesized in the presence of bulky organic alkylammonium cations known as structure-directing agents or templates.

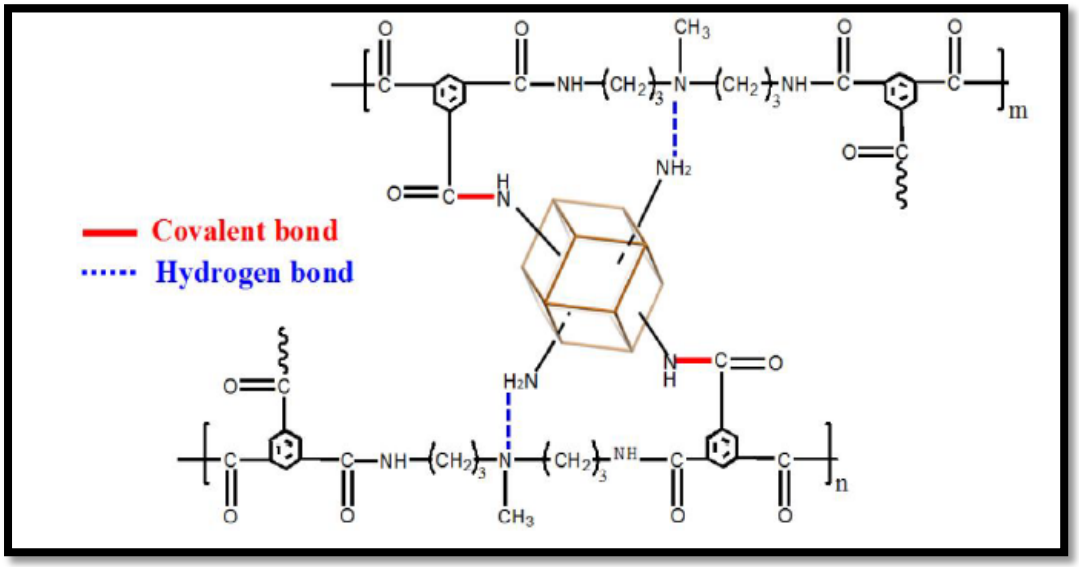


Fig 3.5: Schematic illustration of covalent bonds and hydrogen bonds between NH2-ZIF-8 and PA.

Next figure (fig 3.6) represents Fundamental reaction steps in the sol–gel process based on tetrialkoxysilanes [2].

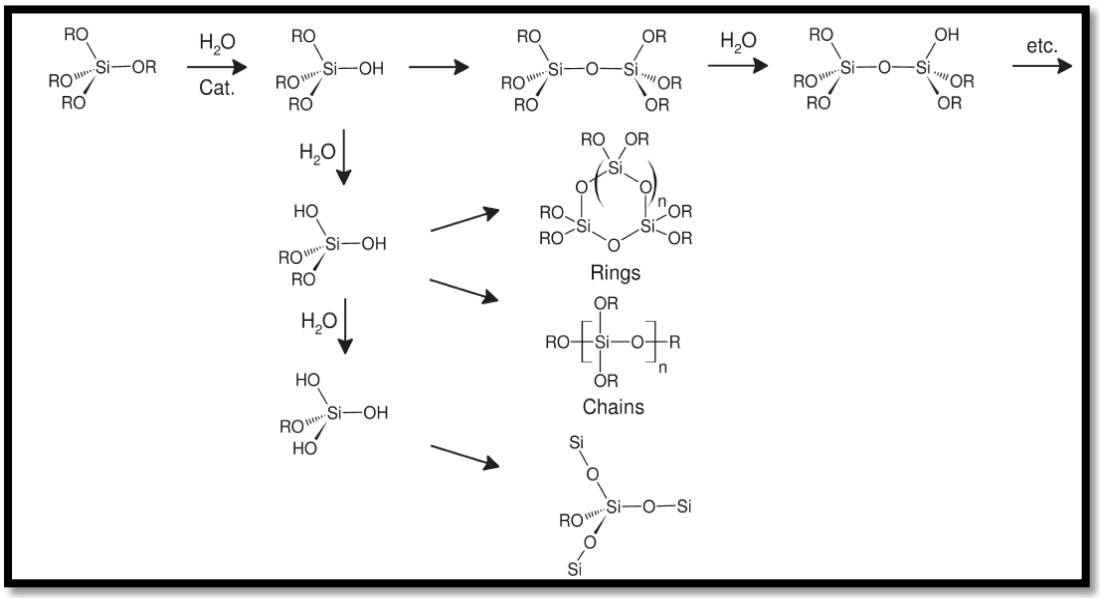


Fig 3.6: Fundamental reaction steps in the sol–gel process based on tetrialkoxysilanes.

2.2. Self-Assembly Process:

In 1992, researchers of Mobil Oil Company discovered a new type of mesoporous silicas, so-called M41S. M41S family includes hexagonal MCM–41, cubic MCM–48, and lamellar MCM–50(Fig 3.7). MCM is an abbreviation of "Mobil Crystalline Materials". Notwithstanding their amorphorous pore walls, these organic-inorganic hybrid compounds exhibit a long-range ordered array of uniform and controllable mesopores with sizes ranging between 2–10 nm. Mesostructure compounds have high specific surface areas (greater than 1000 m^2/g) and the pore size of these materials enables them to adsorb much larger molecules than is possible for zeolites. These compounds are used for catalysis, gas adsorption, *etc*. Other types of ordered mesoporous silicas are Santa Barbara Amorphous (SBA) (e.g., SBA–15), Michigan State University (MSU) (e.g., MSU–2), folded sheets mechanism (FSM) (e.g., FSM–16), *etc* [7].

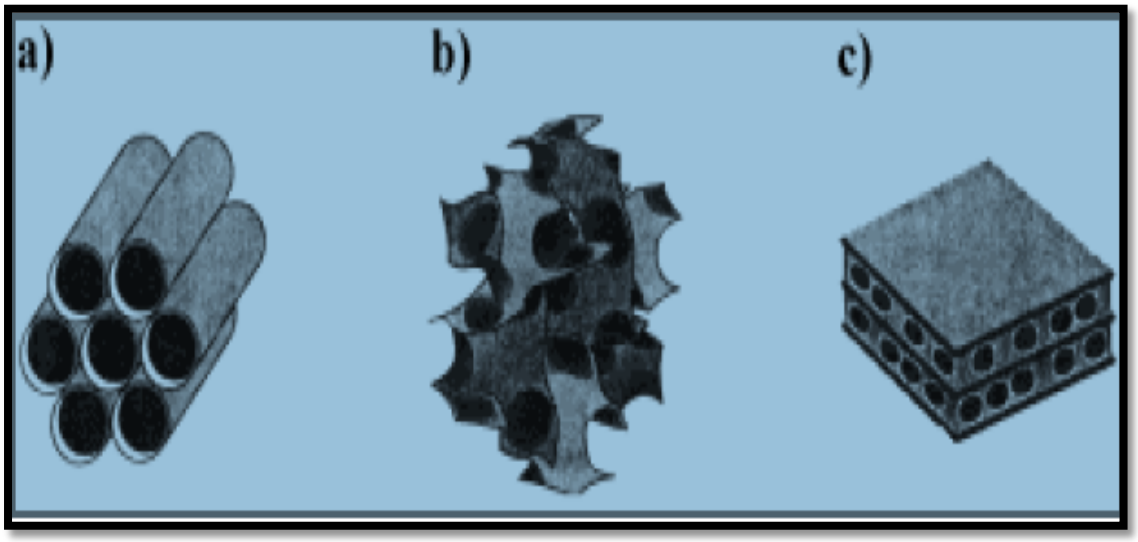


Fig 3.7: Representation of mesoporous M41S compounds including (a) MCM–41; (b) MCM–48 and (c) MCM–50.

In recent years, attempts of scientists resulted in syntheses of non-silica mesoporous metal oxides such as TiO_2, ZrO_2, Al_2O_3, Nb_2O_5, SnO_2, mixed oxides such as SiAl$O_{3.5}$, SiTiO_4, carbon nanocage, mesoporous carbon nitride, *etc*. The formation of mesoporous materials is depicted schematically in (Fig 3.8), based on "liquid crystal templating" mechanism. Even Through route (a): surfactant concentrations above its critical micelle concentration (CMC), or through route (b): surfactant concentrations below CMC [7].

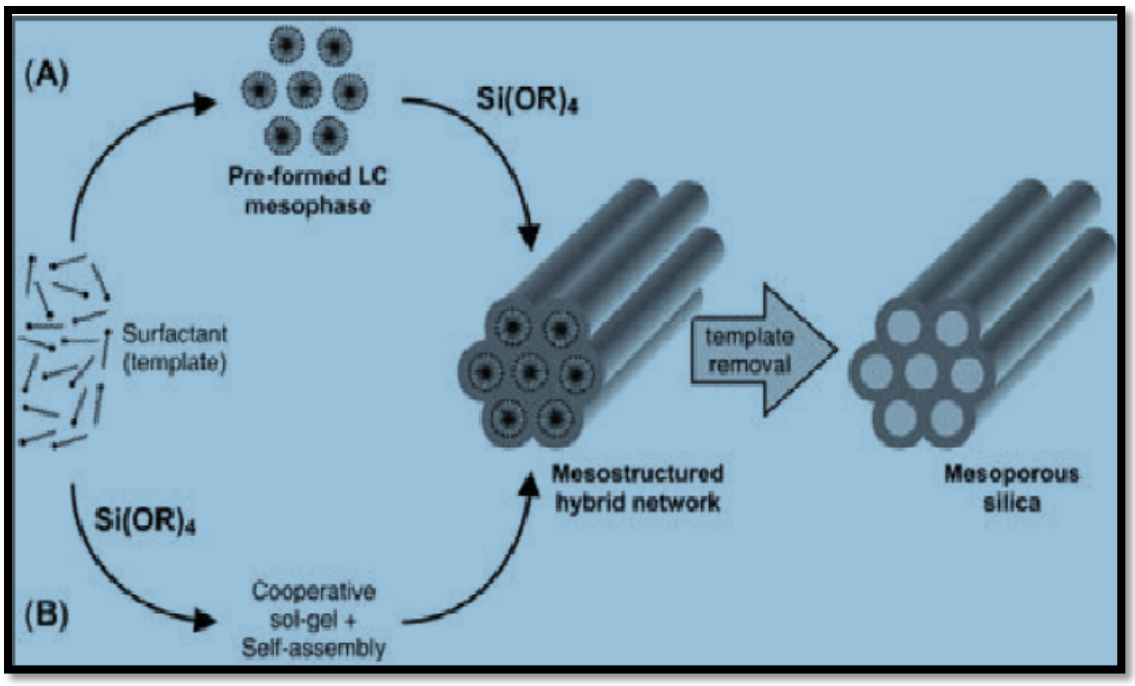


Fig 3.8: Synthesis of mesoporous compounds in the presence of template through (A) liquid-crystal template or (B) cooperative liquid-crystal mechanisms.

In recent years, mesoporous silicas have been used as supports for preparations of organic-inorganic hybrid polymers and have many applications in lasers, drug delivery, pollutant adsorption, *etc*. In these compounds, different organic functional groups are located on the robust, thermally stable and porous inorganic substrate [7].

As illustrated in (Fig 3.9), these organosilica compounds are prepared through (a) grafting or post-synthetic fictionalization; (b) co-condensation or one-pot synthesis and (c) synthesis of periodic mesoporous organosilicas (PMOs) [7].

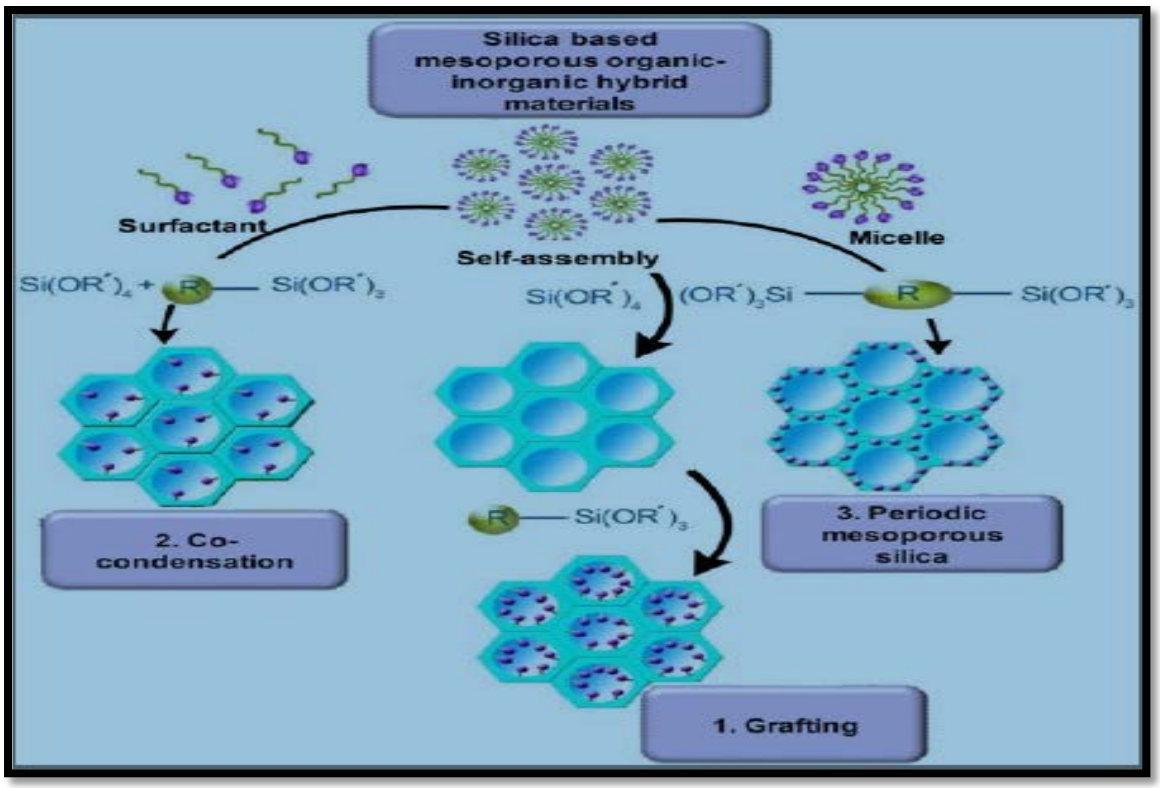


Fig 3.9: Different methods for the synthesis of organic-inorganic hybrid mesoporous silica: 1. Grafting, 2. Co-condensation or in situ grafting and 3. Synthesis periodic mesoporous organosilicas (PMOs).

2.3. Assembling or Dispersion of Nanobuilding Blocks (NBBs):

The interest in nanoscale materials originates from this fact that their properties are a function of their size, composition, and structural order. Here, a series of compounds called as nanobuilding blocks (NBBs) are used for preparing organic-inorganic hybrid polymers. NBBs are capped with polymerizable legands or connected through organic spacers, e.g., telechelic molecules or functional dendrites. These compounds maintain their integrity and fulfill certain (chemical or physical) functions in the final material. NBBs are classified as (1) clusters; (2) organically *in situ*- or post-functionalized nanoparticles; (3) layered compounds and (4) core-shell nanocompounds [7].

2.3.1. Clusters:

Metallic clusters (e.g., polyoxometalates) are an ensemble of bound atoms and contain a group of two or more metal atoms that bind together by direct Metal-Metal bonding. Clusters are connected either (1) by the polymerization of their ligands and are called cross-linked clusters or (2) by coordinative bonds between coordinating

groups of organic ligands (called as a linker or spacer) to each metal center (called as a connector) of clusters [7].

2.3.2. Organically in Situ- or Post-Functionalized Nanoparticles:

In this method reactive organic groups are bound to the surface of the inorganic moiety by strong ionic or covalent interactions. These organic groups are either grafted to preformed nanoparticles (called as post-functionalization) or are incorporated during the synthesis of nanoparticles (called as *in-situ*-functionalization) . This method is used for metal oxides (e.g., TiO_2), chalcogenides (e.g., CdSe), metallic nanoparticles (e.g., Au) and polyoxometalates (e.g., γ-[SiW10O36]8−), *etc* [7].

2.3.3. Layered Compounds:

To improve the physical properties of polymers, inorganic compounds physically are dispersed in them (as fillers) in various forms such as platelets, spheres, fibers, *etc*. If the size of discrete inorganic components is in the range of 1–100 nm, the resulted organic-inorganic compound is called a nanocomposite. Organic-inorganic hybrid nanocomposites are either as interpenetrating networks or layered inorganic components embedded into the organic matrix.

These compounds are incorporated in organic polymers as (a) a phase-separated structure in which the polymer cannot intercalate within the inorganic layers and the inorganic component is dispersed as aggregates or particles within the polymer matrix; (b) an intercalated structure in which one or more polymer chains are inserted into the galleries (space between layers) of inorganic components and subsequently increase the interlayer spacing and (c) an exfoliated structure in which the insertion of polymer chains between inorganic sheets delaminates the layered compound (Fig 3.10) [7].

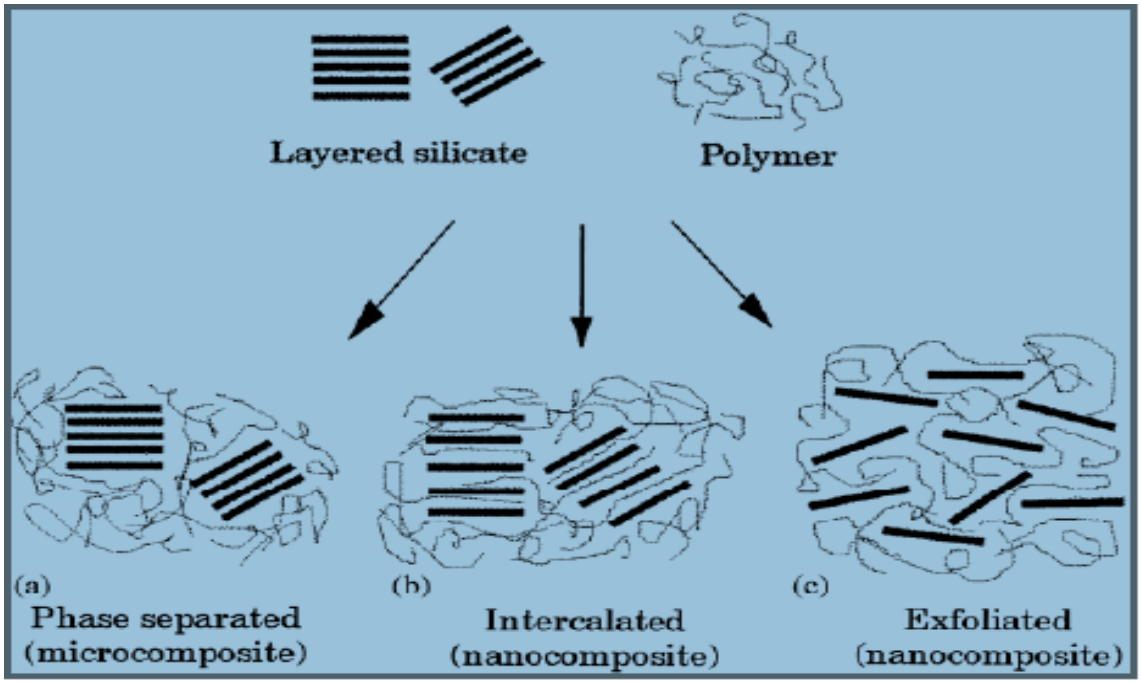


Fig 3.10: Schematic representation of different kinds of composites produced from interaction of layer compound with polymers: (a) phase separated; (b) intercalated and (c) exfoliated structures

2.3.4. Core-Shell Nanocomposites:

Core-shell nanocomposites (CSNs) consist of a core region covered by a shell domain (Fig 3.11). A series of CSNs are polymer-coated inorganic compounds. The encapsulation of an inorganic particles, in a polymer shell, are carried out through (1) the adsorption of monomers on the surface of the inorganic moiety followed by their polymerization in the adsorbed layer and (2) interaction of inorganic particles with preformed polymer as in situ growing inorganic components in a polymer matrix [7].

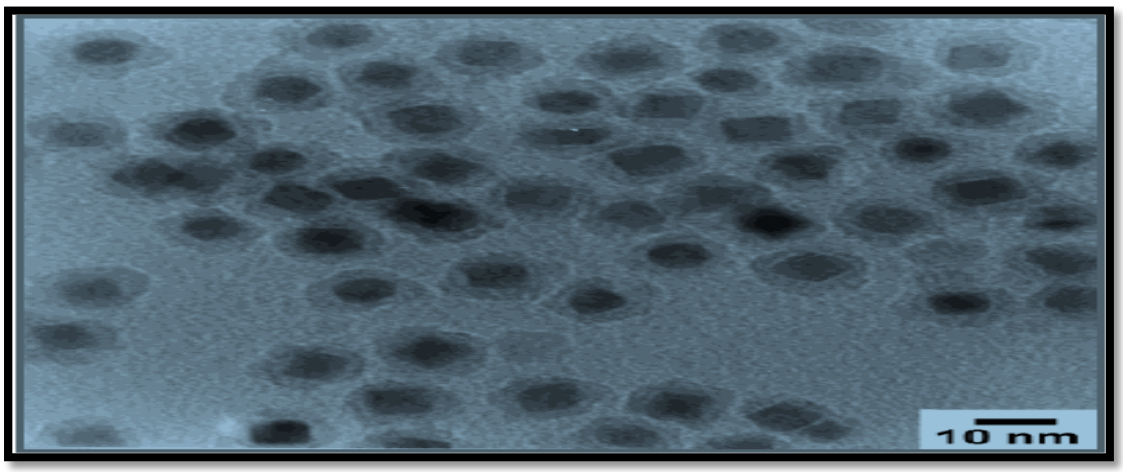


Fig 3.11: TEM of polystyrene-coated Fe_2O_3 particles. The polymer coatings are seen as a shell around the Fe_2O_3 cores.

2.4. Hierarchical Structures:

A hierarchy is a feature of self-assembly, where primary building blocks associate into more complex structures which are integrated into the next size level in the hierarchy. Self-assembly is emerging as an elegant, “bottom-up” method for the construction of nanostructured materials and is distinct from the template-directed assembly . The feature of an integrated chemical, biological, *etc*. system is the assembly of components into a specific architecture that performs a certain function. Many examples of hierarchical structural designs are seen in nature and are characteristic of many self-assembling biological structures (Fig 3.12) [7].

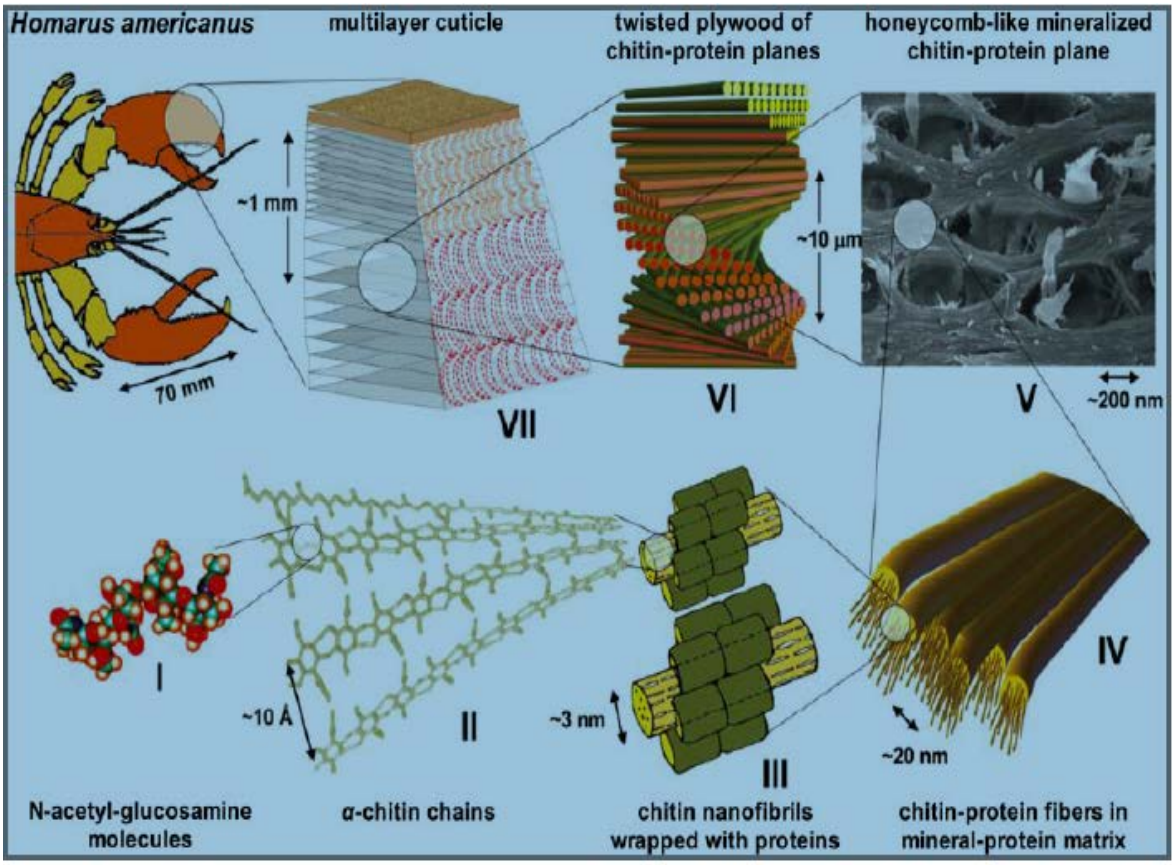


Fig 3.12: Hierarchical structure of lobster cuticle.

The hierarchically structured porous membranes, however, are highly interesting because their performance is not dependent on excessive water uptake WU. Table 3.1 presents characteristics and ion separation performances of some reported asymmetrical structured porous and dense membranes. We selected the membranes in Table 2 based on their morphology, composition, and superiority relative to the other reported membranes of the same category. (Follow) [10].

Table 3.1: Ion Exchange Capacity (IEC), water uptake (WU), proton diffusion coefficient (U_H^+), and separation factor of some reported membranes.

Membranes	Composition	Feature	IEC (mmolg -1)	WU (%)	$U_H^+(10^{-3}$ m $h^{-1})$	S
Hierarchical porous	-QPPO, SilicaIL,carboxylicacid	Zwetterionic Pores	1.98-2.39	65.76-131.9	21-38.6	33.9-62
	-QPPO, Silica IL, hydroxyl groups	Quaternized pores	2.2-2.49	66-158	20-27.3	38.8-86.5
Asymmetrical porous	-BPPO,multisilicon, quaternized amine, hydroxyl groups	Quaternized Pores	1.75–2.45	169-449	20–25	28.6–45.5
	-BPPO, quaternized Amine					
	-BPPO, Polyethyleneimine	quaternized thin layer	1.75–2.45	169-449	20-25	28.6-45.5
		Quaternized pores	0.51-1.43	171-336	9-43	46.6-73.8
Dense	DF-120 membrane	/	1.96	42	9	18.5
	PPO-SiO2	Quaternized Amines	1.7-2.2	16-30	1.5-9	23-30
	-QPPO-PVA, Silica	Quaternized amines and hydroxyl groups	1.2-1.9	51-220	21-45	25-39
	-PVA and glycidyltrimethyl Ammoniumchloride (EPTAC)	Quaternized amines and hydroxyl groups	0.58–1.15	160-270	11-18	18.5-21

Also, the hierarchy has resulted in the discovery of versatile nanoparticles with many applications, synthetic bone implants materials, mesostructured solid electrolytes, TiO2–graphene composite, *etc [10]*.

2.5. Interpenetrating Networks (IPNs):

IPNs comprise organic and inorganic networks that are microscopically phase-separated. However, they seem uniform macroscopically and there are weak interactions between moieties of IPNs (class I interactions). These components are partially interlaced and, upon separating IPNs, chemical bonds are broken. IPNs are synthesized by: Firstly the formation of a secondary network in a primary one (a sequential two-step process); secondly, the simultaneous formation of two networks and finally IPN components connect to each other through covalent bonds in which

the compound is named a dual organic-inorganic hybrid polymer (class II interactions) see (Fig 3.13). In the first method, IPNs are prepared by polymerization in a sol-gel network or sol-gel process in the presence of preformed polymers. In the third case, either bifunctional precursor are used or preformed inorganic or organic polymers are functionalized by the required functional groups for the formation of other types of networks [7].

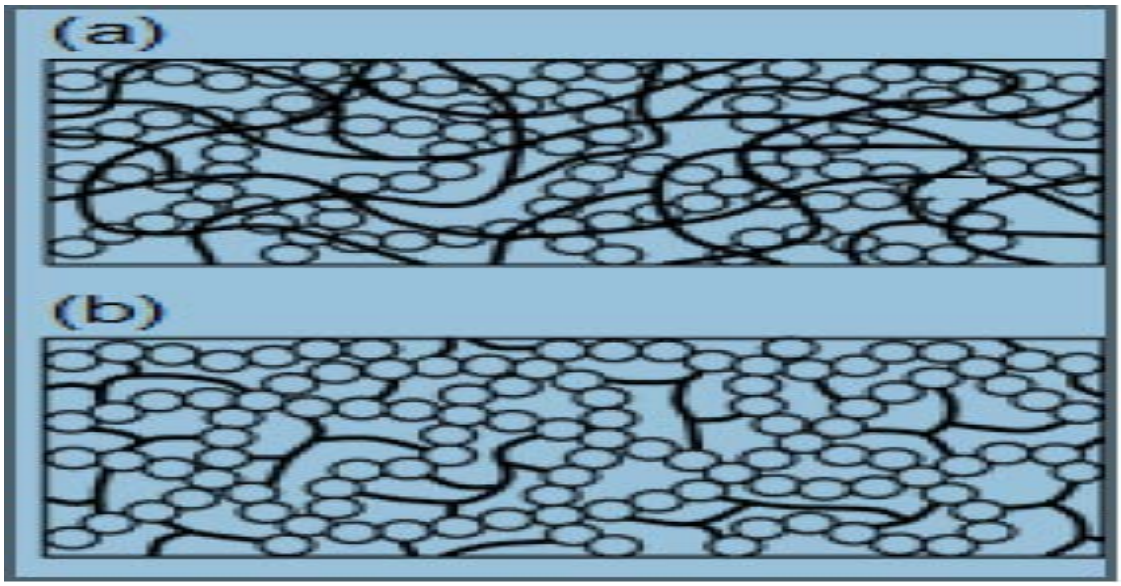


Fig 3.13: Schematic representation of IPNs (a) without chemical bonds between moieties and (b) dual hybrid network.

3. Class II hybrid organic-inorganic membranes synthesis method:

These class II hybrid organic-inorganic membranes can thus be divided in two types depending on the synthesis method (Fig 3.14), in which (1) dip-coating or (2) post-synthetic grafting is applied. The post-synthetic method and the dip-coating method induce distinctly different properties at both the nanometer scale and at the macroscale. Both are explained in more detail below. A focus on general comparison of benefits and drawbacks of the dip-coating and post-synthetic methods and more details about the principles of organosilane and organophosphonic acid grafting are given below [2].

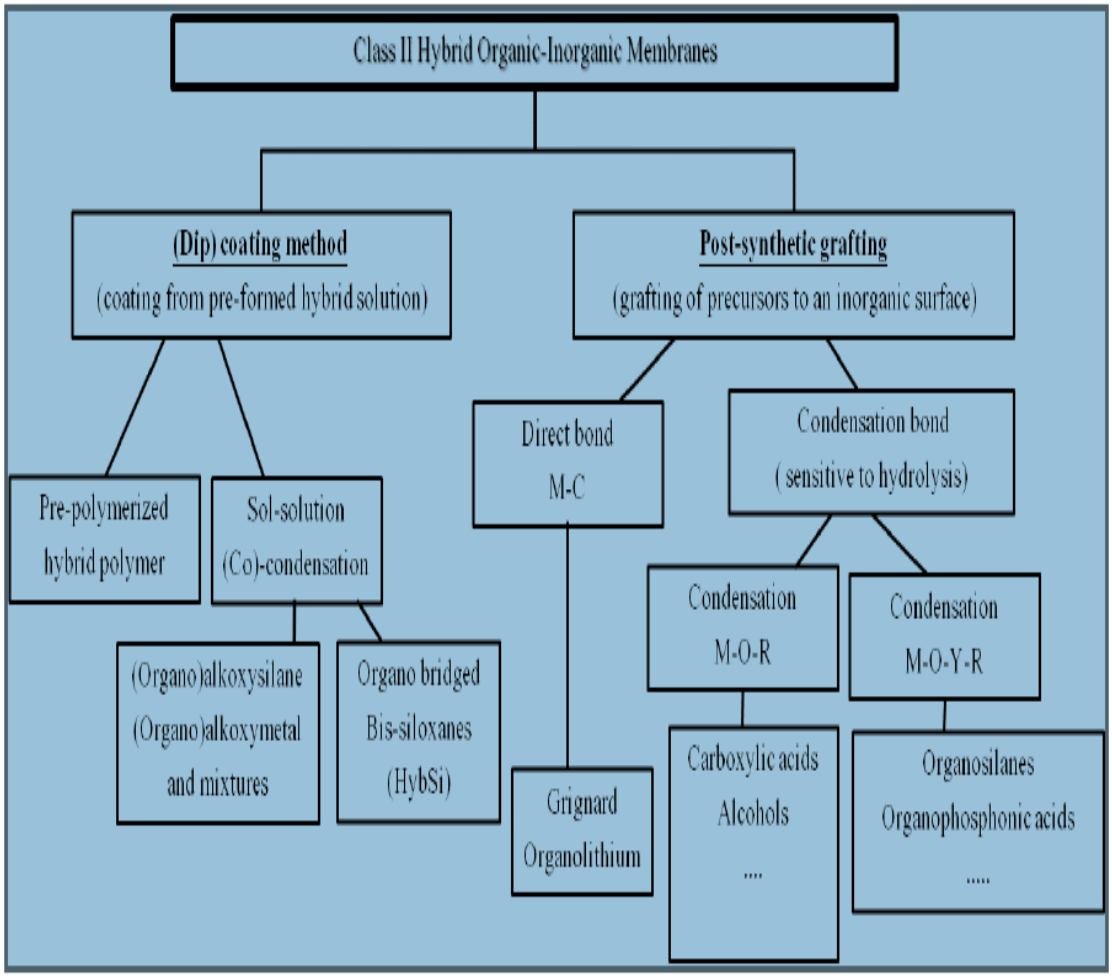


Fig 3.14: Schematic overview of the different synthesis approaches resulting in class II hybrid organic-inorganic membranes. M represents the metal of the metal oxide support, R the functional organic group and Y the bridging heteroatom.

3.1. Dip-coated organic-inorganic hybrid membranes:

Dip- or spin-coated sol-gel hybrid organic-inorganic membranes are mostly applied as gas separation or pervaporation membranes as they are usually microporous (pore diameter < 2 nm). A low-viscosity preformed hybrid sol or polymer solution is applied onto a porous ceramic membrane support. As a separate layer is coated, typical problems can arise that generally also occur in other coated layers. Therefore, the quality of the sol solution is very important and needs to be adjusted to every specific material and desired pore structure. For dip-coated membranes, high permeability and high mechanical, chemical and thermal stability are provided by the open inorganic support, while the denser thin hybrid top layer allows selective transport of molecules from a gas or liquid [2].

The dip-coating method (1) consists of dip coating a sol containing pre-condensed monomeric (pre-polymerized polymeric) species onto the surface of a ceramic support. The sol has a hybrid character, i.e. it contains both inorganic and organic moieties that are covalently bound. An extra selective top layer is thus formed in which the hybrid top layer and the (inorganic) support layer are clearly visible separately. This category also encompasses other possible application methods of a separate top layer such as spin coating [2].

The precursors for these dip-coated synthesized membranes can be very different in nature (Fig 3.15), and are basically either (1) polymeric with two reactive groups, (2) organosilane monomers with three reactive groups and one pendant organic group, or (3) organically bridged bissilyl monomers with multiple reactive groups. In (2) and (3), oligomeric species are produced by condensation or co-condensation of the precursors in a solvent [2].

This sol is subsequently dip-coated onto the support.

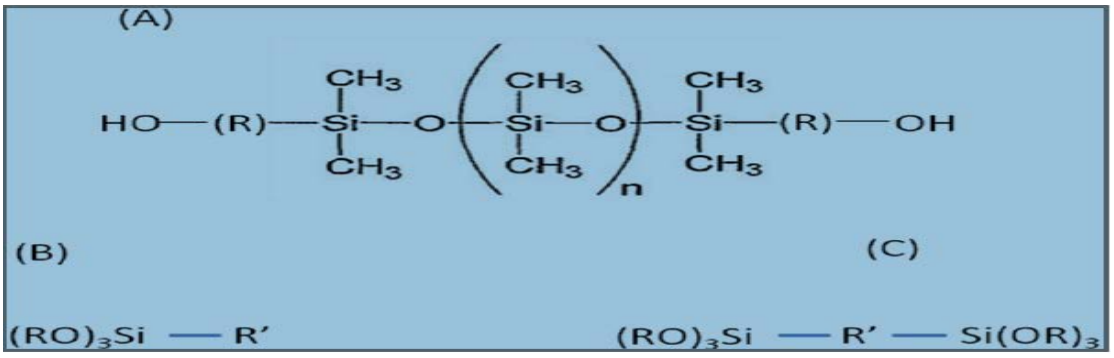


Fig 3.15: Schematic representation of the different precursors. (A) Hydroxy-terminated PDMS polymer (with n the number of monomer repetitions and (R) an optional organic hydrocarbon chain), (B) classical sol-gel precursors (example of monofunctional precursor with 3 reactive alkoxy groups), (C) bridged organic bissilyl precursor.

3.1.1. Polymer (PDMS) coated ceramic membranes:

These membranes were composed of a separate selective hybrid layer of polymeric material on the support, show a similar behavior and interactions at the molecular level as purely organic polymers. One of the most extensively studied polymer-coated ceramic membranes is PDMS/ceramic nanocomposite membranes made by dip-coating dissolved silicon oil on ceramic membrane supports. To prevent

infiltration in the support layer, the dip-coating solution needs to have a sufficiently high PDMS concentration [2].

3.1.2. (Co)-condensed membranes based on sol-gel chemistry:

While polymer-coated membranes are simply produced by coating of a polymer solution onto the support, (co)condensation of precursors with 3 or more reactive groups allows much wider control over the materials properties as more variation is possible during preparation of the sol-solution.

(Co)-condensed membranes can be formed in different ways. The general principle is the condensation of one type of precursor or co-condensation of 2 or more different precursors (e.g. organoalkoxysilane and TEOS) to form a sol, which is then dip-coated onto the ceramic support. After drying, the coated sol gives rise to a hybrid top-layer. The intrinsic properties of the sol (controlled by the synthesis conditions of the sol-solution) in combination with the dip-coating conditions and subsequent drying and thermal consolidation procedures determine the specific character and performance of the selective hybrid top layer [2].

The surface properties can be further modified by applying mixtures with other precursors. Variation of the preparative conditions leads to a great variety of membrane properties. The internal pore structure is essentially determined by the concentrations of the hybrid silica precursor, water and acid or base (including concentration and type), the reaction temperature and time. Other preparation parameters that require control are the choice of solvent, the drying rate and the structure and pretreatment of the porous multilayer system [2].

Oligomeric colloidal structures are formed during sol-gel synthesis as the result of condensation reactions. While these would ultimately condense to a continuous network gel with high viscosity, thin-film coating of defect-free layers requires a sol with low viscosity. Careful tuning of the condensation time and/or of the reactant concentration is required to obtain optimum coating conditions, which depends largely on the structure of the precursor molecule [2].

3.2. Post-synthetic organic-inorganic hybrid membranes:

Post-synthetic grafting is also known as surface modification. A covalent bond is formed between the precursor molecules and the pore surface of the membrane. Ideally, this results in the formation of a (sub)monolayer or of only a few layers in case of polymerization. The small dimensions make it more difficult to image the organic layer separately in comparison to the coated hybrid layers. In surface-

modified membranes, all organic groups are only situated on the pore surface of the selective layer, making them fully accessible. Grafting can be done on commercial ceramic membranes. The grafting will thus only change the physico-chemistry of the surface and sometimes reduce the pore size. This is a clear advantage compared to the dip-coating method [2].

In the post-synthetic method (2) organic functional groups are grafted onto the pore surface of the inorganic porous support. Specific individual precursor molecules (e.g. organoalkoxysilanes, organohalosilanes, organophosphonic acids, Grignard reagents, complexing agents like sulfates or carboxylic acids etc.) form a covalently bound (partial) monolayer or in some cases thin multilayers on the pore surface of the membrane [2].

3.2.1. Grafted organic-inorganic membranes with a direct oxygen bond:

M-O-R bonds are typically made via etherification reactions between alcohols or carboxylic acids and the hydroxyl groups of the inorganic membrane top layer. The method is easy, straightforward and warrants high surface coverage of the organic functional groups. Nevertheless, it is not widely applied. The main reason is the fast hydrolysis of the M-O-R bond in the presence of water or substitution reactions of other alcohols or carboxylic acids with the surface-grafted groups. While stability and applicability depend strongly on the functional group (hydrophobicity, branching degree, surface coverage) and the operating conditions, they are usually limited compared to the other grafting methods [2].

3.2.2. Condensation via a heteroatom:

By far the most applied method for grafting of ceramic membranes is condensation via a heteroatom to produce M-O-Y-R bond. Different types of precursors are applied, including organoalkoxysilanes, organohalosilanes and organophosphonic acids, which will be further detailed below:

3.2.2.1. Organosilane-modified membranes:

The best-known method is the use of organosilanes. Typically, a chemically stable Si-C bond is attached to the surfac0e via a reaction with an organosilane with one, two or three reactive groups, resulting in the formation of M-O-Si-C bonds. Organosilanes constitute the most versatile type of coupling agents with a broad range of organic functionalities commercially available. The choice in type of functional groups in combination with the type and number of reactive groups is enormous, exceeding that

of all other coupling with an order of magnitude. A virtually unlimited variety of hybrid membranes can be synthesized by applying this type of precursor [2].

Organosilanes with more than one reactive group can easily polymerize, in contrast to organophosphonic acids. Polymerization of organosilanes occurs more extensively for a lower number of M-OH anchoring groups on the membrane surface, but it also depends on the type of precursor and the synthesis conditions. Two types of polymerization reactions can occur: horizontal (between neighboring organosilanes parallel to the support) or vertical (perpendicular to the support). Moreover, vertical polymerization can introduce defects that can negatively affect the separation selectivity. The competitive reaction between homocondensation (polymerization) and horizontal bonding (anchoring to the surface) is determined by their relative reaction rates. It is influenced by the reaction conditions: water content, temperature, solvents, type of reactive groups and presence of amine catalysts, which can either be added to the solution or an integral part of the functional organic group [2].

Water assists in the grafting process but its quantity also determines horizontal and/or vertical polymerization between the organosilanes (Fig 3.16).

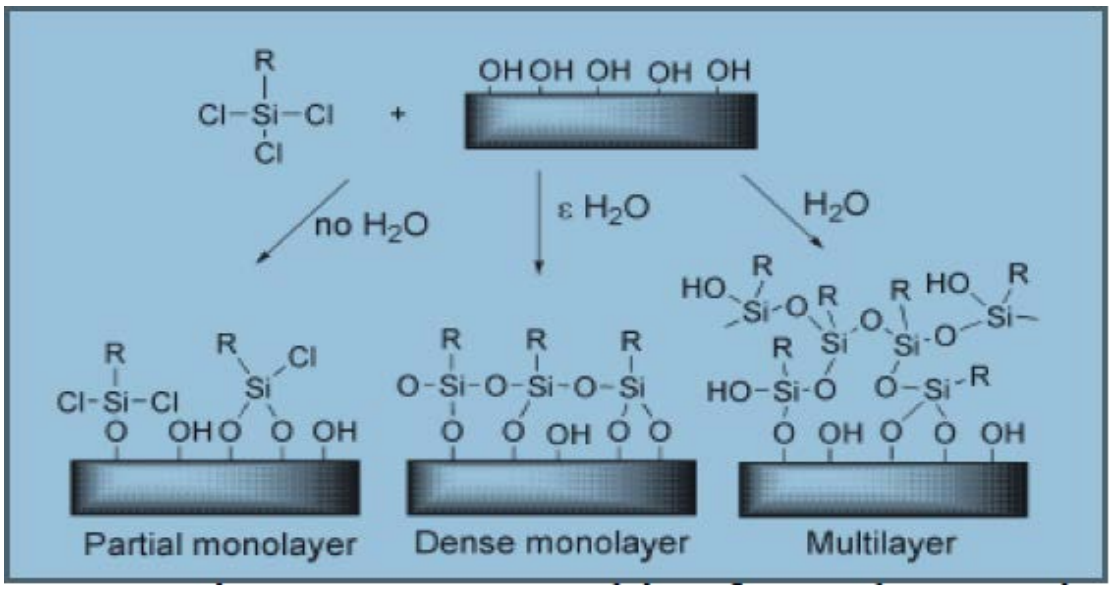


Fig 3.16: Schematic representation of the influence of water on the grafting of organosilane with multiple reactive groups. The dense monolayer shows horizontal polymerization, the multilayer vertical polymerization.

3.2.2.2. Organophosphonic acid-modified membranes:

As organophosphonic acids bond strongly onto transition metal oxide surfaces, the modification is fast and cheap. Modification can be done in organic solvent or water, depending on the solubility of the chosen precursor.

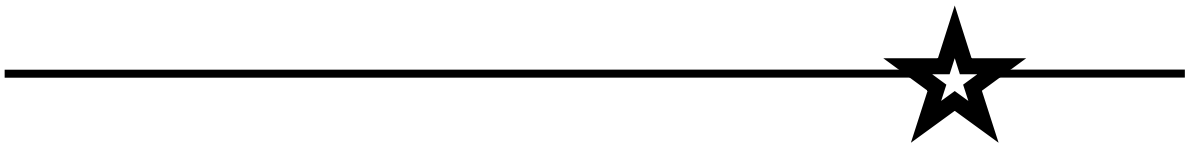
The most applied phosphonic acids have 3 reactive groups (P-OH, P-OR and/or P=O depending on the applied phosphonic or phosphinic acid). Similar to organosilanes with 3 reactive groups, multiple bonds can be formed with the surface but polymerization reactions are generally not occurring. Mono-, di- and tridentate bonds on metal oxides have been reported, with additional bonding variants depending on which type of reactive group (P-OH or P=O) interacts with the surface. The control over the bonding type, grafting density, etc. depends on the type of phosphonic acid, the support and the synthesis conditions applied. It is important to note that in most cases a dangling P-OH or P=O bond is left, which is not attached to the surface. The presence of this dangling bond can substantially influence themembrane separation properties [2].

3.2.3. Organometallic-modified hybrid membranes:

The use of organometallic chemistry for the preparation of surface-modified hybrid membranes has only recently been developed. This method applies organometals such as Grignard reagents or organolithium to directly from M-C bond without intermediate oxygen or a heteroatom. As organometallic reagents are highly reactive, the modification has to be done in dry ethers as solvents, on pretreated supports and under an inert atmosphere. The membranes are subsequently dried at slightly elevated temperature under vacuum to remove the solvents or loosely bond volatile molecules from the surface [2].

4. Conclusions:

- Organic-inorganic hybrid polymers are obtained through sol-gel processes, self-assembly processes, assembling or dispersion of nanobuilding blocks, hierarchical structures and interpenetrating networks.
- Includes the correlation between the precursors and synthesis conditions to produce the various hybrid membranes with their stability under operating conditions.
- We have focused on the various types and subtypes of class II hybrid membranes. For the presence of covalent bonds between organic and inorganic moieties.



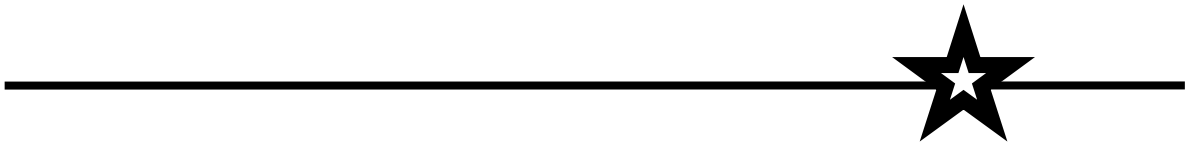
Chapter II

NEURONAL MODELING FOR THE PREDICTION OF PERMEABILITY



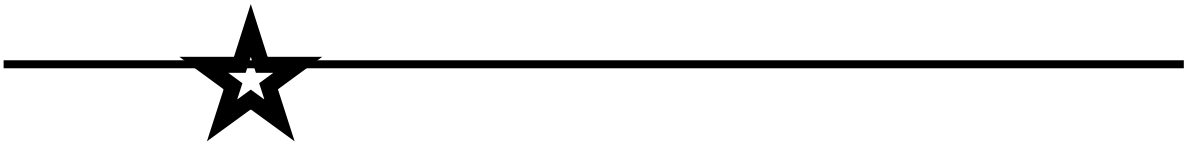
1. Introduction:

This chapter deals with the permeability prediction of hybrid polymers. For this to do so, we will start with a first part entitled "elaboration of the database". This will involve the collection and representation of the molecular structures of hybrid polymers belonging to different classes up to the calculation of the descriptors by the appropriate software; the second part presents the reduction of the number of descriptors using iteratively retaining informative variables (IRIV) as a method for reducing the size of the descriptors database. The third part is devoted to the neuronal modeling of data and the optimization of the parameters of the elaborated neural networks model. The neural network is a powerful computer model capable of capturing and representing complex Input / Output relationships. It is inspired from the biological nervous systems; offer the promise of a general and cost-effective method for process modeling, tool for approximating complex systems, effective for nonlinear and complex systems, capable of learning and adapting with examples, processing multiple systems at once and determine the traceability of the modeled parameters.



Part -1-

“Development of the database”



2. Part-1-

2.1.*Software and materials used:*

We started the calculations with a workstation tower equipped with intel (R) core ™ i7cpu; 3.6 GHz, 32 GB RAM operating under windows 64-bit system.

2.2. *Collection of data:*

In this step we have collected and selected 45 hybrid polymers from the different articles containing experimental CO_2 permeability. They belong to 5 main classes of polymers: norbornenes, polyacetylenes, silicones, Polysiloxane imides (PSI) and Poly (phosphazenes). Their monomeric formulas can be found in the table II.1. The different stages of realization of the descriptors database are presented in (Fig II.1).

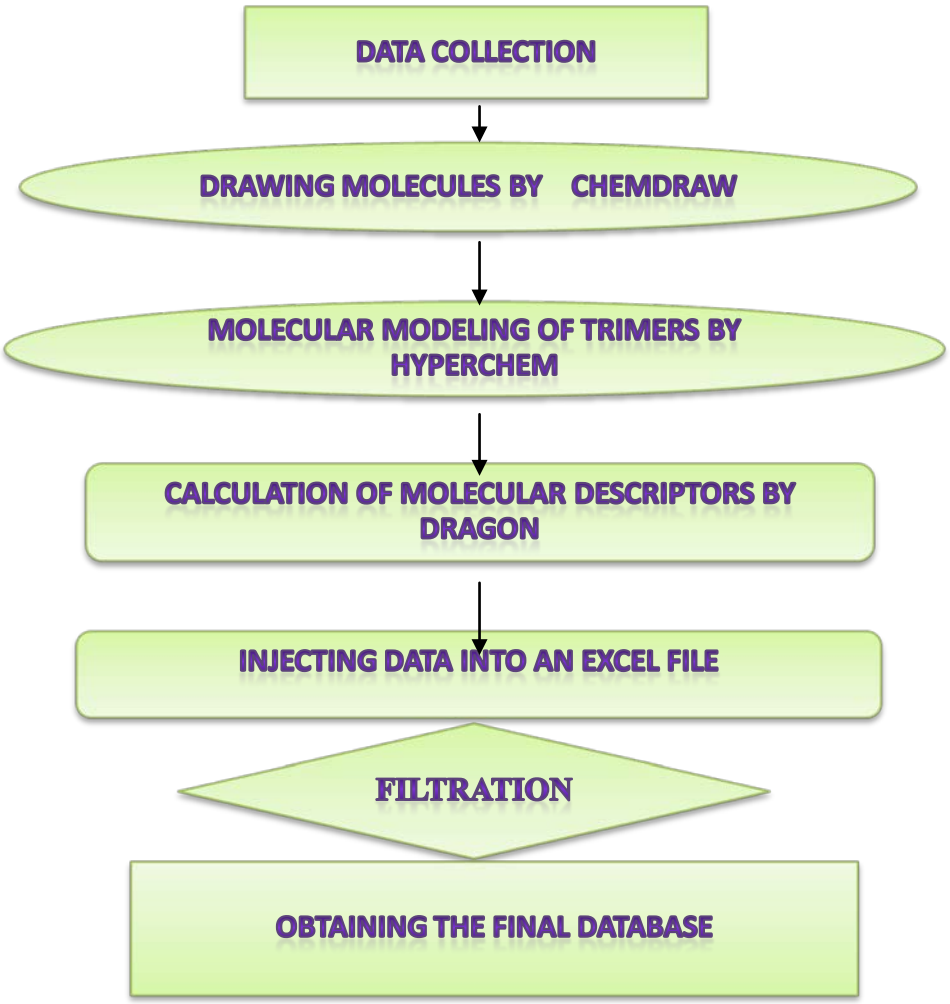


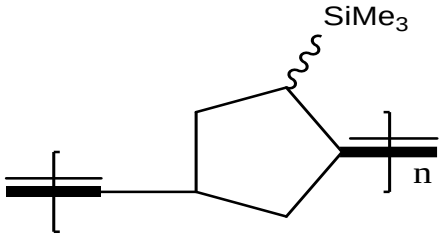
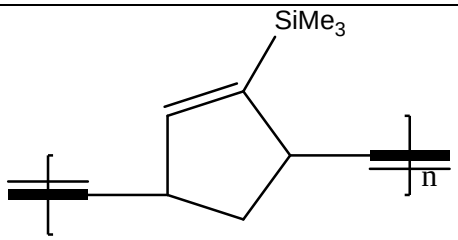
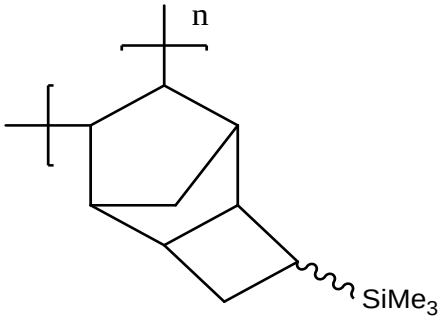
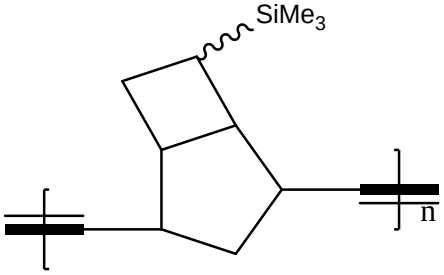
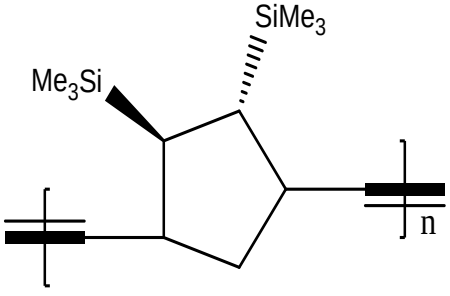
Fig II.1: Flowchart of the different stages of realization of the database.

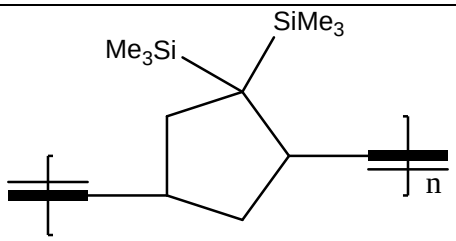
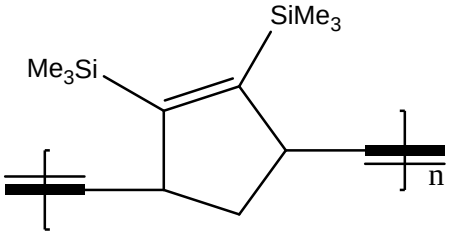
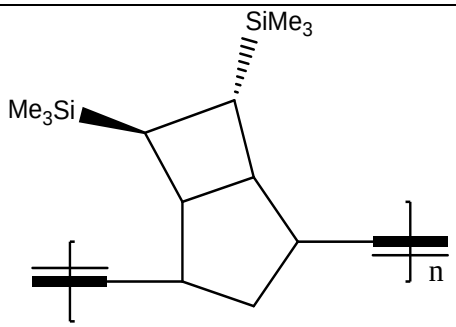
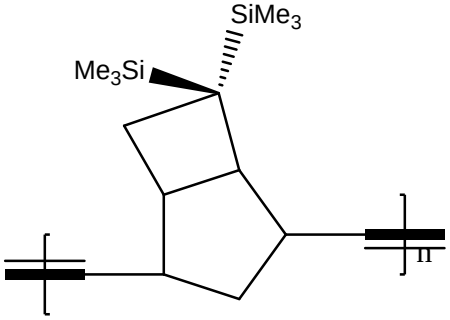
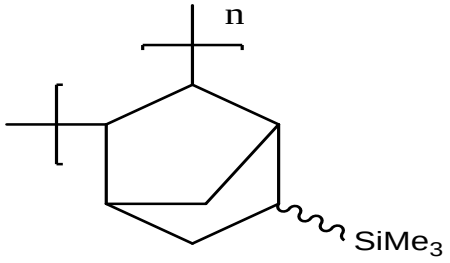
2.3.*Class of hybrid polymers collected used in this work:*

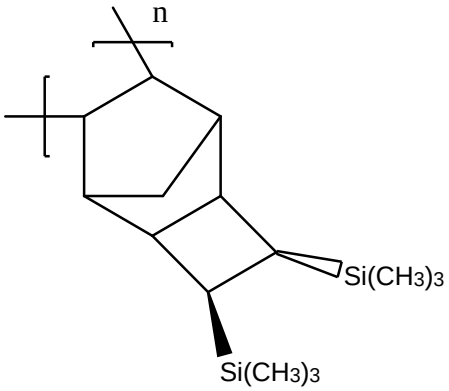
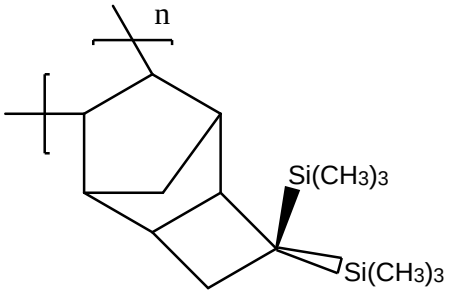
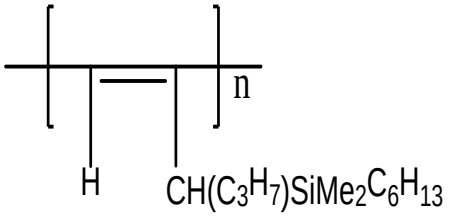
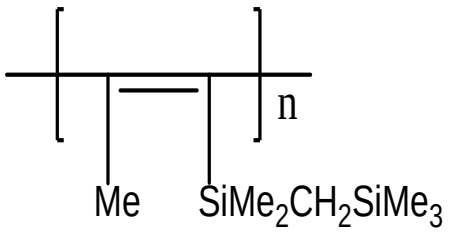
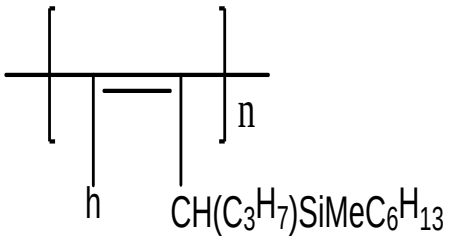
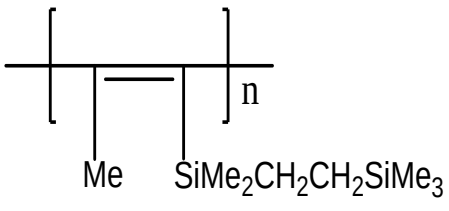
The polymers in this work are the most used in the published work on gas permeability

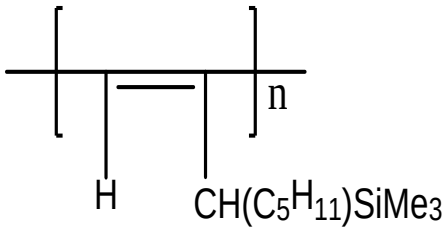
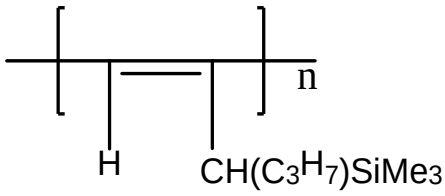
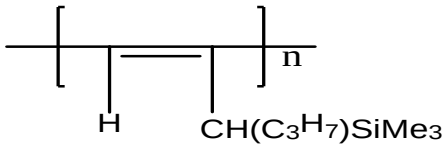
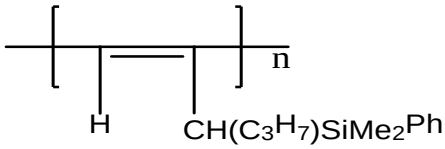
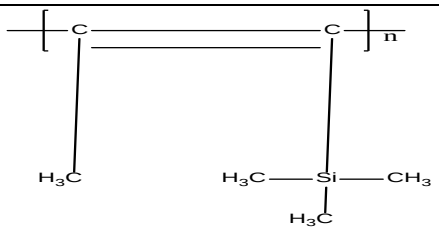
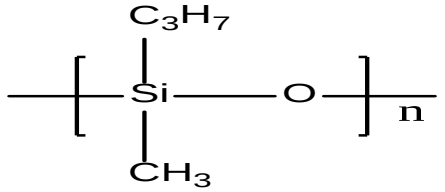
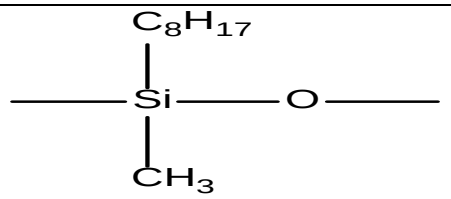
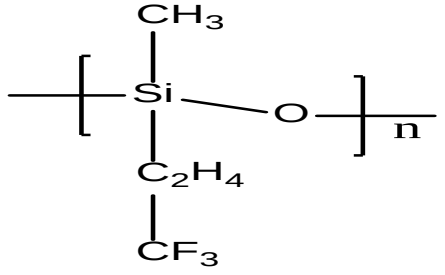
- The norbornenes: are glassy polymers having a glass transition temperature higher than ambient temperature. Their experimental permeability for CO_2 is shown in (Table II.1) [11].
- Polyacetylenes: experimental data on the permeability of CO_2 gas through polyacetylenes is shown in Table II.1, [11]
- Silicones: silicones are characterized by weak intermolecular forces and binding energy. They belong to the family of elastomers, amorphous hybrid polymers existing above their glass transition temperature, so that much segmental motion is possible, the (Table II.1) presents the experimental data of the permeability of CO_2 through silicones [11].
- PSI: Are elastomeric copolymers consisting of two fragments: the first is a polyimide PI (glassy) and the second is a fragment of siloxane (elastomer). These copolymers have two interesting properties: - The hardness and resistance of PIs; - The flexibility of polysiloxanes. (Table II.1) [12]
- Phosphazenes: These hybrid polymers endowed an organic part contained both the aromatic and the polyether components; however, they were individually attached to the phosphazene backbone resulting in a random terpolymeric structure[13].
- And other hybrid polymers: PI / SILICA [14] [15] and PEDS-P [16] [17].as illustrated in table II.1 bellow:

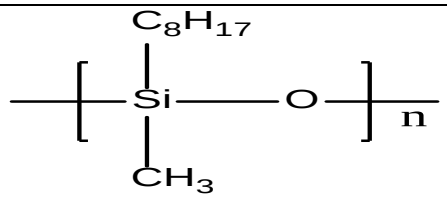
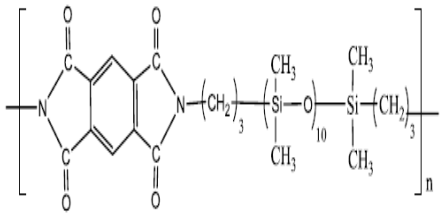
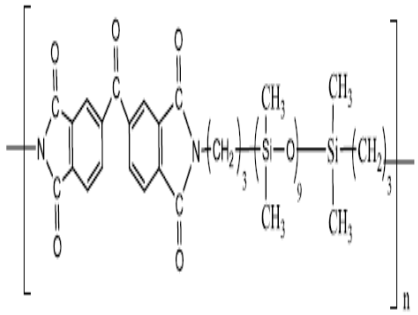
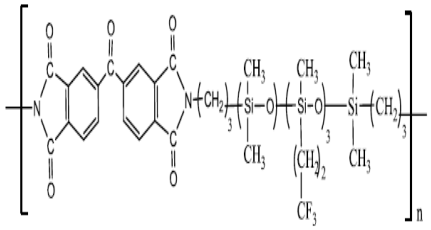
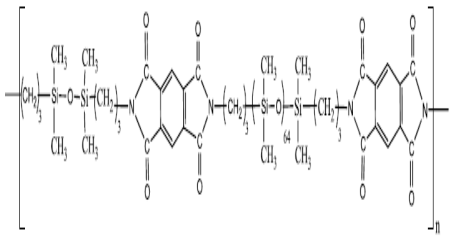
Table II.1: Selected hybrid membranes and their permeability at deferent temperature

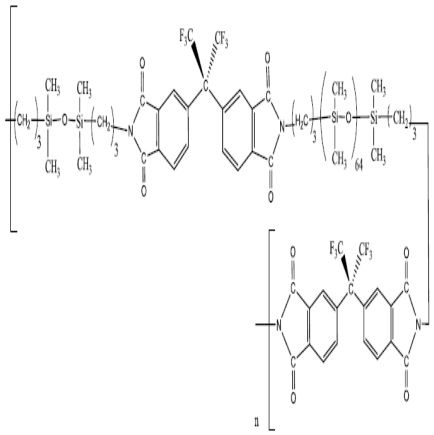
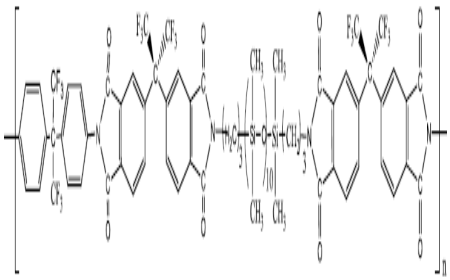
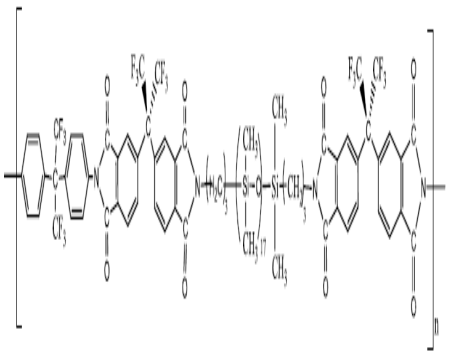
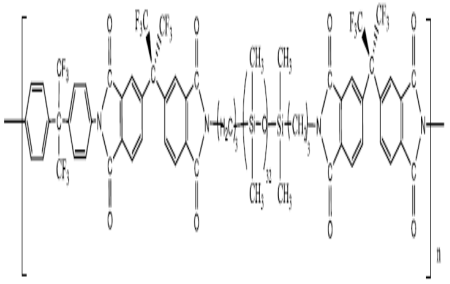
Hybrid polymers	T°	P CO_2 (Barrer)	Structures	Group	Ref
PNBSi	24	79		norbornene	[11]
	24	64		norbornene	[11]
PNBSiCSi	24	67		norbornene	[11]
PTCNSi	24	112		norbornene	[11]
P(6.5-$NBSi_2$)	24	455		norbornene	[11]

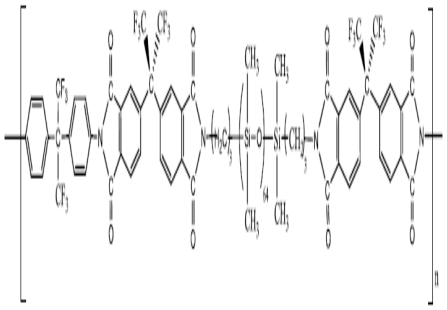
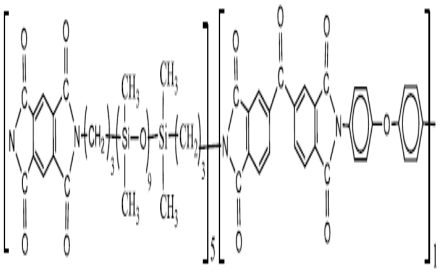
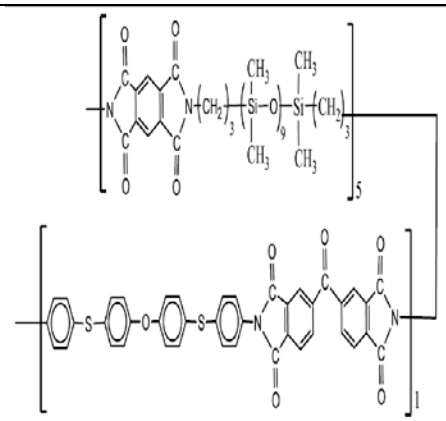
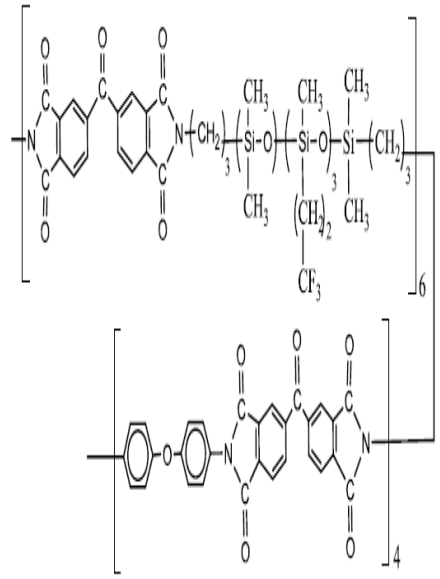
P(5.5-NBSi$_2$)	24	277		norbornene	[11]
P(2,3- NBDSi$_2$)	24	358		norbornene	[11]
P(3,4-TCNSi$_2$)	24	396		norbornene	[11]
P(3,3-TCNSi$_2$)	24	258		norbornene	[11]
APNBSi	24	4350		norbornene	[11]

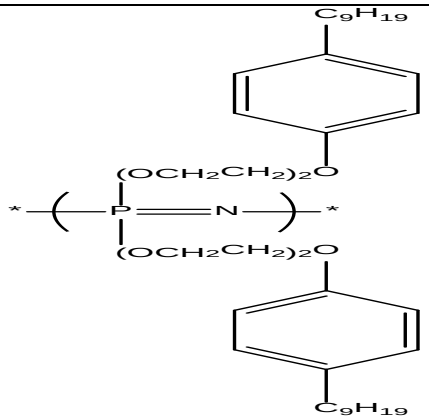
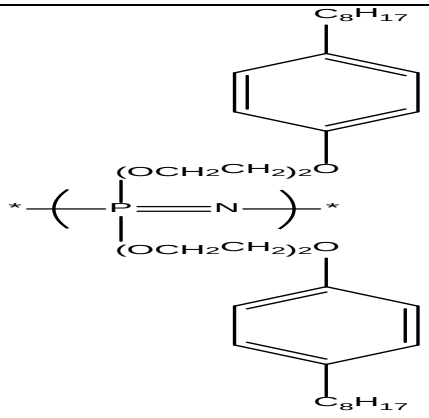
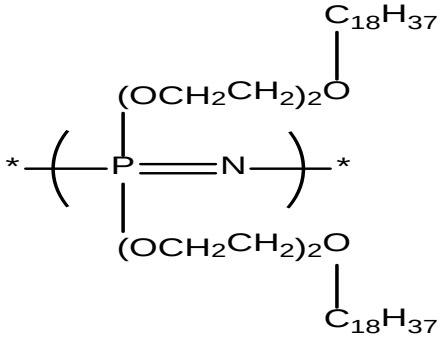
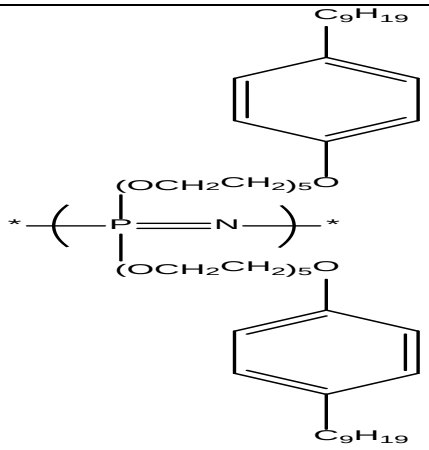
APTCNSi	24	2230		norbornene	[11]
PTCNSi2V	20	11280		norbornene	[11]
PTCNSi2g	20	19900		Polyacetylene	[11]
[C(Me)=C(SiMe$_2$CH$_2$CH$_2$SiMe$_3$)]	25	310		Polyacetylene	[11]
[C(Me)=C(SiMe$_2$CH$_2$SiMe$_3$)]	25	150		Polyacetylene	[11]
C(H)=C(CH(C$_3$H$_7$)SiMe$_2$C$_6$H$_{13}$	25	71		Polyacetylene	[11]

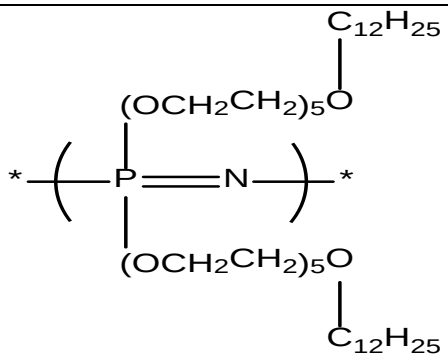
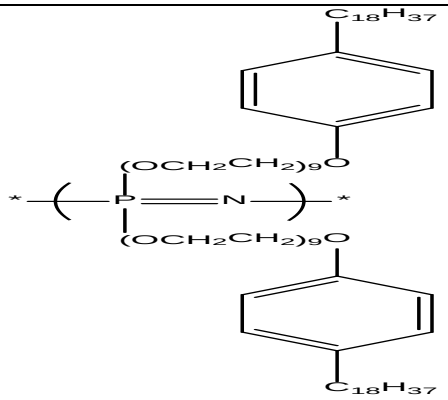
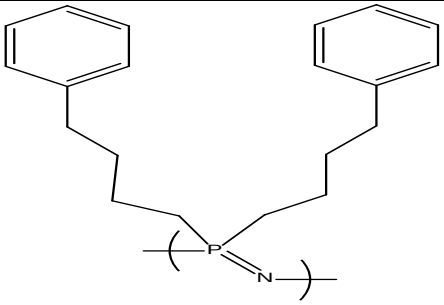
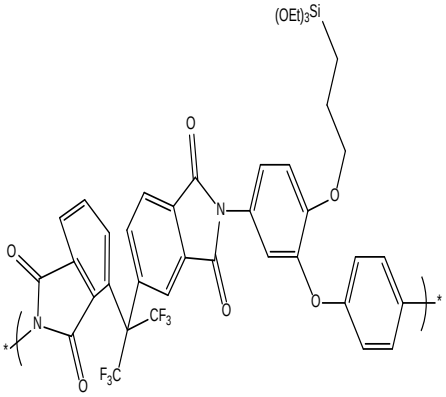
[C(H)=C(CH(C$_5$H$_{11}$)SiMe$_3$)]	25	120		Polyacetylene	[11]
C(H)=C(CH(C$_3$H$_7$)SiMe$_2$C$_6$H$_{13}$	25	70		Polyacetylene	[11]
HCH(C$_3$H$_7$)SiM$_3$	25	15		Polyacetylene	[11]
[C(H)=C(CH(C$_3$H$_7$)SiMe$_2$Ph)]	25	54		Polyacetylene	[11]
Polyacetylens		190		Polyacetylene	[11]
CH$_3$C$_3$H$_7$SiO	35	1520		Silicones	[11]
CH$_3$C$_8$H$_{17}$SiO	35	917		Silicones	[11]
CF$_3$C$_2$H$_4$)CH$_3$S	35	1210		Silicones	[11]

$(CH_3)_2Si CH_2$]	35	542		Silicones	[11]
P900	25	3930		PSI	[11]
PSI-2	35	2380		PSI	[12]
PSI-7	35	148		PSI	[12]
PD5000	25	4780		PSI	[12]

FD5000	25	3720		PSI	[12]
T1	25	665			[12]
T2	25	2160			[12]
T3	25	3940		PSI	[12]

T4	25	5550		PSI	[12]
PSI-4	35	1710		PSI	[12]
PSI-5	35	1660		PSI	[12]
PSI-6	35	524		PSI	[12]

Phosphazenes alkylated phenol ethoxylate Polyether chain length (x) :1.63 Aliphatic chain ($\mathbf{C_mH_{m+1}}$) (m) :9.19	30	45		Phosphazenes	[13]
Phosphazenes alkylated phenol ethoxylate Polyether chain length (x) :1.52 Aliphatic chain ($\mathbf{C_mH_{m+1}}$) (m) :8.31	30	12		Phosphazenes	[13]
Phosphazenes mono-alkylated ethoxylate. Polyether chain length (x) 2.36 Aliphatic chain ($\mathbf{C_mH_{m+1}}$) (m)18.21	30	8.03		Phosphazenes	[13]
Phosphazenes alkylated phenol ethoxylate Polyether chain length (x) 4.75 Aliphatic chain ($\mathbf{C_mH_{m+1}}$) (m)9.20	30	132		Phosphazenes	[13]

Phosphazenes mono-alkylated ethoxylate. Polyether chain length (x) 4.89 Aliphatic chain ($\mathbf{C_mH_{m+1}}$) (m)12.19	30	386		Phosphazenes	[13]
Phosphazenes alkylated phenol ethoxylate Polyether chain length (x) 8.57 Aliphatic chain ($\mathbf{C_mH_{m+1}}$) (m) 2*9.11	30	275		Phosphazenes	[13]
poly[bis-(3-phenyl-propoxy) phosphazene]	30	107		Phosphazenes	[13]
PI/SILICA	80	41		PI	[14],[15]

2.4.Drawing of hybrid polymers structures by ChemDraw:

To accomplish this task, we chose the ChemBioDraw software as a drawing tool; we considered the polymers (fig II.2) as trimers of the repeating building block for the following considerations:

- A trimer is a very simple representation of a polymer and is valid for its geometric optimization in order to evaluate a maximum of intermolecular interactions. The advantage of working with a trimer lies in the speed of the optimization of the structure and the ease of calculating the descriptors.
- The trimer segment best represents the original structure of the polymer is that of the medium (repetitive unit), as it is by the physicochemical, electronic and steric characteristics of adjacent units and also preserves the structural characteristics of the hybrid polymer ...

One faith the molecule drawn, it is saved as a MDL Mol file extension (* .mol) for the next step which is pre-optimization by HyperChem.

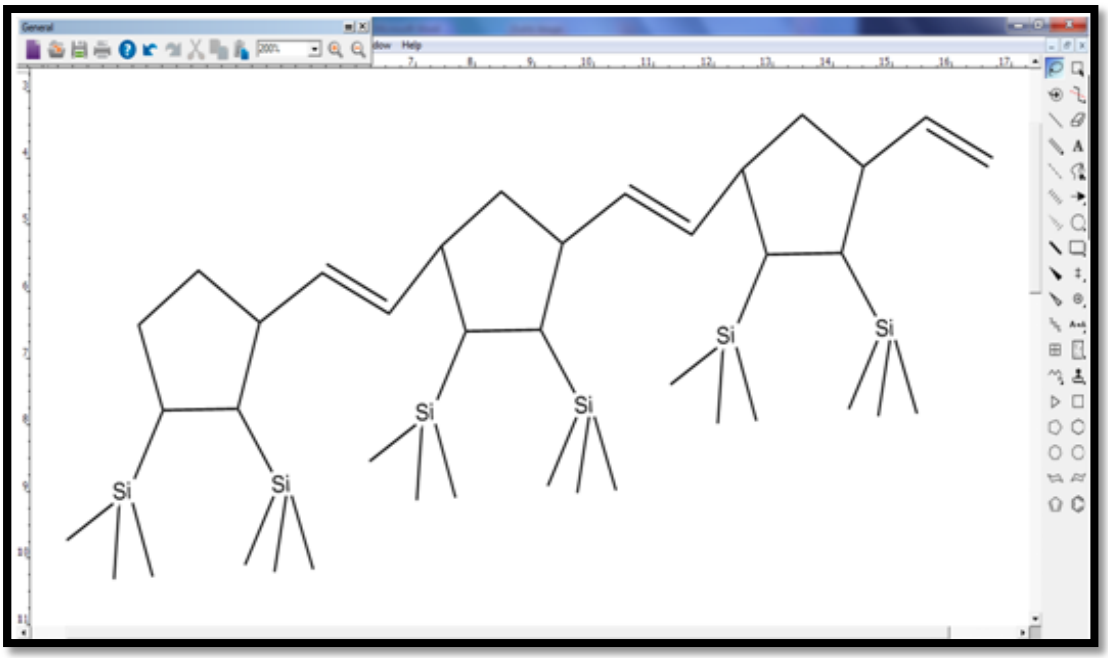
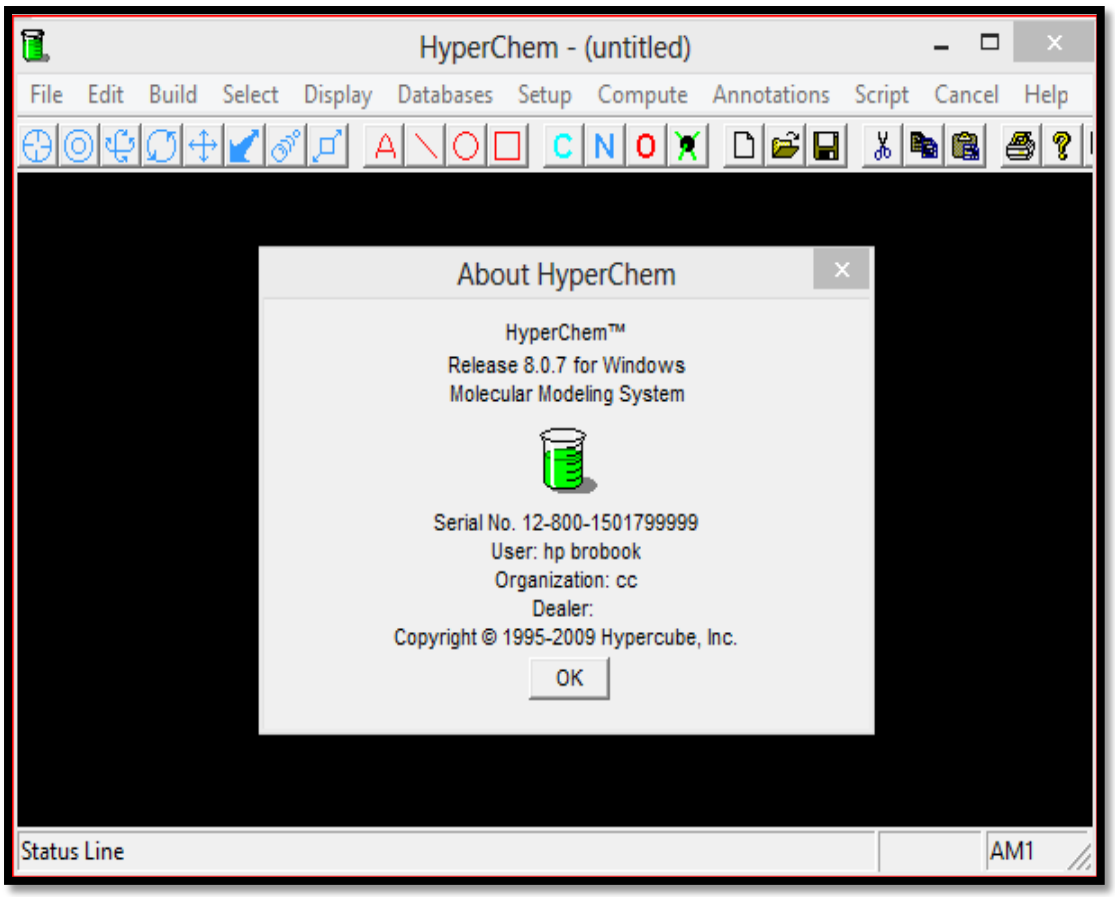


Fig II.2: Stage of representation of a polymer structure by ChemDraw.

2.5.Molecular modeling of trimers by HyperChem:

The HperChem (Fig II .3) is software very appreciated by the scientists because of the diversity of the modules that it presents as well as its power presented through the various methods of modeling and geometrical optimization. These laste one is provides in following the steps:



II .3: HyperChem version 8.0.7 for molecular modeling of trimers.

- Opening the HyperChem interface will call the file containing the extension file (* .mol) already prepared by ChemDraw and then perform a pre-optimization of the structures that consists of a procedure based on the molecular mechanics of fields Force (MM +: Force Field Molecular). With the following instructions:

  (Setup / MolecularMechanics / MM + / Compute / GeometryOptimization / Gradient conjugate polakRibière). Once the calculations converge, the preoptimized 3D structure is saved in HIN file extension.

- The final optimization of our structure was done by the semi empirical molecular orbitals method AM1 with the polak-Ribiere algorithm with a limit value of the RMS of the gradient = 0.01 KcalA°. This step is very long, it takes considerable time, sometimes several hours or days, but indispensable for calculating descriptors. (Fig II.4)

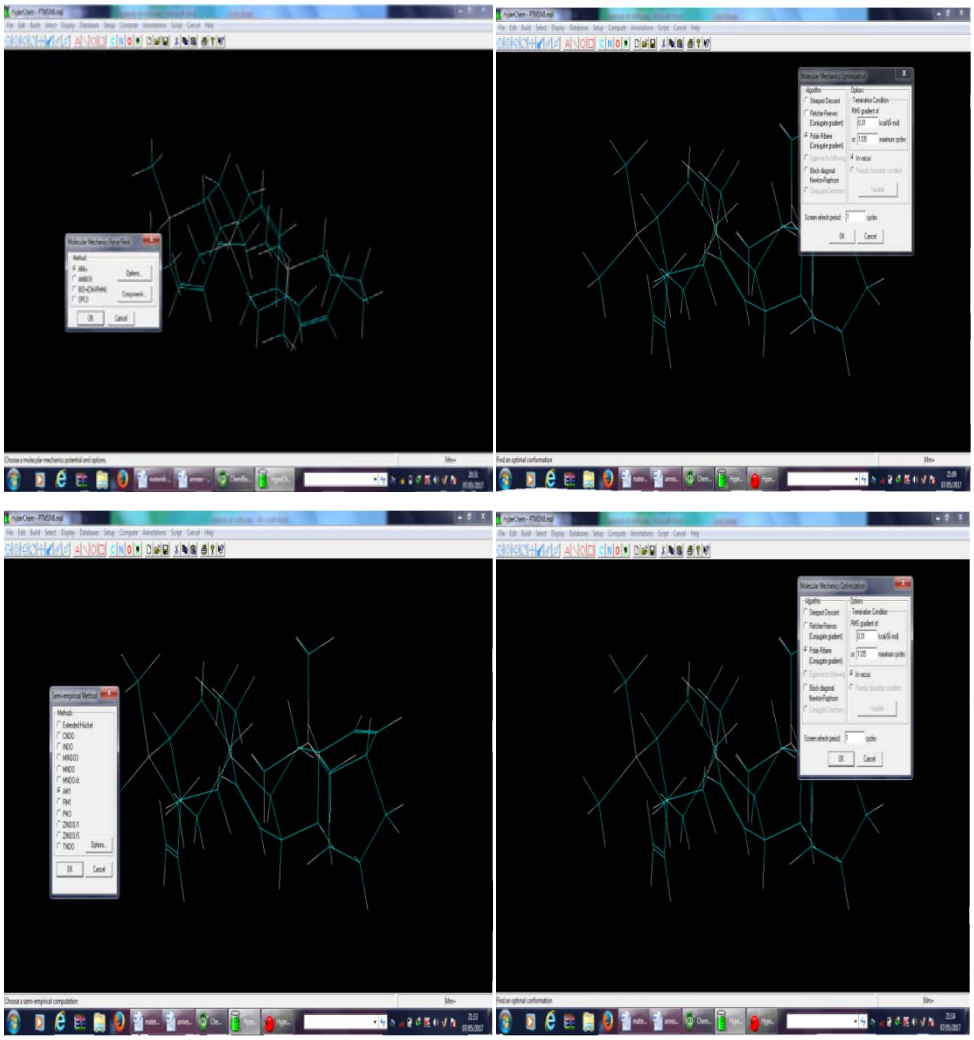


Fig II.4: Steps of the pre-optimizations and optimization of the polymers structures.

In our work, molecular modeling has been employed in order to obtain the most stable energy conformation - the one of which the energy is smaller possible.

- Once the convergence is reached, the optimized structure of the polymer is saved in the form of an extension file (* HIN) in order to make it compatible with the calculation of the descriptors by the Dragon software.

2.6.Descriptor calculation by DRAGON:

Once our structures have been optimized, the descriptors are calculated using the molecular descriptor calculation software most widely used in the majority of structural modeling type research that is DRAGON version 5.5- Year 2007 (Fig II .5).



Fig II .5: The interface of the DRAGON software version 5.5.

The blocks of the chosen molecular descriptors and the methodology for calculating the various descriptors by the DRAGON software are summarized in (Fig II.6 and 10).



Figure II.6: First steps for calculating descriptors by DRAGON

To calculate the descriptors, we open the files (* .HIN), because it does not link the extension files * .Mole and we choose all 22 blocks of available descriptors whose last two are the novelty of this version for all the structures (0D, 1D, 2D, 3D) then once the batch calculations of all studied polymers were finished, we save the results descriptors matrix as text files (. * Txt). Look (Fig II.7 and 8)

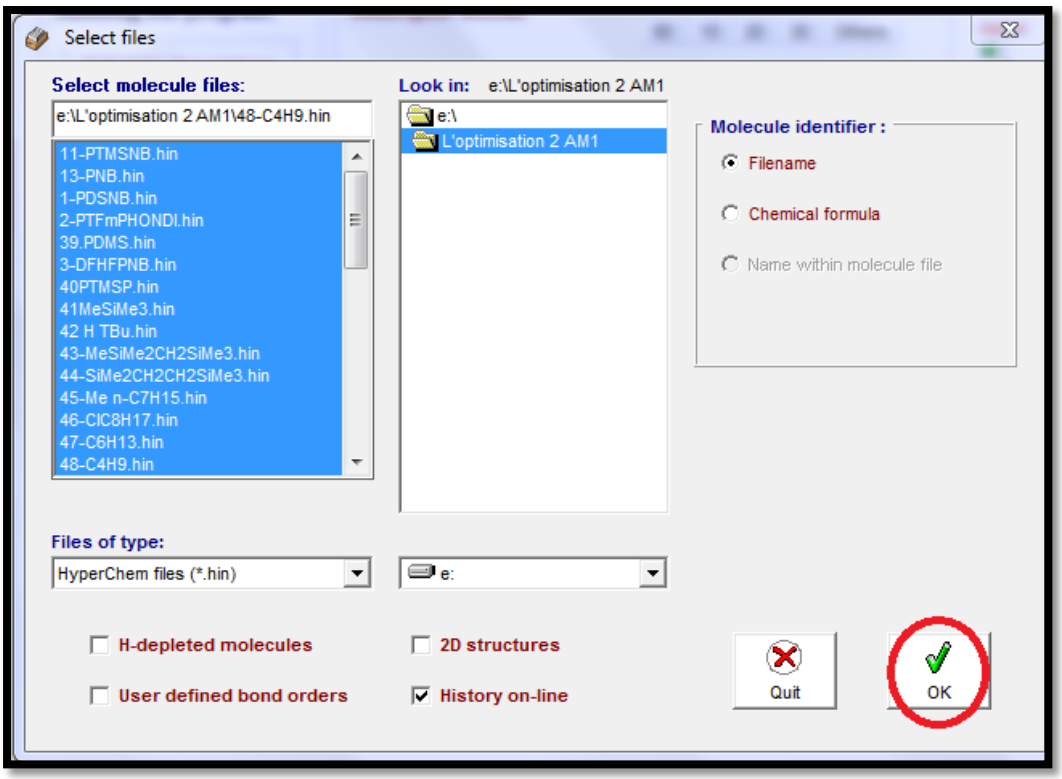


Fig II.7: Second steps for calculating descriptors by DRAGON.

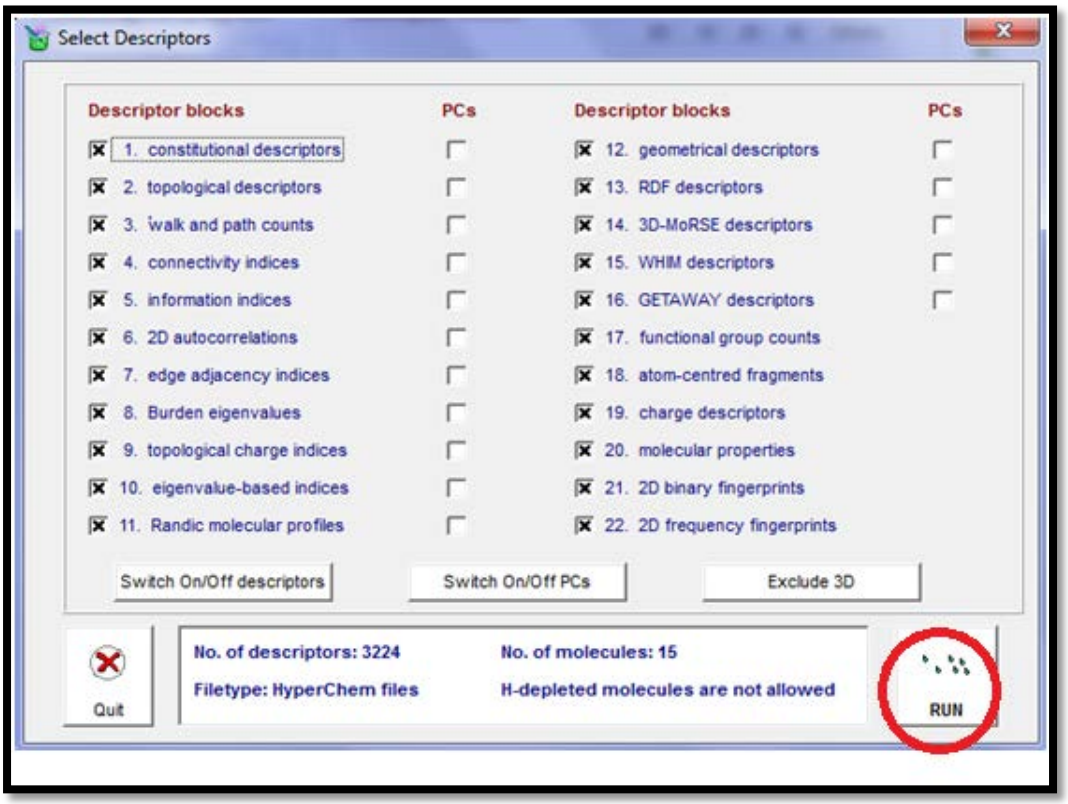


Fig II.8: Third step for calculating descriptors by DRAGON.

We have calculated all descriptors (Table II.2) because in our study we need the maximum of structural information to predict the relationship between polymer structure and their CO_2 gas permeability (QSPR). (Fig II.9)

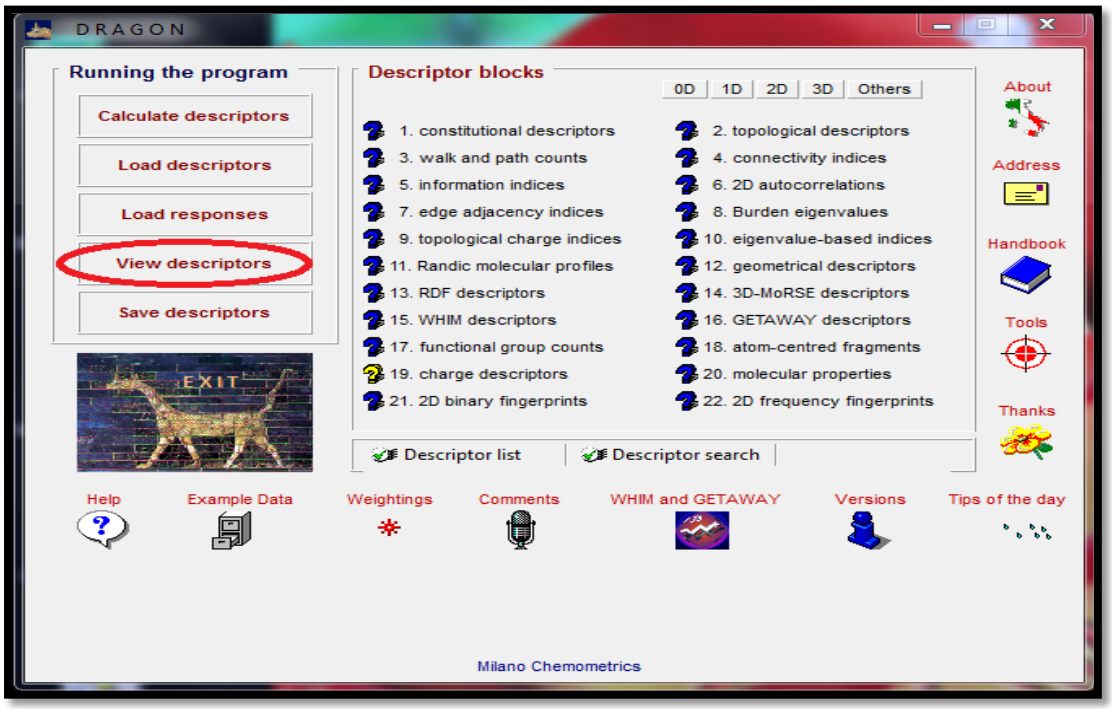
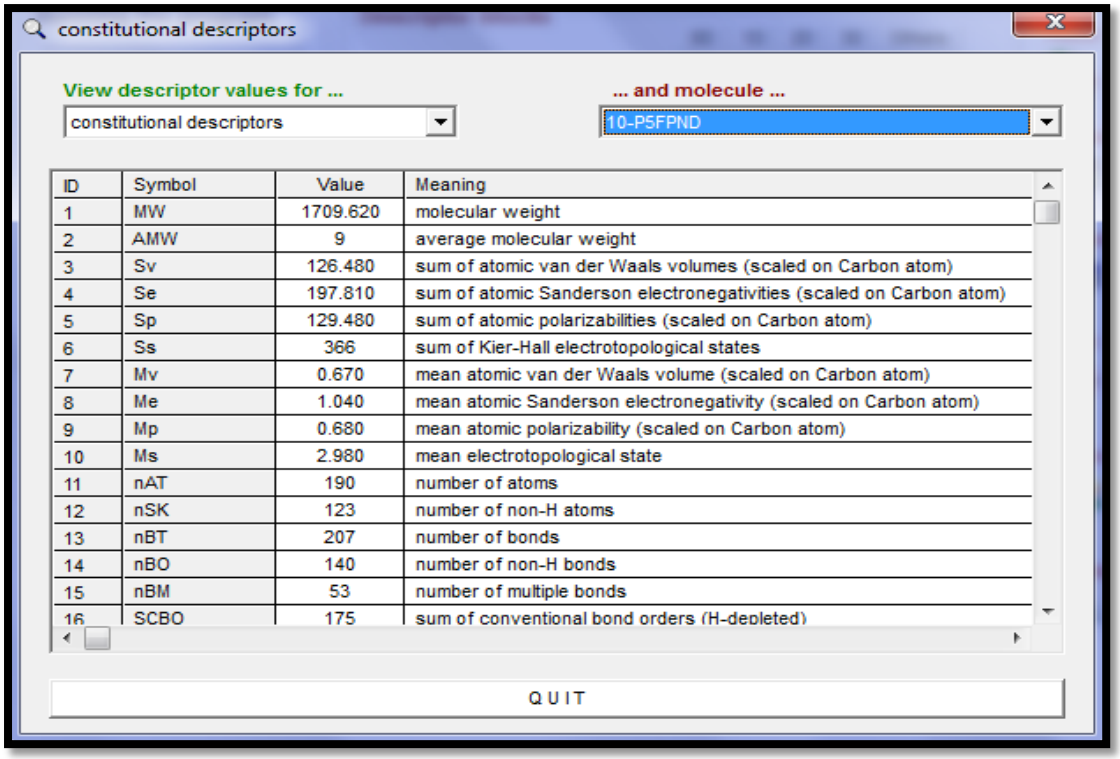


Fig II.9: Fourth step for calculating descriptors by DRAGON



ID	Symbol	Value	Meaning
1	MW	1709.620	molecular weight
2	AMW	9	average molecular weight
3	Sv	126.480	sum of atomic van der Waals volumes (scaled on Carbon atom)
4	Se	197.810	sum of atomic Sanderson electronegativities (scaled on Carbon atom)
5	Sp	129.480	sum of atomic polarizabilities (scaled on Carbon atom)
6	Ss	366	sum of Kier-Hall electrotopological states
7	Mv	0.670	mean atomic van der Waals volume (scaled on Carbon atom)
8	Me	1.040	mean atomic Sanderson electronegativity (scaled on Carbon atom)
9	Mp	0.680	mean atomic polarizability (scaled on Carbon atom)
10	Ms	2.980	mean electrotopological state
11	nAT	190	number of atoms
12	nSK	123	number of non-H atoms
13	nBT	207	number of bonds
14	nBO	140	number of non-H bonds
15	nBM	53	number of multiple bonds
16	SCBO	175	sum of conventional bond orders (H-depleted)

Fig II.10: Fifth step for calculating descriptors by DRAGON.

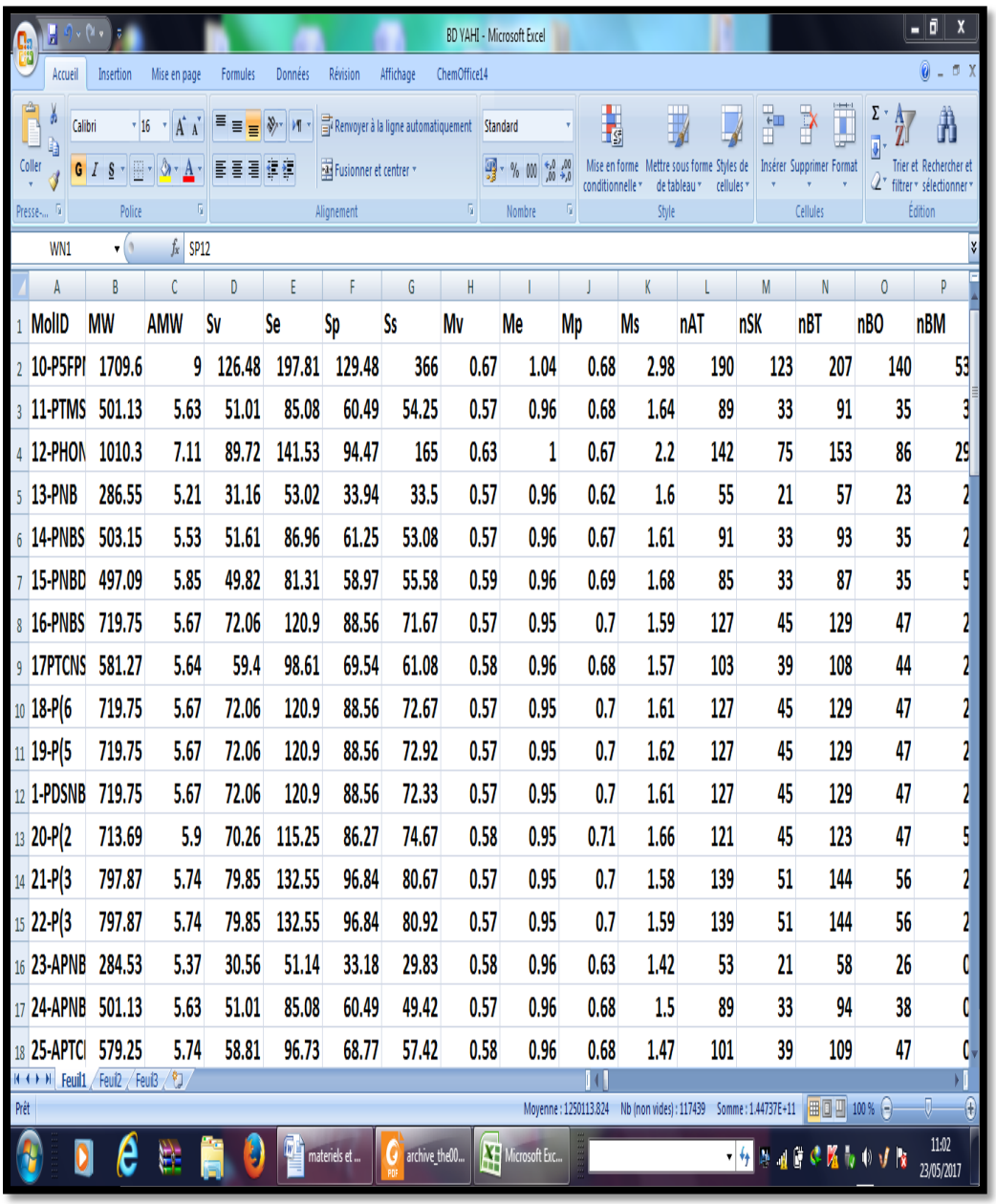
Table II.2: Number of descriptors calculating by DRAGON.

Name of descriptors	Number of descriptors
ConstitutionalDescriptors	48
TopologicalDescriptors	119
Walk and Path counts Descriptors	47
Connectivity Indices	33
Information Indices	47
2D Autocorrelations	96
EdgeAdjacency Indices	107
Burden Eigen values	64
Topological Charge Indices	21
Eigenvaluebased Indices	44
RandicMolecular Profiles	41
GeometricalDescriptors	74
RDF Descriptors	150
3D MoRSEDescriptors	160
WHIM Descriptors	99
GetawayDescriptors	197
Functional Group Counts	154
Atomcentered fragments	120
Charge descriptor	14
MolecularProperties	29
2D binary fingerprints	780
2D frequency fingerprints	780
Total	3222

.

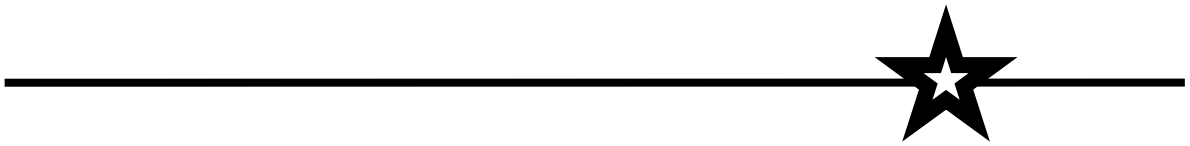
2.7.Converting descriptors data in an EXCEL file:

Our descriptors calculated by DRAGON saved in a text format file containing the name of the polymer and the number of calculated descriptors (in our study 3222 descriptors, the names of each descriptor and its value). The contents of the text files are imported into an EXCEL file. The first line contains the names of the descriptors and the first column the names of the hybrid polymers (Fig II.11).



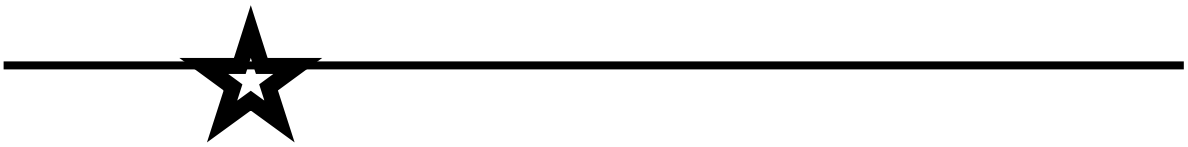
	A	B	C	D	E	F	G	H	I	J	K	L	M	N	O	P
1	MolID	MW	AMW	Sv	Se	Sp	Ss	Mv	Me	Mp	Ms	nAT	nSK	nBT	nBO	nBM
2	10-P5FPI	1709.6	9	126.48	197.81	129.48	366	0.67	1.04	0.68	2.98	190	123	207	140	53
3	11-PTMS	501.13	5.63	51.01	85.08	60.49	54.25	0.57	0.96	0.68	1.64	89	33	91	35	3
4	12-PHOI	1010.3	7.11	89.72	141.53	94.47	165	0.63	1	0.67	2.2	142	75	153	86	29
5	13-PNB	286.55	5.21	31.16	53.02	33.94	33.5	0.57	0.96	0.62	1.6	55	21	57	23	2
6	14-PNBS	503.15	5.53	51.61	86.96	61.25	53.08	0.57	0.96	0.67	1.61	91	33	93	35	2
7	15-PNBD	497.09	5.85	49.82	81.31	58.97	55.58	0.59	0.96	0.69	1.68	85	33	87	35	5
8	16-PNBS	719.75	5.67	72.06	120.9	88.56	71.67	0.57	0.95	0.7	1.59	127	45	129	47	2
9	17PTCNS	581.27	5.64	59.4	98.61	69.54	61.08	0.58	0.96	0.68	1.57	103	39	108	44	2
10	18-P(6	719.75	5.67	72.06	120.9	88.56	72.67	0.57	0.95	0.7	1.61	127	45	129	47	2
11	19-P(5	719.75	5.67	72.06	120.9	88.56	72.92	0.57	0.95	0.7	1.62	127	45	129	47	2
12	1-PDSNB	719.75	5.67	72.06	120.9	88.56	72.33	0.57	0.95	0.7	1.61	127	45	129	47	2
13	20-P(2	713.69	5.9	70.26	115.25	86.27	74.67	0.58	0.95	0.71	1.66	121	45	123	47	5
14	21-P(3	797.87	5.74	79.85	132.55	96.84	80.67	0.57	0.95	0.7	1.58	139	51	144	56	2
15	22-P(3	797.87	5.74	79.85	132.55	96.84	80.92	0.57	0.95	0.7	1.59	139	51	144	56	2
16	23-APNB	284.53	5.37	30.56	51.14	33.18	29.83	0.58	0.96	0.63	1.42	53	21	58	26	0
17	24-APNB	501.13	5.63	51.01	85.08	60.49	49.42	0.57	0.96	0.68	1.5	89	33	94	38	0
18	25-APTCI	579.25	5.74	58.81	96.73	68.77	57.42	0.58	0.96	0.68	1.47	101	39	109	47	0

Fig II.11: The database of final descriptors.



Part-2-

Reduction of the number of descriptors



3. Part-2-

After optimization of the three-dimensional structures, the determination of descriptors which can be correlated with the property of interest, in our case the permeability (P). The resulting database needs pretreatment to reduce its size. The selection of relevant variables in relation to the quantity to be modeled; it aims at three essential points:

- Reduction of the dimension of the space of the representation of the variables of the model.
- Eliminate entries that have no or little influence on the exit.
- Selecting descriptors having great effect on polymer permeability

3.1.Pretreatment of the database:

The preprocessing of the database is intended to eliminate the descriptors that are not relevant in order to avoid the phenomenon of over-learning.

Our database called "initial database" is a table of 45* 3222 descriptors, we proceeded to a preliminary elimination of insignificant values as follows:

- ✓ The invariant descriptors have been removed manually.
- ✓ Any descriptor having more than 75% identical values was deleted.
- ✓ All descriptor with a RSD (Relative standard deviation) <0.05 is deleted

Hence the pre-reduction of more than 44% of the descriptors possessing little or not significant. This database called "new database" has become 45 * 1416 which will undergo another reduction by the IRIV method.

Nowadays, with a high dimensionality of dataset, it faces a great challenge in the creation of effective methods which can select an optimal variable subset. In this study, a strategy that considers the possible interaction effect among variables through random combinations was proposed, called iteratively retaining informative variables (IRIV). Moreover, the variables are classified into four categories as strongly informative, weakly informative, uninformative and interfering variables. On this basis, IRIV retains both the strongly and weakly informative variables in every iterative round until no uninformative and interfering variables exist. Three datasets were employed to investigate the performance of IRIV coupled with partial least squares (PLS). The results show that IRIV is a good alternative for variable selection strategy when compared with three outstanding and frequently used variable selection methods such as genetic algorithm-PLS, Monte Carlo uninformative variable

elimination by PLS (MC-UVE-PLS) and competitive adaptive reweighted sampling (CARS) [18]

The detailed approach of IRIV is illustrated as follows (Fig II.12).

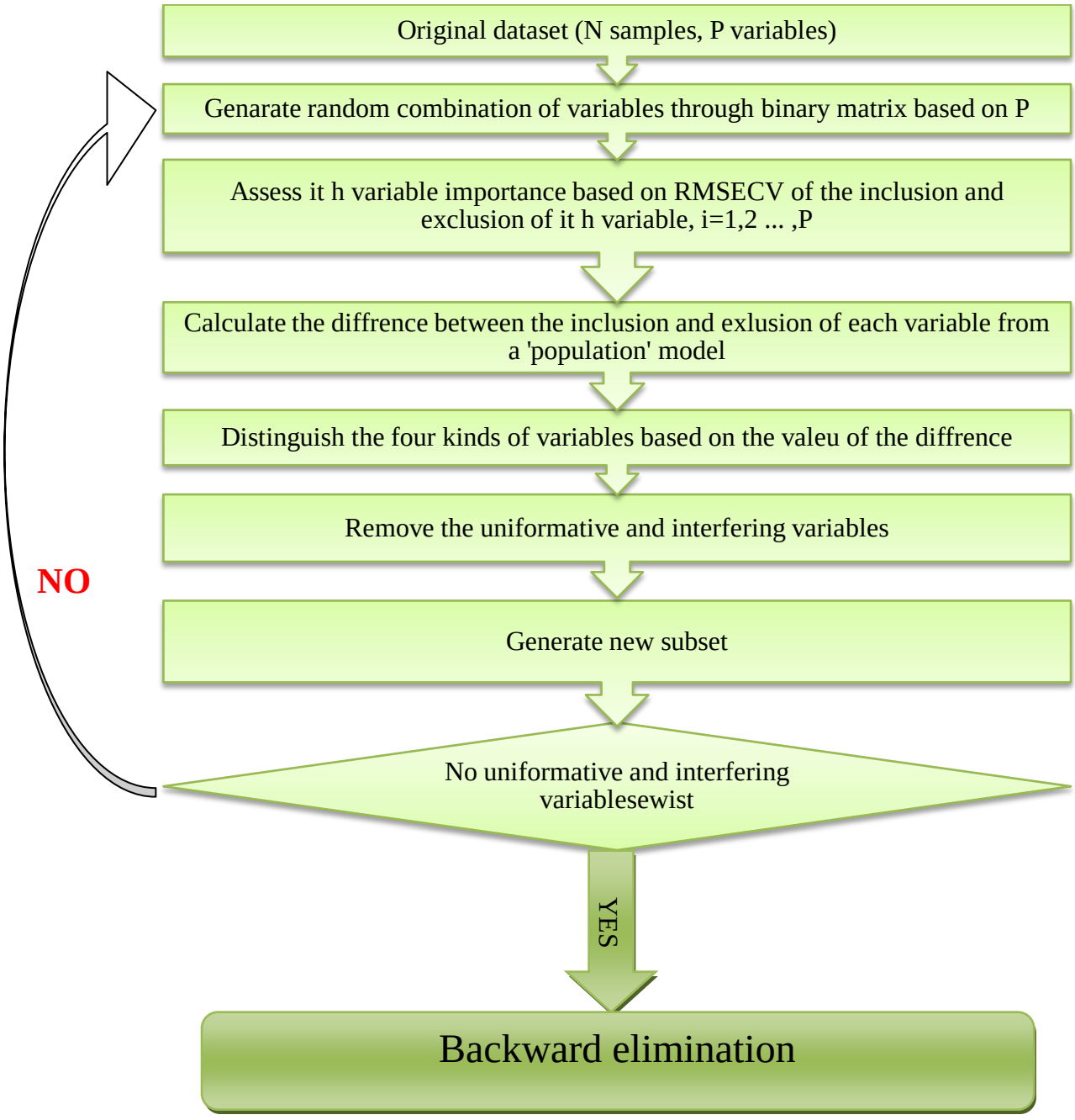
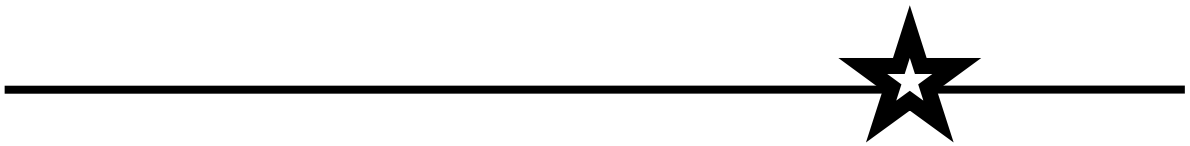


Fig II.12: The flow chart of IRIV algorithm. The number of the variables, P, changes after removing the uninformative and interfering variables. Correct this flow chart. No start from the conditional diagram and not above it.

We applied the method through the interface of Matlab R2010b Mathematical Calculation Software Version 7.11.0.584, 64 bit. The IRIVS is implemented in the software library; the results are shown in the (table II.3).

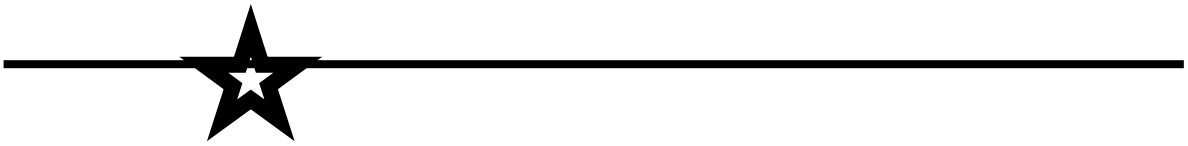
Table II.3: Calculation results of molecular descriptors of CO_2.

The descriptor blocks	The number of descriptors in each block	The number of descriptors after the reduction
Topological descriptors	78	2
Walk and path counts	46	1
Connectivity indix	33	2
Burdeneigen values	63	1
Geomitrical desctiptors	74	1
2D frequencyfingerprints	61	1
3D-morse descriptors	160	3
GETAWAY decriptors	195	1
WHIM descriptors	99	1
Total		13



Part-3-

Neural modeling for permeability prediction



4. Part-3-

The previous first part of our study allows us to obtain a dimension database. When we can use them to establish a quantitative structure property relationship (permeability) QSPR, to achieve this relationship, we use the artificial neural network.This part of our study is divided into three stages:

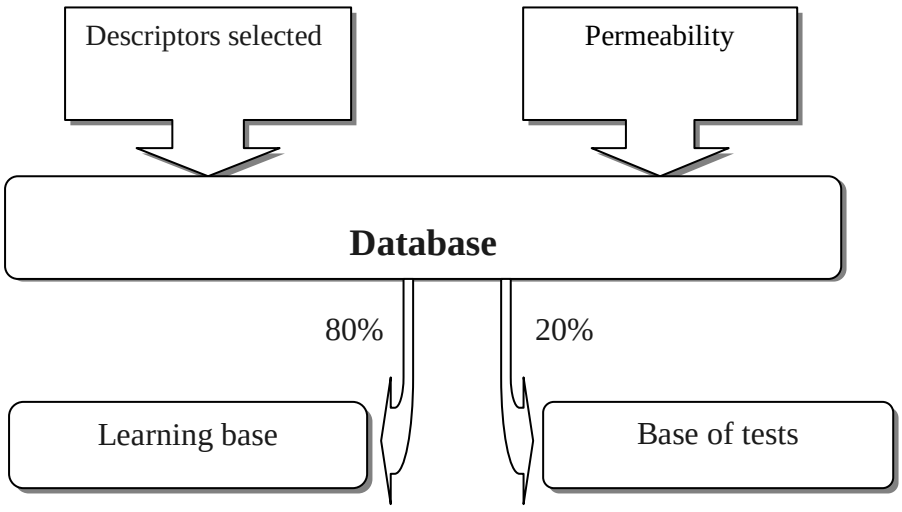
- The first one looks at the architecture of the network and the optimization of the parameters that affect it.
- The second step presents the results of prediction of the model obtained and its performances with respect to existing models.
- The last is concerned with the validation of models obtained by statistical parameters.

4.1.Distribution of data:

In this step, the data is subdivided into two subsets:

- A set for learning.
- A set for the test.

Certainly, there are no rules for the determination of this sharing in a quantitative way. The experimental database contains 45 polymers chosen for the different polymeric structures; the structure of the final database is shown schematically in (Fig II.13). (80% for the learning phase and 20% for the test phase)



FigII.13: General schematization and distribution of the contents of the database.

4.2.Optimization and design of the neural network:

There are many types of neural networks; each with its advantages and disadvantages, the choice depends on:

- The task to be performed (classification, association, control ...)
- The nature of the data.

Different types of neural networks are available in the simulation software (Matlab) that we intend to use or develop its own program.

The main objective of this part is to know which is the best architecture that can be able to process the available database for the design and optimization of neural model.

In this work, three steps were followed:

- The first is to test the fundamental parameters: the activation function and the learning algorithm.
- The second part is to draw the best networks and see the effect of some standardization functions on their performance.
- The third part is devoted to the study of the effect of the number of neurons and the number of hidden layers.

There are several languages or softwares where we can build a prediction model based on ANN such as: Lazy 1071, Fortran 77 and Matlab. We have chosen in this work Matlab because of its frequent use in publications such as Wessling [19], Mazdak [20] and our mastery of this software in our previous works JMS [21].

In Matlab, the steps for creating a neural model result in the instructions given in Table II.4.

Table II.4: The meanings of some Matlab instructions.

Instruction	Signification
newff	Create a new MLP network
Init	Initializes the MLP network
Train	The learning phase
Sim	Simulate the neural network

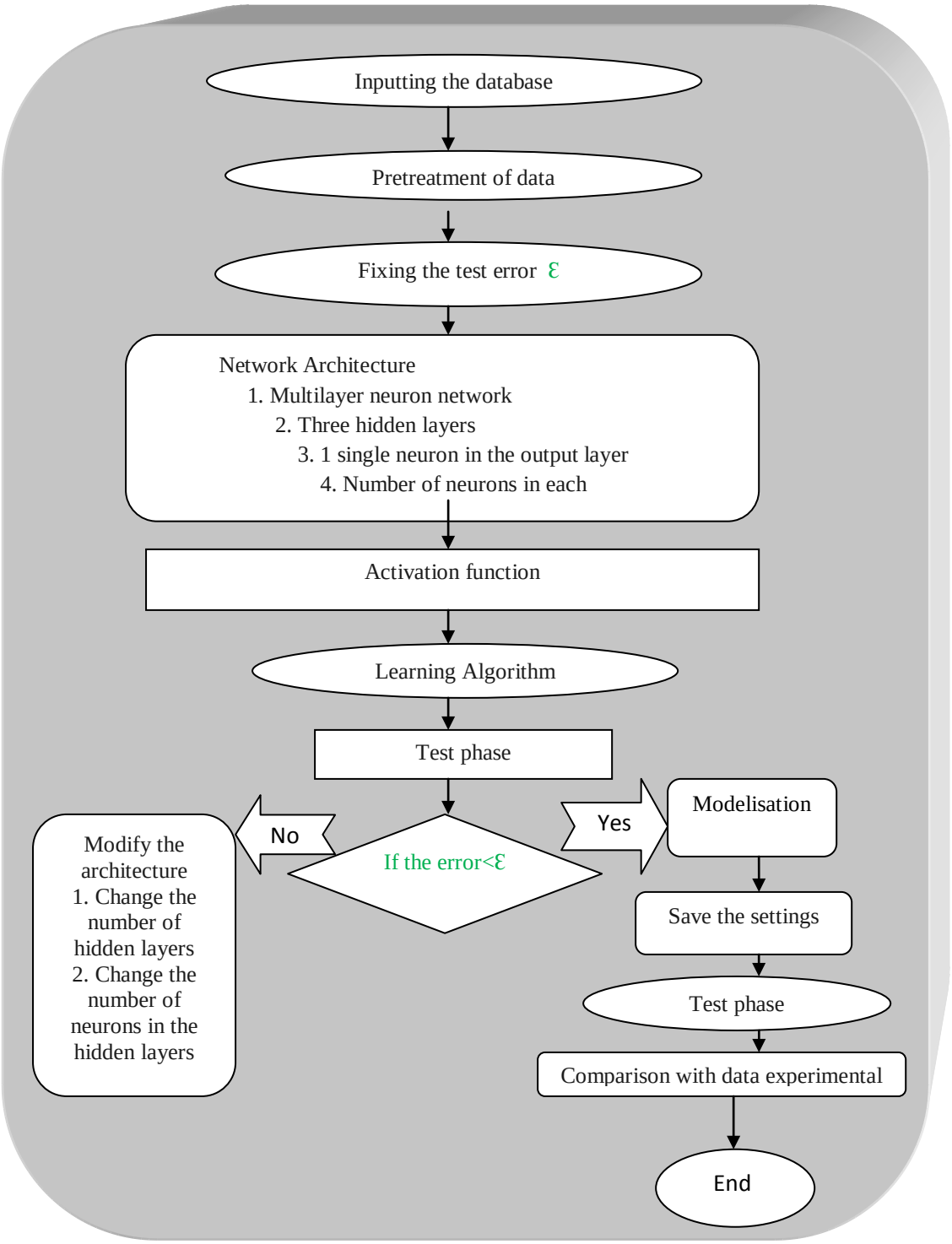
The emergent property of an ANN is its learning ability, from any state. It relies on a learning algorithm, adapting the value of synaptic weights to provide a similar true answer to the problem being addressed. There are different learning techniques for determining optimal synaptic weight values.

Supervised learning is retained in this study. It consists of supplying the network with input datasets (chemical descriptors of hybrid polymeric structure) for which the desired response is known (the coefficient of the permeability). The architecture of a network is optimized to minimize the root of the network:

- ✓ Mean square error.
- ✓ The network of type "feedforward" is the most used network for the approximation of the functions of the static data.
- ✓ The codes of the different learning functions used in the tests are shown in the following table II.5:

Table II.5. The codes of deferent learning functions used in the test.

Algorithm	Matlab Code	Acronym
Levenberg-Marguardt	Trainlm	LM
Scaledconjugate Gradient	Trainscg	SCG
Bayesianregularization	Trainbr	BR
Resilient Back propagation	Train rp	RP
BFGC quassi-Newton	Trainbfg	BFG



FigII.14: Flowchart of Optimal Static Neural Network (OSNN) Methodology.

4.3.Optimization of the CO_2 prediction network architecture:

4.3.1. Step 1: Effect of the learning algorithm:

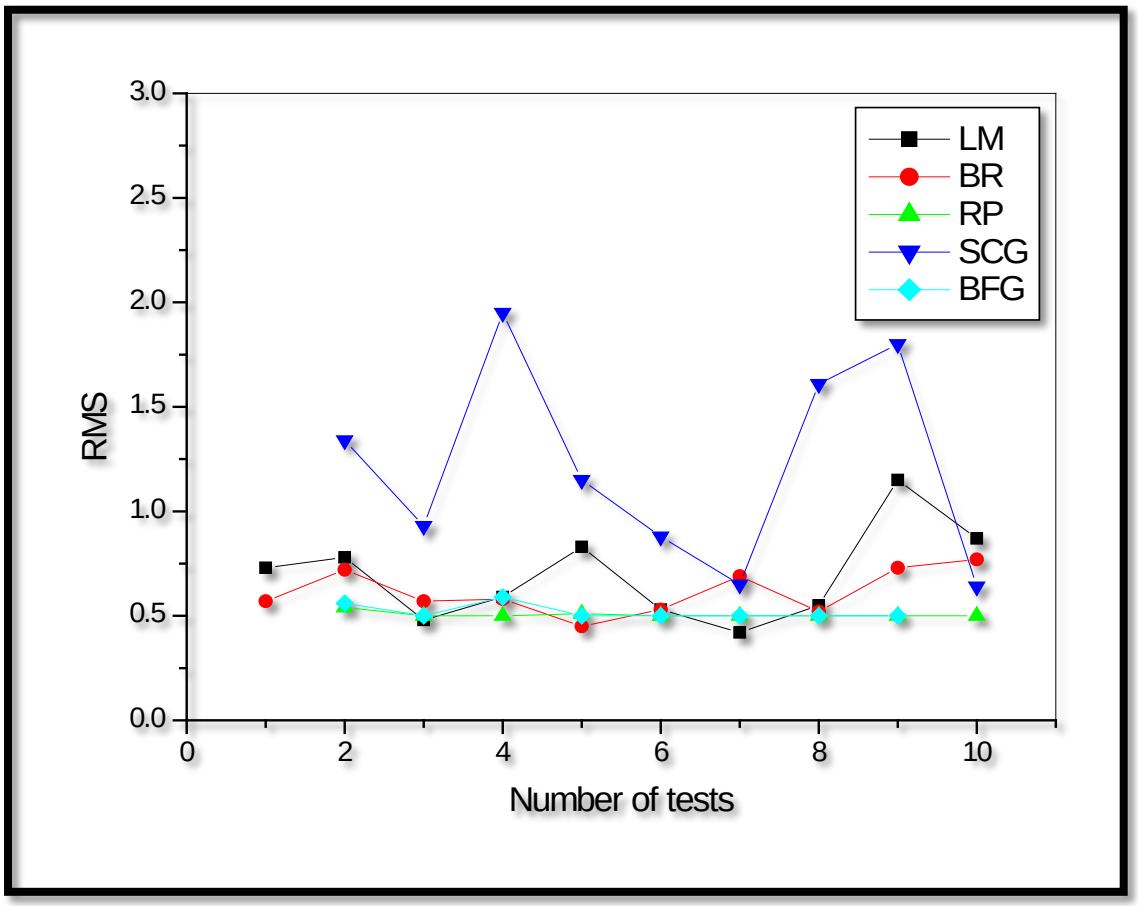
To follow the effect of the variation of the learning algorithm, several algorithms are used which are listed Up in (Table II.5).

The goal is to have the (RMSE) Root of the Mean Squared Error minimum regardless of the algorithm:

$$\mathbf{RMSE} = \sqrt{\frac{1}{n}\sum_{i=1}^{n}(y_{prédite} - y_{observée})^2} \qquad \text{II.1}$$

With $y_{predicted}$ and $y_{observed}$ values respectively predicted and experimental.

After the learning phase of the algorithms, train BR and train LM, the learning outcomes are shown in (Fig II.15)



FigII.15: Effect of the learning algorithm on the performance of the neural network.

4.3.2. Step 2: Effect of standardization

Numeric data has been standardized to improve optimization, and normalization is done by one of the following functions: mapminmx, mapstd.

These functions follow the formulas shown in Table II.6.

Table II.6: Standardization algorithms.

	The algorithm
Mapminmx	$\boldsymbol{y = (y_{max} - y_{min}) * \frac{(x - x_{min})}{(x_{max} - x_{min})} + y_{min}}$
Mapstd	$\boldsymbol{y = (x - x_{moy}) * \left(\frac{y_{std}}{x_{std}}\right) + y_{moy}}$

And y: is the normalized value.

x: is the original value.

From step 1, both BR train algorithms, LM train, were obtained. These results make it possible to test the normalization effect on the two networks obtained.

✓The algorithm that gives the best result is LM with mapstd.

The normalization effect on the convergence of the neuronal model is shown in (FigII.16) and (Fig.II.17)

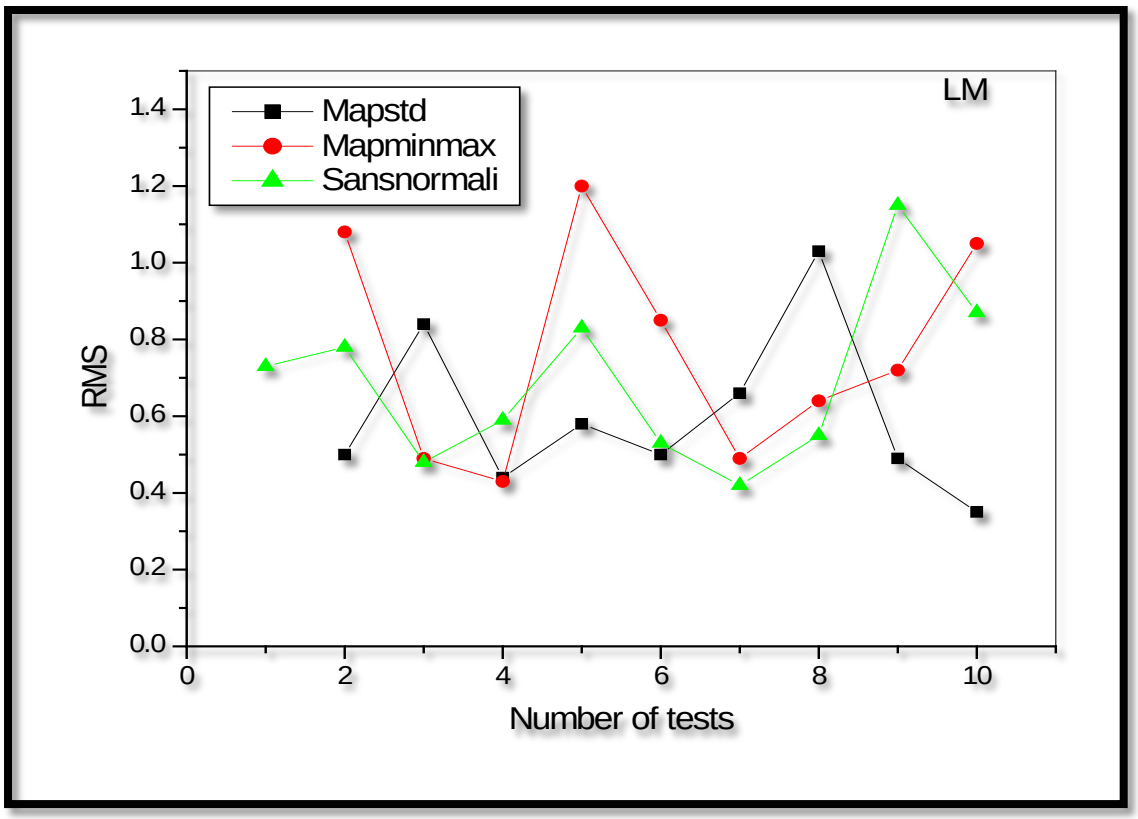


Fig II.16: Effect of normalization on the learning performance of the neural network, train LM.

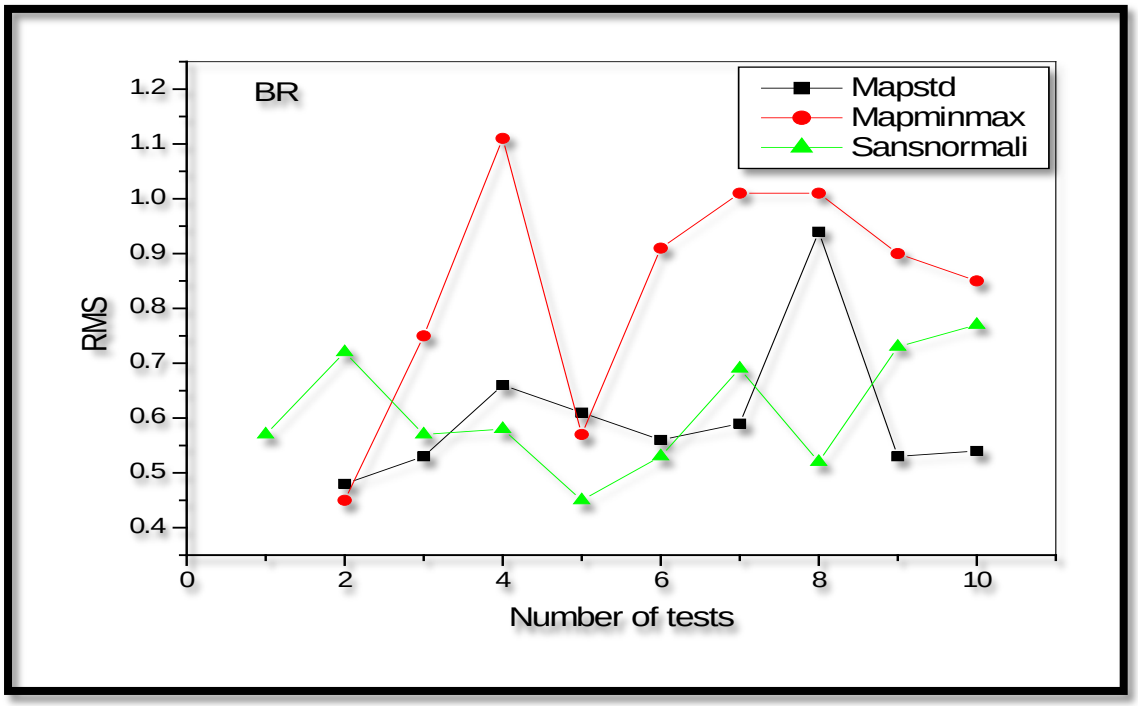


Figure II.17: Effect of normalization on the learning performance of the neural network, BR train.

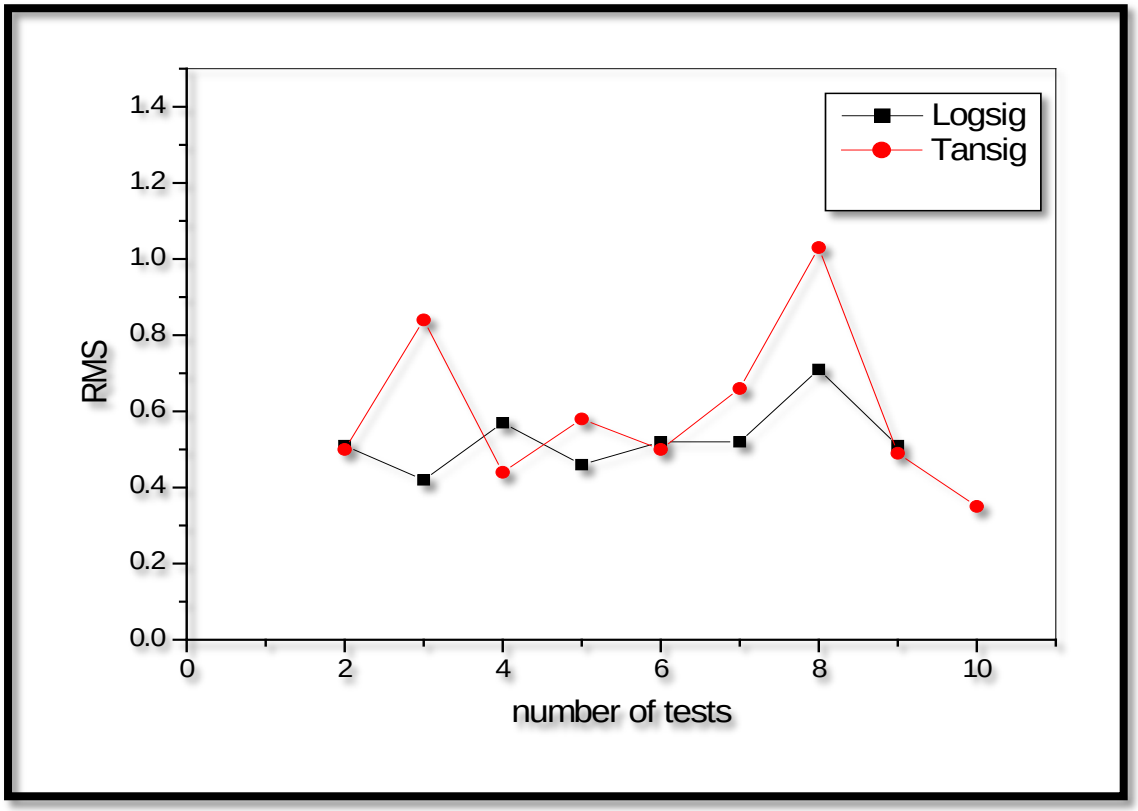
✓ In terms of RMSE (Fig II.16 and 17) show that the Mapstd standardization method gives the best performance.

4.3.3. Step 3: Activation function effect:

Two activation functions have been applied (Table II.7) to have a single activation function which gives the root of the least squared error, (Fig II.18) shows the variation of the root of the squared error. Average (RMSE) with different activation functions.

Table II.7 Different activation functions used in the design phase of the neural model.

Transfer function	Code MATLAB
Tan- Sigmoidtransferfunction	Tansig
Log-Sigmoidtransferfunction	Logsig



FigII.18: Effect of the activation function on the performance of the neural network.

✓ The activation function that has been chosen for the hidden layers is Tan-Sigmoid and the Purelin Identity function for the output layer.

4.3.4. Step 4:

This step was devoted to testing different architectures by modifying the number of neurons in each hidden layer and the number of hidden layers. (Fig II.19)

A. Effect of the number of neurons:

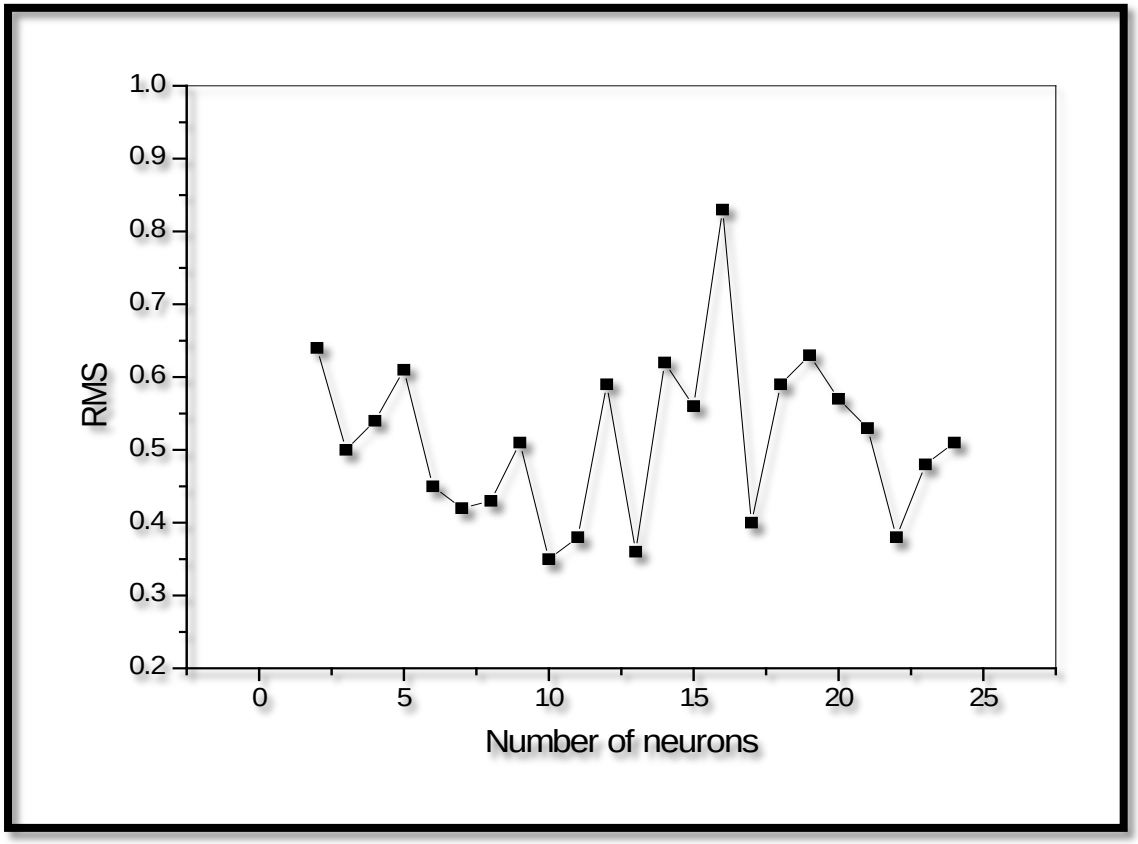
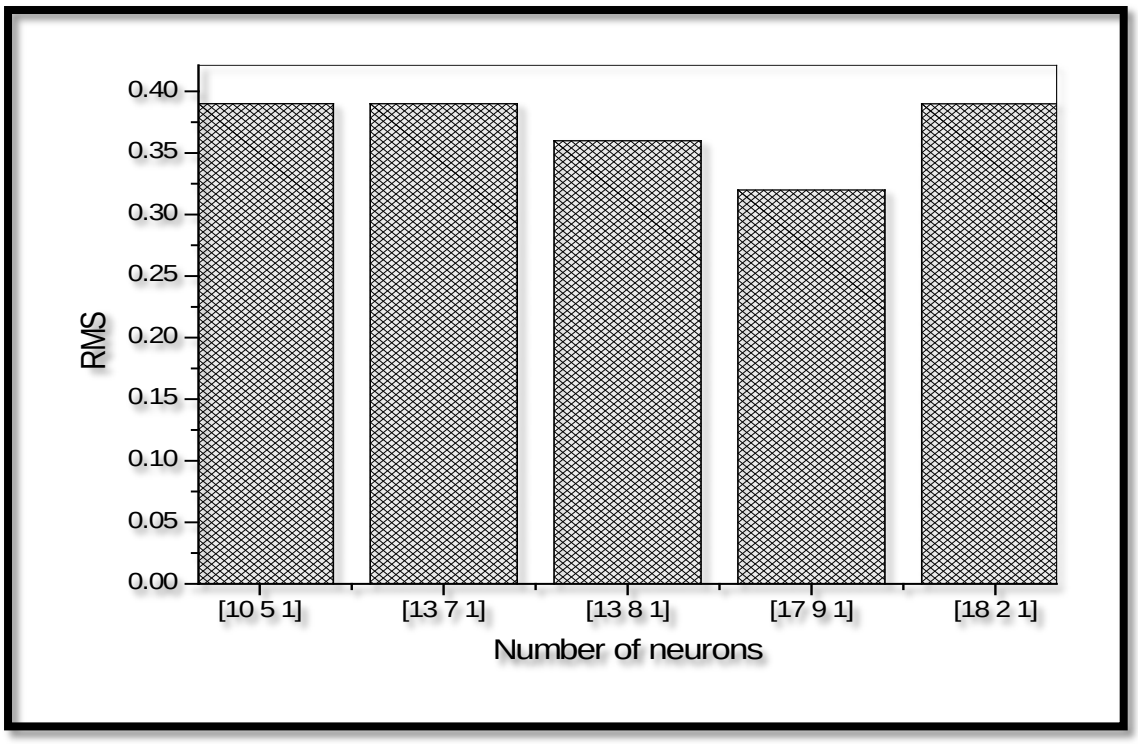


Fig II.19: Effect of number of neurons of the hidden layer on the learning performance of the neural network.

✓ According to (Fig II.19), the network gives a better performance for 10 neurons in the hidden layer.

B. Effect of the number of hidden layers:

The structure of the neural network has been further modified by integrating a third hidden layer. The best result obtained with the architecture of [13 18 6 4 1] gives a RMSE of 0.23.



FigII.20: Effect of the number of hidden layers on the learning performance.

5. *Result of the optimization:*

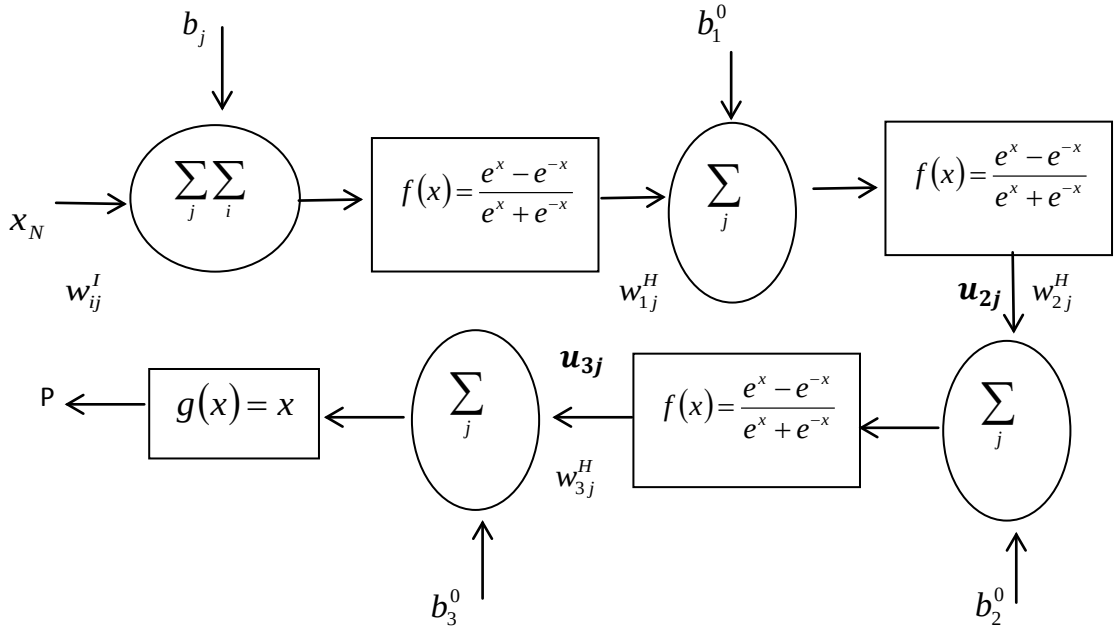
The constitution of the networks obtained is presented in Table II.8.When the learning is done; the networks are tested on new sets of input / output which form the basis of generalization. This step makes it possible to check the behavior of the networks on untrained cases.

Gas	Type of network	Entry layer	First hidden layer		Second hidden layer		Third hidden layer		Exit layer		Algorithm of learning weaving
		Number of neurons (Nn)	Nn	Activation function (Af)	Nn	Af	Nn	Af	Nn	Af	
CO_2	SNN MLP[a]	13	18	Tansig	6	Tansig	4	Tansig	1	Purlin	Train LM

Table II.8: Structure of optimized neural networks.

a: Static neural network multi-layer perception.

These networks are schematically represented in Fig II.21 for the CO2 network



FigII.21: Optimized CO_2 neuron network architecture.

The mathematical expression of the model obtained is given below:

$$P_{CO2} = g\left\{\sum_{j=1}^{4}\left(w_{3j}^H u_{3j} + b_3^0\right)\right\} \quad \text{..... (II.1)}$$

$$u_{3j} = f\left\{\sum_{j=1}^{6}\left(w_{2j}^H u_{2j} + b_2^0\right)\right\} \quad \text{..... (II.2)}$$

$$u_{2j} = f\left\{\sum_{j=1}^{18}\left(w_{1j}^H u_{1j} + b_1^0\right)\right\} \quad \text{..... (II.3)}$$

$$u_{1j} = f\left\{\sum_{i=1}^{13}\left(w_{ij}^I x_N + b_j\right)\right\} = \left[\frac{e^{\left(\sum_{i=1}^{13} w_{ij}^I + b_j\right)} - e^{-\left(\sum_{i=1}^{13} w_{ij}^I + b_j\right)}}{e^{\left(\sum_{i=1}^{13} w_{ij}^I + b_j\right)} + e^{-\left(\sum_{i=1}^{13} w_{ij}^I + b_j\right)}}\right] \quad \text{..... (II.4)}$$

With:

x_N represents the inputs

w^I_{ij} represents the weights that connect the inputs to the "j" neurons of the hidden layer

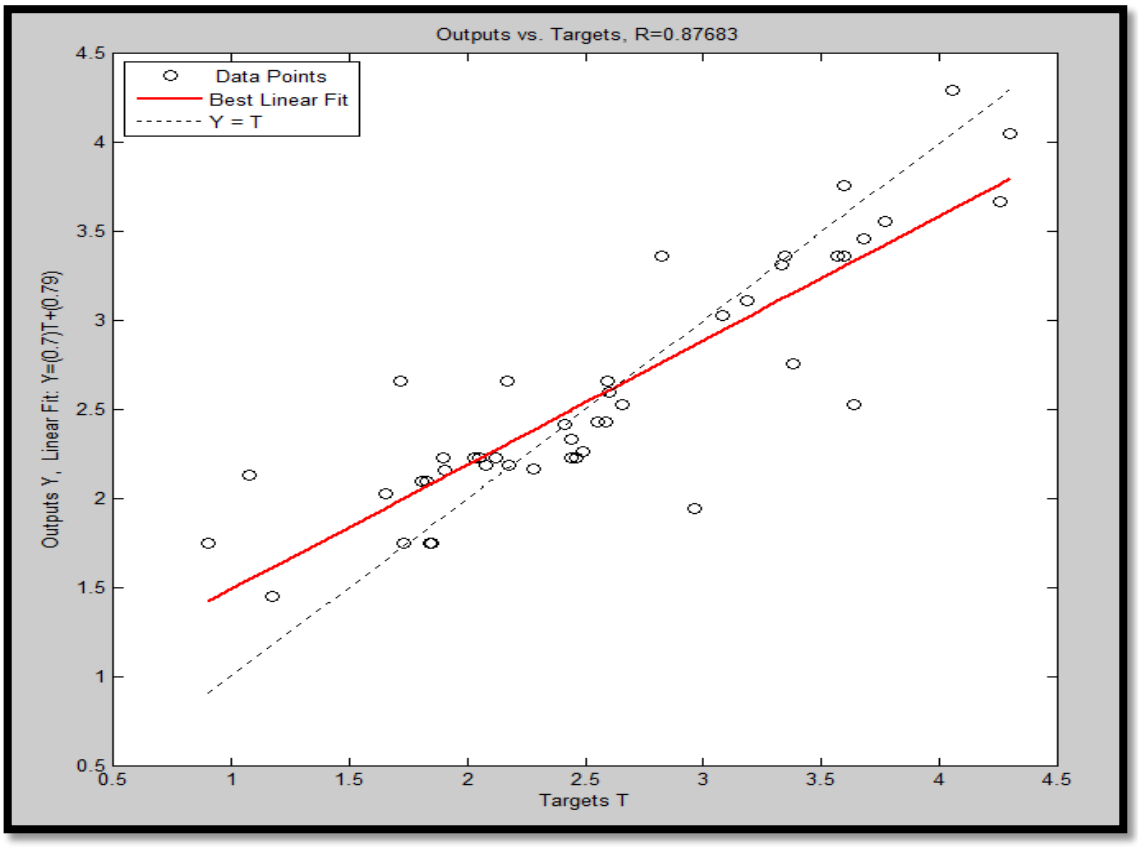
b_j is the weight biases connecting the inputs to the "j" neurons of the hidden layer

w^H_{1j} , w^H_{2j} represent the weights of the "j" neurons of the hidden layer going to the exit

b^0_1, b^0_2 are the hidden layer weight bias

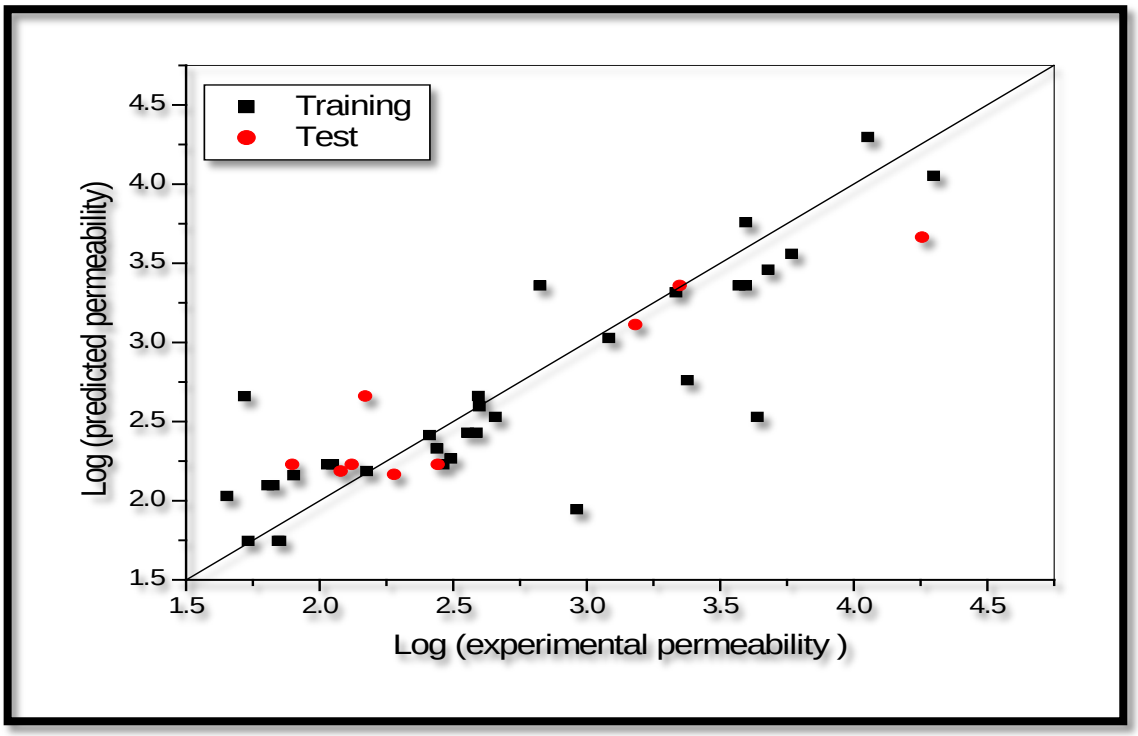
P is the desired output (permeability in the case of our study). The weights of weight and bias of networks optimized for CO_2.

The graphical presentation between the desired output and the network response is performed by the function (Postreg, Matleb). The results obtained are shown in (FigII.22 and FigII.23).



FigII.22: the estimatedpermeability as a function of the experimental permeability for CO_2 and their linear equation by the postreg function of MATLAB.

With $$CO_2 : P_{estimated} = (0,7) \times P_{experimantal} + 0.79$$



FigII.23: Comparison between the experimental permeability and the estimated permeability for CO_2.

6. *Statistical parameters:*

Statistical parameters are required to evaluate the performance of the developed model.

6.1.Coefficient of correlation Z:

$$\mathbf{Z = 1 - \frac{\sum_1^n (y_i - y_i^t)}{\sum_1^n (y_i - y_0)^2}} \qquad \text{(II.6)}$$

With $$\mathbf{y_0 = [\frac{1}{n}(\sum y_i - y_i^t)^2]^{1/2}} \qquad \text{(II.7)}$$

Or $\mathbf{y_i}$ is the experimental value, $\mathbf{y_i^t}$ the predicted value.

- ✓ The Z is a simple indicator; it is easy to understand that the closer it gets to the value 1, the more interesting the model.

6.2. Prediction coefficient($\boldsymbol{Q^2_{train}}$):

$$\mathbf{Q^2_{train} = 1 - \frac{\sum (y_{exp(train)} - y_{pred(train)})^2}{\sum (y_{exp(train)} - \bar{y}_{exp(train)})}} \qquad \text{(II.8)}$$

✓ This parameter informs us about the robustness of the model developed (in general, it is preferable that it be greater than 0.6.

6.3.Prediction coefficient (Q^2_{test}):

$$\mathbf{Q^2_{test}} = \mathbf{1} - \frac{\sum(\mathbf{y_{exp(test)}} - \mathbf{y_{pred(test)}})^2}{\sum(\mathbf{y_{exp(test)}} - \bar{\mathbf{y}}_{\mathbf{exp(train)}})^2} \qquad \text{(II.9)}$$

✓ This parameter informs us about the predictive power of the model. The value greater than 0.8 stipulates, the model performs very well.

6.4. Performance factor (C):

$$C = \frac{\sum_1^n |(y_{pred} - y_{exp})|}{\sum_1^n |(y_{exp} - \bar{y}_{exp})|} \qquad \text{(II.10)}$$

✓ The neural network functions predictively if C is less than 1.

6.5.Average absolute relative error (AARE):

$$\text{AARE} = \frac{1}{n}\sum_{i=1}^{n}\left(\frac{y_{exp} - y_{cal}}{y_{exp}}\right) \qquad \text{(II.11)}$$

Or y_{exp} is the experimental value, y_{cal} the calculated value.

The values of these parameters are shown in Table II.9.

Table II.9: The values of the statistical parameters.

Paramètres statistiques	CO_2
n	45
RMSE	0.23
$AARE_T(\%)$	8.32
$AARE_g(\%)$	14
Z_T	0.87
Z_G	0.89
Q^2_{test}	0.8
Q^2_{train}	0.604
C	0.41
P_{min}	8.03
P_{max}	19900

7. Results analysis:

To evaluate the performance of the obtained neural models, a graphical representation of the obtained predicted permeability values as a function of the experimental values for the learning and test sets is given in (Fig II.18 and II.19). A close correlation between the values calculated by the RNA model and the experimental values of the permeability was observed.

The true utility of QSPR (Quantitative Structural Permeability Relationship) models is not only their ability to replicate known data, but also to have predictive potential. For this reason, the characteristic parameters of the model are given in Table II.9.

Table II.9 shows an excellent value of 0.8 concerning the parameter Q^2_{testce} which shows us that our model has a predictive power and is very efficient; concerning the $Q^2_{learning}$ we found the values 0.6 it means that our model is perfectly robust and stable. On the other hand, the value of the Root Mean Square Error (RMSE), too, is a good predictive power of the model.

Our model presents an $AARE_T$ of 14 and an $AARE_g$ of 8.32 shows the reliability of RNA in the prediction of the permeability.

The networks obtained give a correlation coefficient of 0.89 this value confirms the deviation of the predicted permeability with respect to the experimental ones and this is due to the widened experimental permeability interval used to build the CO_2 database and also to the values poorly predicted by ANN.

The problem of poorly predicted permeability was solved by the expansion of the database.

Prediction related to several parameters, they can handle:

- The size of the database
- The nature of the molecules selected in the database;
- The statistical method of selecting the most relevant descriptors;
- The number and nature of these descriptors;
- The nature and difficulty of representing hybrid materials and limit of the Dragon version used in this work.
- And finally, the properties of the optimized neural network.

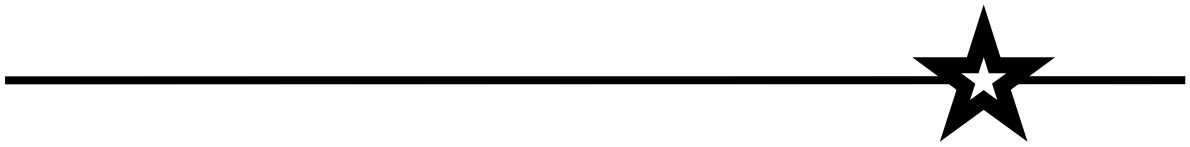
The residuals for the values observed in the learning and validation sets were determined and presented in (Fig II.20). The model did not show proportional

and systematic error because the distribution of residues on both sides of the midline is random.

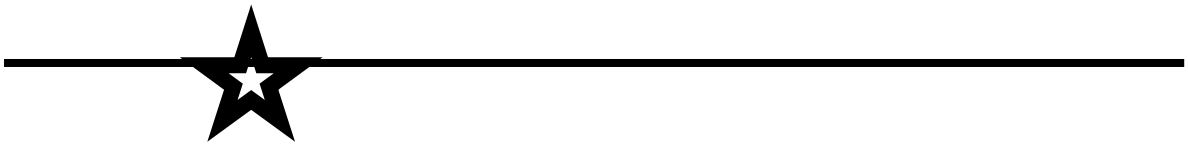
All other satisfactory Table II.9 parameters indicate that the QSPR models we have built are reliable and predictive.

8. Conclusion:

In this part of our study, we have succeeded in establishing a suitable neural architecture for predicting the (CO_2) gas permeability of a set of hybrid materials. This prediction capacity can be evaluated by performing a preliminary treatment on the initial data base. Using an "IRIV" method, the latter allows us to determine the optimal number of input variables for neural modeling that ensures a minimal error (RMSE). The various optimization studies performed on the gas allow us to evaluate confidence intervals for the predictive ability of the neural models designed for the CO_2 gas. It should be noted here that the best predictive performance has been found in the case of CO_2; good predictive capabilities for this gas are reported.



General Conclusion



General conclusion

- Hybrid materials are not only a physical mixture of two phases, but they are characterized by an intimate mixture of the organic and inorganic phases, with their interfaces consequently playing an important role in their properties and generating unusual features or improved performance of the hybrid materials. Depending on the nature of the bonding between the organic and inorganic phases, two classes of organic– inorganic hybrids have been defined, and used as membrane for gas separation processes. To understand the relationship between the microstructure of hybrid materials and their permeability to gases, a model based on artificial neural network was established using the microstructure of macromolecules.
- The modeling of micromolecules properties constitutes an important field of research; the traditional methods of modeling establish relations between the properties studied and the structural characteristics of the molecules, called descriptors. Their main drawbacks lie in the difficulty of choosing descriptors. We have developed a modeling approach that overcomes these problems by establishing a direct relationship between molecular descriptors and the modeled property through the use of an "IRIV" method to determine the most relevant descriptors.
- This method of modeling using artificial neural networks is part of new techniques under the aegis of computational intelligence or cognitive science and it allows developing models ensuring the correlation and the prediction of permeability of hybrid polymers to gas.
- The calculation of the descriptors is ensured by Dragon software and require different softwares (Chembiooffice, Hyperchem), to draw and optimize the microstructure. A large number of different descriptors have been calculated from optimized microstructure of hybrid polymers.
- Different bonding between two moieties O-I may open new opportunities to be develop their modeling methods.
- Different modeling prediction of gases permeability might be use to define different descriptors.

References

[1].*Site web: http://www.open.edu/openlearn/science-maths-technology/science/chemistry/introduction-polymers/content-section-0.*

[2]. *V.Meynen,L Hessel . C and A. Buekenhoudt. Class II Hybrid Organic-inorganic Membranes Creating New Versatility in Separations. Article in Current Organic Chemistry · October 2014.* DOI: 10.2174/1385272819666140806200931. Seen March 26th.2018.

[3]. *N. Physica E. Physica '' Quantum dot solar cells" E 14 (2002) 115 – 120. Seen March 26th.2018.*

[4]. *G. Kickelbick. "Hybrid Materials. Synthesis, Characterization, and Applications". Copyright © 2007 Wiley-VCH Verlag GmbH & Co. KGaA, Weinheim. ISBN: 978-3-527-31299-3. Seen March 3rd .2018.*

[5]. *O. TRABELSI. « Etude des matériaux hybrides organiques-inorganiques élaborés par le procédé sol-gel ». THESIS to obtain the rank of DOCTOR OF THE UNIVERSITY. Univ Riems Champagne-Ardonne. 12/12/2011.*

[6]. *F. Mammeri, E. Le Bourhis, L. Rozesa and C. Sanchez." Mechanical properties of hybrid organic–inorganic materials".* This journal is _ The Royal Society of Chemistry 2005*. Seen 6 Mai 2018.* .

[7]. *C.Boulard. A.Chassenieux. M.Ribaud, M. Barré: Matériaux hybrides et mésoporeux, biomatériaux (4 ECTS). Seen March 27th. 2018.*

[8]. *K. Masakoto,Y.Kazuya, Y.Tomohisa, T.Toshinori. "Organic–inorganic hybrid silica membranes with controlled silica network size:Preparation and gas permeation characteristics". Journal of Membrane Science 348 (2010) 310–318. Seen April 3rd 2018.*

[9]. *Y.Shuwen, L.Shichun, H.Shiliang, Z.Zehua, C.Sheng, L.Yu. "Covalently Bonded Zeolitic Imidazolate Frameworks and Polymers with Enhanced Compatibility*

in Thin Film Nanocomposite Membranes for Gas Separation". Journal of MembraneScience,http://dx.doi.org/10.1016/j.memsci.2017.06.047. Seen April 3rd. 2018.

[10]. *E.Bakangura, C.Cheng, L.Wu, X.Ge, J.Ran, M.Imran khan, K.Emmanuel, N.Afsar, M.Irfan, A.Shehzad and T.Xu), "Hierarchically Structured Porous Anion Exchange Membranes Containing Zwetterionic Pores for Ion Separation", Journalof Membrane Science, http://dx.doi.org/10.1016/j.memsci.2017.05.007). Seen March 18th.2018.*

[11]. K.YAHI and M. KHALFI. "MODELE QSPR POUR LA PREDICTION DE LA PERMEABILITE DES POLYMERES. Master's thesis in Process Engineering. Univ MEDEA. 2016/2017.

[12]. *H.HASNAOUI. « Utilisation des réseaux de neurones dans la prédiction de la perméabilité des polymères aux gaz et aux vapeurs ». . DOCTORAL THESIS 2017/2018. Univ Medea.*

[13] J. Christopher . R.John . K.Mason, A.Thomas, S.Eric, F.Frederick. "Gas permeability in rubbery polyphosphazene membranes". Journal of Membrane Science 280 (2006) 175–184. Seen May 23rd ,2018.

[14]. J.*Christopher , R.John ,K.Mason , A.Thomas ,S. Eric ,F.Frederick.." Gas permeability in rubbery polyphosphazene membranes". Journal of Membrane Science 280 (2006) 175–184. Seen April 9th. 2018.*

[15]. *G. Ragosta*, P. Musto. "Polyimide/silica hybrids via the sol-gel route: High performance materials for the new technological Challenges". Artcle Available online at www.expresspolymlett.com. No.7 (2009) 413–428. Seen March 12th. 2018.*

[16]. *S. Kaur, M.Gallei, and E. Ionescu. " Polymer–Ceramic Nanohybrid Materials". DOI: 10.1007/12_2014_282. © . Seen Mai 6th.2018.*

[17]. *L.CHER HON. » MATERIAL DESIGN AND HYBRIDIZATION FOR GREEN CARBON DIOXIDE CAPTURE ». A THESIS SUBMITTED FOR THE DEGREE OF DOCTOR OF PHILOSOPHY. Flinders University. 2011.*

References

[18]. *Y.Yun, W. Wang, M. Tan, Y.Liang, H.Li , D.Cao, H.Lu, Q. Xu. "A strategy that iteratively retains informative variables for selecting optimal variable subset in multivariate calibration* ".jou rn al h om epage: www.elsevier.com/locate/aca. Seen March 25th.2018.

[19]. *M.Wessling, M.H.V.Mulder," Modelling the permeability of polymers: a neural network approach", Journal of membrane Science, v86, 193-198, 1994. Seen March 27th.2018.*

[20]. M. Shokrian, M. Sadrzadeh, "C3H8 separation from CH4 and H2 using a synthesized PDMS membrane: Experimental and neural network modeling", Journal of Membrane Science, V346, 59-70, 2010. Seen April 27th.2018.

[21]. H.Hasnaouia, M.Krea,D.Roizard." Neural networks for the prediction of polymer permeability to gases": Journal of Membrane Science 541 (2017) 541–549. Seen May 25th .2018.